ABSTRACT

Title of Thesis: INVESTIGATING THE MICROBIAL DIVERSITY AND ECOPHYSIOLOGY OF FILAMENTOUS CYANOBACTERIA ON THE SUSQUEHANNA FLATS, CHESAPEAKE BAY

Shayna Aryn Keller, Master of Science, 2024

Thesis Directed By: Dr. Judith M. O'Neil, Associate Research Professor, Marine, Estuarine, and Environmental Science, the University of Maryland Center for Environmental Science

The Susquehanna Flats is a biodiverse and resilient submerged aquatic vegetation (SAV) bed just below the mouth of the Susquehanna River in the Chesapeake Bay. The Susquehanna River, the largest tributary of the Chesapeake Bay, discharges more water than all other tributaries in the Bay combined. This makes the SAV bed at the Susquehanna Flats important for nutrient removal of the water discharged into the headwaters of the Bay. The Susquehanna Flats is also a unique part of the oligohaline portion of the Chesapeake Bay as it is one of the most prolific and diverse SAV beds that make up ~8% of SAV in the Chesapeake Bay. The SAV bed was devastated by Hurricane Agnes in 1972 and did not reappear until the early 2000s when an extended dry period and long-term reductions in nutrient loading facilitated its resurgence. Since then, it has recovered to be the most abundant and biodiverse SAV bed within the upper Chesapeake Bay. However, a nitrogen fixing filamentous Cyanobacteria, morphologically identified as *Microseira* (*Lyngbya*) *wollei*, has seasonally bloomed at the Susquehanna Flats since the early 2000s. Over the ensuing decade, anecdotal evidence suggested an overall increase of Cyanobacteria on the SAV beds on the Susquehanna Flats, which raised concerns about the impact of this growth on the resilience of the recovering SAV bed. Despite the consistent summer blooms, the filamentous

Cyanobacterial mats and its microbiome at the Susquehanna Flats has not been molecularly identified and its characteristics have not been investigated to date. Additionally, new DNA sequencing technology has become more readily available, and the identification and taxonomy of the Cyanobacteria family Oscillatoriaceae, of which *Microseira* (*Lyngbya*) *wollei* is a part of, has become more refined and organized. Due to this, molecularly identifying the filamentous Cyanobacterial mats and investigating its microbiome has become much easier with current methods that can provide detailed taxonomic information that can help implement management strategies. Using PacBio long-read amplicon sequencing on the 16S rRNA genes and Illumina short-read amplicon sequencing on the *nifH* genes of the filamentous Cyanobacteria mats and a newly observed mucilaginous Cyanobacteria mat collected at the Susquehanna Flats, the host organisms and microbial compositions were revealed. The results indicate that the dominant filamentous Cyanobacterial mat host is *Microseira* (*Lyngbya*) *wollei* and these mats contain a complex microbial community. The host of a newly observed mucilaginous mats was revealed to be a novel strain of *Phormidium sp*. To understand the basic nutrient requirements and preferences of the *Microseira* (*Lyngbya*) *wollei* at the Susquehanna Flats, nutrient bioassay growth and nitrogen fixation experiments were initiated to assess its growth and nitrogen fixation qualities. Samples received nutrient treatments of nitrate, phosphate, nitrate + phosphate, and ammonium compared to the growth of control samples that did not receive nutrient treatments in the summers of 2022 and 2023. The results demonstrated that *Microseira* (*Lyngbya*) *wollei* has variable growth rates, with higher rates in the mid to late part of the summer season, with significant growth stimulations from added nitrogen and phosphorus. In terms of nitrogen fixation, rates were higher in the beginning of the season, with significant stimulation with phosphorus additions. It is likely that lower rates measured at the end of the season, were due to

the increased availability of regenerated nitrogen within the system. More detailed investigation of the seasonal nutrient dynamics are warranted to fully understand the dynamics between these Cyanobacterial mats and the SAV beds.

INVESTIGATING THE MICROBIAL DIVERSITY AND ECOPHYSIOLOGY OF FILAMENTOUS CYANOBACTERIA ON THE SUSQUEHANNA FLATS, CHESAPEAKE BAY

by

Shayna Aryn Keller

Thesis submitted to the Faculty of the Graduate School of the
University of Maryland, College Park, in partial fulfillment
of the requirements for the degree of
Master of Science
2024

Advisory Committee:
Dr. Judith M. O'Neil, Associate Research Professor, Chair
Dr. Jacob Cram, Assistant Professor
Dr. Jeffrey Cornwell, Research Professor

Dedication

This master's thesis is dedicated to my Mom and Dad.

Acknowledgements

Thank you to my advisor, Dr. Judith M. O'Neil, who without her patience, expertise, and mentorship, this thesis and my graduate school path would not have been possible. You took a chance on me as a student, and I am beyond grateful. I have learned so much professionally and personally from you. Thank you for being there during the highs and lows of my time at Horn Point Laboratory. Your grace and can-do approach to everything really inspired me and pushed me to continue even when things pushed me to the brink. You taught me how to have a true work-life balance, pushing me to take time for myself and take care of myself, especially after my accident. Thank you, Dr. Jeffrey Cornwell, for always being such a calming presence and inspiring me to always look for and ask questions. And thank you Dr. Jacob Cram (and Pongo). You taught me how to program in R, which I still cannot believe I learned how to do. You taught me about DNA, bioinformatics, microbial ecology, and did it with such patience that still astounds me. Not only were you a great teacher, but a truly inspiring mentor and friend.

Thank you to Mike Owens, Dr. Clara Fuchsman, Dr. Louis Plough, and Dr. Greg Silsbe for helping me with areas of my thesis and teaching me field, laboratory, programing, and imagery methods. I would like to express my gratitude to ChatGPT, an AI language model developed by OpenAI, for providing invaluable assistance in refining and clarifying my writing throughout this project.

Thank you to the Susquehanna Flats crew, Catherine Wazniak, Amy Hamilton, Brooke Landry, and Kaitlyn Scowen from Maryland Department of Natural Resources, Dr. Cassie Gurbisz from St. Mary's College of Maryland, and Mike Owens from University of Maryland Center for Environmental Science. I learned so much from everyone in the field and had so much fun with this group.

Thank you to our Research Experience for Undergraduate team members, Dana Sanchez and Ana Vader. It was so much fun working with you both during the summers and sharing many laughs in the lab. Thanks for teaching me and being amazing friends during the harsh summer field and laboratory work. A big thank you to all my friends at Horn Point Laboratory. Your friendship is something I will treasure forever. You all individually made me feel at home at Horn Point and the laughs I shared with everyone is something I will always cherish.

Mom and Dad, thank you for saying "sure, whatever you say" and supported me immediately when I told you I wanted to be a marine biologist when I was 12. Your dedication to my education and your support for my sense of wonder is something I am so thankful for. I would not have been able to achieve this much without you. Sierra, you always challenge my way of thinking and make me laugh. Thank you for being a great sister and always supporting me. Thank you Mommom for nourishing my love for the environment and driving my homework to school when I forgot it. And thank you to my extended family for always being there for me. And finally, thank you to my wonderful boyfriend, Matt. You moved with me so I could pursue my master's, and I am so grateful that I got to pursue it with you (and Kevin and Jax). I would not have been able to do this without your patience, love, and of course, your computer.

This thesis would not have been possible without funding from National Oceanic and Atmospheric Administration Maryland Sea Grant. Thank you for funding my curiosities and work towards my thesis. I am so appreciative of the Horn Point Lab Education Committee, which funded me to finish my thesis work and provide travel grants to learn at other institutions.

Table of Contents

Dedication ii
Acknowledgements iii
Table of Contents v
List of Tables vii
List of Equations viii
List of Figures ix
List of Images x
Chapter 1: Background of the Susquehanna Flats and Emerging Cyanobacteria Harmful Algal Blooms 1
Introduction 1
Background 5
Cyanobacteria 5
Harmful Algal Blooms 6
Cyanobacteria Harmful Algal Blooms 7
Goals and Objectives 13
Chapter 2: Molecular Identification of Filamentous Cyanobacteria at the Susquehanna Flats 16
Abstract 16
Introduction 17
Oscillatoriaceae Taxonomy 17
Background of the 16S rRNA Gene and Pacific Biosciences (PacBio) Sequencing 22
Background of the *nifH* Gene and Illumina MiSeq Paired End (Illumina) Sequencing 23
Methods 25
Field Collections 25
DNA Extraction 27
DNA Sequencing 29
Divisive Amplicon Denoising Algorithm (DADA2) 29
Ecological Analyses 31
Results 32
Cyanobacteria Mat Host Identification 32
Associated Microbial Communities 41
Associated Nitrogen Fixing Microbial Community 47

Discussion 53
Woolly Mat Host- *Microseira wollei* Ecotype 53
Associated Microbial Community of *Microseira wollei* Dominated Mats 56
Mucilaginous Mat Host- *Phormidium* Ecotype 58
Associated Microbial Community of *Phormidium sp.* Dominated Mats 60
Management Implications 62
Chapter 3: *Microseira* (*Lyngbya*) *wollei* Ecophysiology 64
Abstract 64
Introduction 65
Methods 69
Study Site and Sample Collection 69
Nutrient Bioassay Growth Experiment 70
Microseira (*Lyngbya*) *wollei* Nitrogen Fixation Experiments 73
Sediment Nitrogen Fixation Experiments 74
Results 74
Susquehanna Flats Bottom Nutrients and *Microseira wollei* Abundance 74
Nutrient Bioassay Growth Rates 80
Microseira (*Lyngbya*) *wollei* and Sediment Nitrogen Fixation Rates 83
Discussion 88
Overall Conclusions 94
Works Cited 98

List of Tables

Table 2.1 16S rRNA ASV (sASV) table of the top 20 most abundant 16S sASVs found in *Microseira wollei* mats collected from the Susquehanna Flats.

Table 2.2 *nifH* ASV (nASV) table of the top 20 most abundant 16S nASVs found in *Microseira wollei* mats collected from the Susquehanna Flats.

Table 3.1 Nutrient bioassay growth rate experiment.

Table 3.2 NOAA tide levels at Havre de Grace, Maryland.

Table 3.3 Pearson r-values and *p*-values of *Microseira wollei* abundance and NH_4, NO_x, and SRP levels.

Table 3.4 Nitrogen fixation rates (N/g/h) from sediment samples collected in June and July 2022.

Table 3.5 Nitrogen fixation rates (N/g/h) from sediment samples collected in June 2023.

List of Equations

Equation 1: Biological Nitrogen Fixation

Equation 2: Acetylene Reduction Assay

List of Figures

Figure 1.1 the Susquehanna Flats location.

Figure 1.2 Map of *Microseira* (*Lyngbya*) *wollei* blooms in Chesapeake Bay.

Figure 2.1 Percent relative abundance of the 20 most abundant 16S rRNA sASVs.

Figure 2.2 Phylogenetic tree of the 10 most relatively abundant sASVs, their closest sequenced relative in GenBank, and the *M. wollei* clade from the McGregor and Sendall (2015) 16S rRNA phylogenetic tree.

Figure 2.3 Percent relative abundance of the 20 most abundant *nifH* nASVs.

Figure 2.4 Phylogenetic tree of the 20 most relatively abundant nASVs, their closest sequenced relative in GenBank, and the *M. wollei* clade from the McGregor and Sendall (2015) *nifH* phylogenetic tree.

Figure 2.5 Canonical correlation analysis of the microbial communities sequenced by their 16S rRNA genes.

Figure 2.6 Canonical correlation analysis of the microbial communities sequenced by their *nifH* genes.

Figure 2.7 Ratios of the sample's non-host 16S rRNA ASV microbial count to the host microbial count.

Figure 2.8 Scatter plots portraying the ratio of each non-host phylum count to the host phylum count sequenced using 16S rRNA genes.

Figure 2.9 Scatter plots of the 16S rRNA ASV ratio of each non-host genus count to the host genus count within the Cyanobacteria phylum.

Figure 2.10 Scatter plots portraying the *nifH* ASV ratio of each non-host phylum count to the host phylum count.

Figure 2.11 Scatter plots of the *nifH* ASV ratio of each non-host genus count to the host genus count within the Cyanobacteria phylum.

Figure 2.12 Scatter plots of the nASV ratio of each non-host genus count to the host genus count within the Cyanobacteria phylum

Figure 2.13 Scatter plots of the nASV ratio (along a $\log_{10}$ scaled axis) of each non-host genus count to the host genus count within the Pseudomonadota phylum.

Figure 2.14 Scatter plots of the nASV ratio of each non-host genus count to the host genus count within the Thermodesulfobacteriota phylum.

List of Images

Image 1.1 Planet Labs imagery of the Susquehanna Flats.

Image 2.1 Mucilaginous mat at the surface of the water column at the Susquehanna Flats.

Image 3.1 Removal of excess water from *Microseira wollei* samples with use of salad spinner, to establish uniform wet-wet measurements.

Chapter 1: Background of the Susquehanna Flats and Emerging Cyanobacteria Harmful Algal Blooms

Introduction

Susquehanna Flats

The Susquehanna Flats (hereafter referred to as "the Flats") is a shallow shoal on a subaqueous delta below the mouth of the Susquehanna River at the head of the Chesapeake Bay (Figure 1.1). The Susquehanna River is the largest tributary of the Chesapeake Bay, equal in flow volume to all other tributaries combined (Schubel and Pritchard, 1986). It is 16 kilometers downstream of the Conowingo Dam, which makes the Flats an important area of nutrient removal from the ~1,100 $m^3 s^{-1}$ of discharged water into the Chesapeake Bay (Schubel and Pritchard, 1986). The aquatic grasses, or submerged aquatic vegetation (SAV), on the Flats is currently the most extensive and biodiverse in Maryland (CheseapeakeBay.net, 2019).

In 1972, Tropical Storm Agnes caused flooding inundation with large amounts of sediment on the Flats, which caused a major decline in SAV. Low density and population of the SAV continued until the early 2000s (Bayley et al., 1978), until the surrounding water clarity increased possibly due to an extended dry period and long-term reductions in nutrient loading (Orth et al., 2010; Gurbisz and Kemp, 2014). As the SAV grew back, the water became clearer, which in turn allowed the SAV to grow more and increase the water quality. This positive feedback loop resulted in a resilient and biodiverse SAV bed. At its peak in 2008, the SAV bed

covered ~50 km^2 (Figure 1.1), making it the largest SAV bed in the Chesapeake Bay watershed (Environmental Protection Agency, 2016), which can be seen via satellite imagery (Image 1.1).

In 2011, Tropical Storm Lee hit the Chesapeake Bay area, causing major flow and sediment discharge down the Susquehanna River; however, this time, the Flats was relatively stable, with only small reduction and therefore resilient enough to withstand the major flooding event (Gurbisz et al., 2016).

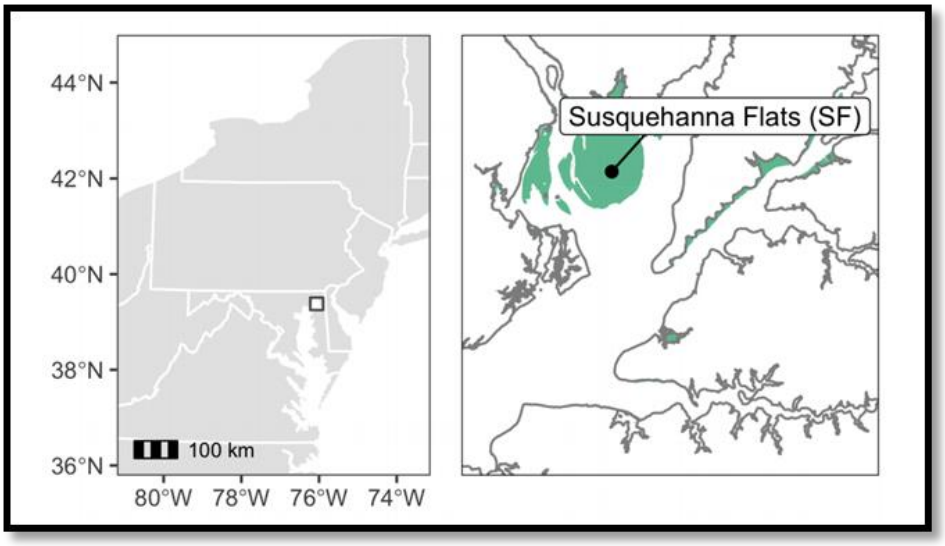

Figure 1.1 the Susquehanna Flats at the fresh headwaters of the Chesapeake Bay at the mouth of the Susquehanna River. (~50 km^2, 1 m average depth). (Figure by Dr. Cassie Gurbisz).

Image 1.1: Planet Labs imagery of the Susquehanna Flats from 17 September 2022. (Image from Planet Labs Imagery, accessed by Dr. Greg Silsbe.

Researchers have documented that SAV beds improve water quality by reducing water column nutrient concentrations (Moore, 2004; McGlathery et al., 2007; Caffrey and Kemp, 1992; Bartoli et al., 2008), decreasing wave energy, and settling suspended particles (Ward et al., 1985; Gambi et al., 1990; Granata et al., 2001; Peterson et al., 2004), and benefiting benthic organisms and shorelines (McDevitt-Irwin et al., 2016; Minello et al., 2003; Lefcheck et al., 2017; Fourqurean et al. 2012, Lefcheck et al. 2019). In conjunction with these positive attributes, SAV beds like those that exist on the Flats are critical to the positive feedback loop and overall health of the Chesapeake Bay (Gurbisz and Kemp, 2014; McGlathery et al., 2007; de Boer, 2007). SAV beds also provide crucial habitat for fish and invertebrates and nurseries for juvenile fish and have been found to increase juvenile density and growth (Lefcheck et al., 2019).

Today, the Flats is home of up to 13 plant species that make it one of the most prolific SAV beds that make up ~8% of SAV in the Chesapeake Bay (Moore et al., 2000; Orth et al., 2010; Patrick and Weller, 2015; Gurbisz et al., 2016). Due to the dense abundance of SAV, the water column at the center of the Susquehanna Flats has low nutrient concentrations during the summer, specifically dissolved inorganic nitrogen (DIN) (Gurbisz et al., 2016; Russ & Palinkas, 2018). Lower turbidity and current velocity was also found towards the center of the SAV bed, which correlates with the higher clarity at the center of the Flats (Gurbisz et al., 2016). The SAV also adds drag on the water column and decreases shear stress on the bottom, which causes suspended particles to sink and diminishes particle resuspension. In turn, the water becomes less turbid, and sunlight can reach the benthos (Luhar et al., 2008; Koch, 2001). Water column Nitrogen to Phosphorus (N:P) ratios at the Flats are lower than the Redfield Ratio during the summer (July-August), which is also when filamentous Cyanobacteria are observed (Gurbisz, 2016).

The unique biogeochemistry and clear, shallow water column at the center of the Flats create an ideal environment for benthic filamentous Cyanobacteria growth, identified as *Microseira* (*Lyngbya*) *wollei*, which was first noted around 2004 (Gurbisz and Kemp, 2014; Gurbisz, 2016). Over the ensuing decade, anecdotal evidence suggested an overall increase in Cyanobacteria on the SAV beds in the Flats. This raised questions about how the overtopping growth of Cyanobacteria might affect the resilience of the recovering SAV beds. This thesis outlines a part of a Maryland Sea Grant funded project to partially address that question. This thesis focuses on two unresolved questions: 1) The molecular identification of the species of Cyanobacteria that are growing on Susquehanna Flats and their associated microbial communities and 2) The ecophysiology of the filamentous Cyanobacteria at the Susquehanna Flats, including

determination of growth rates and nitrogen fixation by the Cyanobacteria mats, and the effect of the addition of nitrogen and phosphorus on those rates.

Background

Cyanobacteria

Cyanobacteria, originating around 2.5 billion years ago, were the first oxygenic phototrophic organisms on Earth. Their development of a system that utilizes both photosystems to extract electrons from water, producing O_2 as a byproduct, was crucial for oxygenating the atmosphere and enabling the expansion of life on Earth (Knoll, 2008). In addition to their historical evolutionary significance, Cyanobacteria play key roles in the carbon and nitrogen cycles as photosynthetic and nitrogen-fixing (N_2-fixing) organisms.

Dinitrogen gas (N_2), which makes up approximately 78% of the atmosphere, is dissolved in seawater. Certain prokaryotes, including some Cyanobacteria, can fix N_2 into ammonia (NH_3), for their own cellular needs, using their nitrogenase enzyme. This process, known as nitrogen fixation, involves breaking the very stable triple bond of N_2 gas, which is energetically costly. However, this ability to utilize nitrogen that is unavailable to eukaryotes and other non-nitrogen fixing organisms is crucial for primary production in nitrogen-limited environments such as lakes and estuaries (Ben-Porath and Zehr, 1994). Thus, Cyanobacteria are essential contributors to the nitrogen cycle by adding "new" biologically available nitrogen in the form of NH_3 into the system (Paerl and Zehr, 2000; Horne & Viner, 1971; Ashton, 1981; Capone, 1983; Howarth et al., 1988). Additionally, Cyanobacteria can uptake and store phosphorus under high-phosphorus

conditions, such as in benthic environments with phosphorus-rich sediments. They can utilize this stored phosphorus when they are in phosphorus-limited conditions, such as the water column surface (Paerl et al., 2001).

These opportunistic adaptations enable Cyanobacteria to bloom in nutrient rich and in low N:P waters (Smith, 1990; Paerl, 1990). This is concerning as some Cyanobacteria are considered harmful. These Cyanobacteria are referred to as harmful "algae" (as they used to be classified as "bluegreen algae") and tend to include the genera *Anabaena, Aphanizomenon, Lyngbya, Microsystis, Nodularia,* and *Oscillatoria*. These Cyanobacteria harmful algal blooms (cHABs) can produce toxins linked to liver disease, cancer, and death (Fogg, 1969; Reynolds and Walsby, 1975; Paerl, 1988; Sellner, 1997; Paerl and Tucker, 1995; Francis, 1878). Additionally, cHABs can cause hypoxia and anoxia of the water column upon the death of the cells and remineralization by heterotrophic bacteria (Negri et al., 2004).

Harmful Algal Blooms

A cHAB is a type of harmful algal bloom (HAB) that is caused by Cyanobacteria instead of eukaryotic phytoplankton. Understanding characteristics and environmental and nutrient requirements of HABs is essential for helping determine causes of cHABs and potential mitigation strategies. Eukaryotic phytoplankton blooms are considered HABs when they are either “toxic”, “noxious”, or simply a “nuisance” to the ecosystem (Hallegraef, 1993).

HABs can cause hypoxia or anoxia of a water column due to respiration by heterotrophic bacteria as they break down dead or decaying biomass (Graneli et al., 1989; Mahoney and Steimle, 1979), harm filter feeders, and/or produce toxins that can cause massive fish die-offs, and shellfish poisoning in humans (Hallegraeff, 1993). HABs have also caused more economic loss in recent decades due to their increase in frequency and intensity (Chorus and Bartram, 1999; Carmichael, 2001; Carmichael, 2008; Hudnell, 2008; Heisler et al., 2008; Hoagland et al., 2002; Paerl, 2008; Paul, 2008; Paerl and Huisman, 2008; O'Neil et al., 2012) as HABs have been found to thrive with warmer temperatures, and eutrophication, which have been increasing with global climate change. (Paul, 2008; Paerl and Huisman, 2009; Glibert, 2020).

Cyanobacteria Harmful Algal Blooms

A cHAB is a type of HAB but unlike typical HABs caused by eukaryotic algae, cHABs are formed by prokaryotic Cyanobacteria. cHABs thrive in nutrient rich waters with high levels of nitrogen and phosphorus, often caused by runoff from agricultural fields and impervious surfaces, wastewater discharge, and other anthropogenic activities. However, they can occur in oligotrophic systems when under favorable conditions such as warm water temperatures, high light availability, and stable water columns (O'Neil et al., 2012; Fogg, 1969; Reynolds and Walsby, 1975; Paerl 1988; Shapiro, 1990). This is largely due to their nitrogen fixing capabilities.

As cHABs are a type of HAB, they can be detrimental to the environment, wildlife, and human health. Overgrowth of a cHABs can create dense mats on the water surface, blocking sunlight from reaching the submerged aquatic vegetation (SAV) and other benthic organisms.

Additionally, cHABs can cause hypoxia and anoxia of the water column when they die and decompose, leading to fish and benthic fauna mortalities (Paerl & Tucker, 1995; Boyd et al., 1978. Also, cHABs may produce toxins, termed cyanotoxins, such as microcystins, anatoxins, and saxitoxins, which can cause significant fish die-offs and damage fisheries and aquaculture. These toxins pose serious health risks to animals and humans through direct contact or consumption of contaminated drinking water or food (Francis, 1878; Codd & Bell, 1996; Carmichael, 1997). These health risks can include damage to the nervous system, dermatitis, liver disease, cancers, and death (Carmichael, 2001; Carmichael, 1998; Paerl et al., 2001; Brooks et al., 2017; Kirpenko et al., 1981; Fujiki et al., 1984).

Researchers have linked global climate change and increasing human population and activity to an increase in cHAB frequency and intensity (Paul, 2008, O'Neil et al., 2012; Paerl and Huisman, 2009). Freshwater eukaryotic phytoplankton growth rates tend to plateau or decline as water temperatures exceed 20°C. In contrast, Cyanobacteria thrive at temperatures above 30°C (Briand et al. 2004), positioning them to benefit from the warming trends associated with global climate change (Canale and Vogel, 1974; Peperzak, 2003; Paerl and Huisman, 2009).

As waters warm, stratification of the water column intensifies, which will ultimately reduce nutrient availability in surface waters. Since Cyanobacteria are diazotrophic, they can reduce atmospheric N_2 to NH_3 in low nitrogen waters. They can also control their own buoyancy allowing them to sink to nutrient rich bottom waters and rise for direct sunlight for photosynthesis. Consequently, Cyanobacteria can outcompete eukaryotic phytoplankton in

waters with a nitrogen limited water, as long as they have access to available phosphorus. (Smith, 1990; Paerl, 1990).

Excess nitrogen and phosphorus levels have also often driven cHABs in warm, stratified fresh waters. Additionally, eutrophication has caused an increase in HAB and cHAB frequency and intensity (Paerl and Huisman, 2008; Paerl and Huisman, 2009; Paerl and Paul, 2012; O'Neil et al., 2012). Scientists believe that phosphorus-driven eutrophication is the primary nutrient factor for Cyanobacteria blooms, specifically nitrogen-fixing Cyanobacteria, in nitrogen-limited coastal and estuarine waters. If nitrogen levels increase in estuaries and coastal waters with high phosphorus levels or sediment rich in legacy phosphorus, it can create hotspots for cHABs (Putnam et al., 2022; Paerl, 2008; Paerl et al., 2001). One area in the Chesapeake Bay that is particularly vulnerable to a benthic cHAB is the Susquehanna Flats. With high phosphorus content in the sediment, clear water, and low nitrogen levels at the center of this SAV bed, benthic Cyanobacteria are able to outcompete eukaryotic phytoplankton and bloom seasonally (Gurbisz, 2016).

Microseira (*Lyngbya*) *wollei* Presence

Filamentous Cyanobacteria have increased in prevalence and intensity in the Chesapeake Bay (Figure 1.2). Researchers first noted the presence of a benthic, filamentous Cyanobacteria in the SAV bed of the Susquehanna Flats around 2004, and it has bloomed seasonally since (Batiuk et al., 2023). Through microscopic observation, researchers identified the filamentous Cyanobacteria as *Microseira* (*Lyngbya*) *wollei* (Farlow ex Gomont) based on the description by Speziale and Dyck (1992). However, McGregor and Sendall (2015) recently reclassified *Lyngbya wollei* to *Microseira wollei*. Thus, this paper will refer to it as *Microseira wollei* (*M. wollei*).

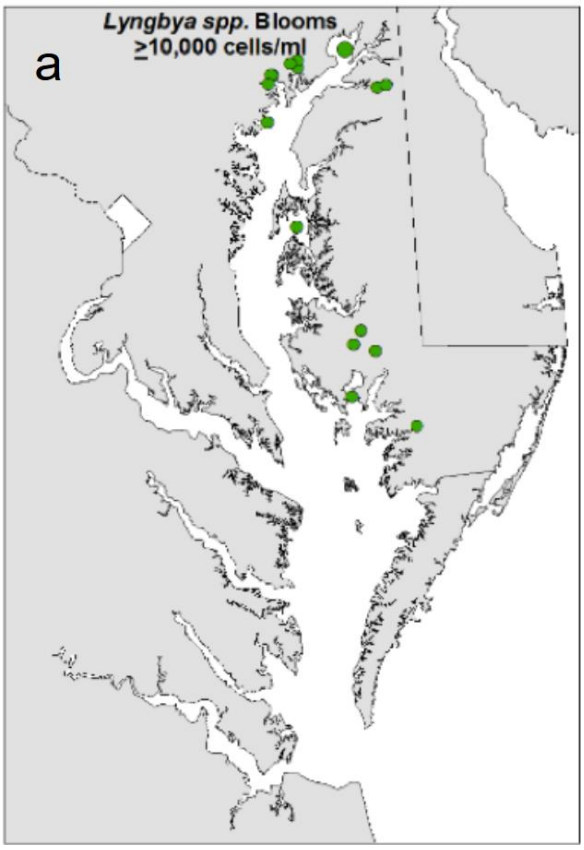

Figure 1.2 Map of *Microseira* (*Lyngbya) wollei* blooms in Chesapeake Bay based on monitoring data from Maryland Department of Natural Resources (MD DNR) and Old Dominion University (2000-2014). Blooms are defined as having more than 1,000 cells/ml or visible mats. Map created by MD DNR (https://dnr.maryland.gov/waters/bay/Pages/algal_blooms/Lyngyba-Distribution.aspx).

Microseira wollei is fresh water filamentous benthic Cyanobacteria (Phlips et al., 1992). Due to its nitrogen fixing capabilities, *M. wollei* can not only thrive in eutrophic conditions, but also in nitrogen limited conditions, such as the Susquehanna Flats, where they can out-compete the eukaryotic phytoplankton. Nitrogen limited conditions can occur after intense phytoplankton growth and decomposition and/or where lush SAV sequesters nitrogen in the water column (Gao et al., 2014a; Gao et al., 2014b; Risgaard-Petersen and Ottosen, 2000; Gurbisz, 2016). Although *M. wollei* nitrogen fixation can be phosphorus and iron limited, the phosphorus and iron rich sediment and fluxes from the benthos of the Flats provides those limiting nutrients to promote *M. wollei* growth (Watkinson et al., 2005; Ahern et al., 2006; Gurbisz, 2016). As the Flats are also shallow with higher wave attenuation and warmer water temperatures (>20 °C), the *M. wollei* has access to ample sunlight and ideal water temperatures for growth (O'Neil et al., 2012; Paerl, 2008).

Ample sunlight in the clear water column that exists in the center of the SAV beds on the Flats, allows the *M. wollei* to grow from the benthos (Luhar et al., 2008; Gurbisz, 2016). Eventually, growth creates "self-shading" of the Cyanobacteria that begins to block sunlight from forming new *M. wollei* growth, and they can potentially grow up over SAV blades. Additionally, gas bubbles from photosynthesis can get trapped in the *M. wollei* filaments and allows portions of the benthic mats to detach and float to the surface of the water column and form dense tangled surface mats, which can also act as a dispersal mechanism to other areas (Albert et al., 2005). These biphasic mats can be malodorous, unsightly, and can potentially blanket the SAV, which can block sunlight and possibly smother them (Speziale and Dyck, 1992; Carmichael et al., 1997; Yin et al., 1997; Butler et al., 2023). Consequently, this can decrease new SAV growth that

requires higher light availability than established SAV (Gurbisz and Kemp, 2014). This ultimately will decrease SAV biomass and co-organism diversity (Tiling and Proffit, 2017).

Microseira wollei and other benthic Cyanobacteria can also alter its surrounding environment in many ways. *Microseira wollei* can cause anoxic conditions by forming dense mats at the benthos, which can then subsequently cause the release of phosphate and iron into the water column (Harrington et al., 2016), which can promote their own growth. Although *M. wollei* can fix nitrogen and alter nutrient conditions, there have not been any studies to measure how much nitrogen the *M. wollei* at the Flats actually fixes. As a result, there is a lack of understanding of its impact on the nutrient conditions at the Flats. This information is crucial to determine in this unique submerged SAV bed that is vital to the health of the Chesapeake Bay. It is also important information for systems beyond the Chesapeake Bay, which may also suffer from excessive nitrogen levels and eutrophic conditions which are increasing globally.

Like other cHABs, researchers have found *M. wollei* to produce cyanotoxins (McGregor and Sendall, 2015), such as a type of neurotoxin, known as saxitoxins, in bodies of freshwater in Alabama, South Carolina, Florida, and other southeastern areas, as well as Canada (Yin et al., 1997, Carmichael et al., 1997, Putnam et al., 2022, Foss et al., 2012, Poirier-Larabie, 2020; Smith et al., 2019; Onodera et al., 1997). They have also found them to harbor harmful bacteria and pathogens (Vijayavel et al., 2013).

Although researchers morphologically identified the filamentous Cyanobacteria on the Flats as *M. wollei*, molecular identification was required to confirm its identity. Historically, researchers identified organisms in the Oscillatoriaceae family only morphologically and/or ecologically (cf. Geitler, 1932; Elenkin, 1938; Starmach, 1966; Wehr et al., 2015; Komárek, 2018a). However, this method can be unreliable because members of this family have very few distinguishing morphological features and often look similar or even identical to one another. This has historically led to frequent misidentification, confusion, and inaccurate taxonomy records. With the advent of molecular tools, the Oscillatoreaceae family is undergoing significant taxonomic revisions (McGregor and Sendall, 2015; Casamatta et al., 2005; Engene et al., 2011; Engene et al., 2012; McAllister et al., 2016). Therefore, molecular identification was employed in this study to correctly identify the filamentous Cyanobacteria with the most up-to-date technology and identification methods.

Goals and Objectives

To better understand the causes and effects of *M. wollei* at the Flats and their potential impact on SAV growth, a three-pronged approach was undertaken in this study, which included field surveys and laboratory experiments to provide information for subsequent ecosystem modelling efforts. This thesis will explore the first two approaches involving field and lab approaches. The laboratory experiments encompassed DNA analysis of the Cyanobacteria mats to investigate the host Cyanobacteria and their associated microbial communities as well as ecophysiology experiments. Water quality parameters were also assessed at the Flats, including nutrient (NO_3^-, NH_4^+, PO_4^{3-}) levels to investigate what roles they may have in promoting *M. wollei* proliferation. The 2022 and 2023 field surveys explored in this paper include measurements of water column

nutrient levels and *M. wollei* abundance. Nutrient bioassay experiments were also conducted to investigate whether nitrogen or phosphorus was the limiting nutrient for the growth of *M. wollei*, as well as to determine nitrogen fixation rates under different nutrient conditions.

In chapter 2, the molecular identification and the associated microbial communities of the Cyanobacteria at the Flats will be discussed. DNA sequencing of the 16S rRNA and *nifH* genes were performed on samples from filamentous Cyanobacteria mats, hypothesized to be *M. wollei*, and a cyanobacterium observed during the 2022 field season, hypothesized to be *Oscillatoria sp.*, at the Flats. The 16S rRNA sequences were used to molecularly identify the morphologically identified *M. wollei* and *Oscillatoria spp.* and their microbiomes. The *nifH* genes were sequenced to investigate the potential diazotrophic microbial communities within the Cyanobacteria mats. The Silva 132 (Quast et al., 2013) training tool assigned the samples taxonomically and the Amplicon Sequence Variant (ASV) was used to document genera and/or species in the National Center for Biotechnology Information (NCBI) GenBank using the Basic Local Alignment Search Tool (BLAST).

Nutrient bioassays growth rates and nitrogen fixation rates will be discussed in chapter 3. To determine the *M. wollei* nutrient limitations, nutrient bioassay experiments were performed on samples in triplicates, with three control samples, three samples that received daily nitrate treatments, three that received daily phosphate treatments, three that received daily nitrate and phosphate treatments, and three that received daily ammonium treatments. Nitrogen fixation experiments using the acetylene reduction assay were performed on *M. wollei* samples taken

directly from the nutrient bioassay samples to investigate nitrogen fixation rates under different nutrient conditions.

Through these experiments, a better understanding of the ecophysiology of the cyanobacterium *M. wollei* at the Susquehanna Flats was gained. By using this information in future ecosystem models and understanding its characteristics and conditions that favor *M. wollei* blooms, management programs may be able to potentially predict and manage *M. wollei* blooms and health officials can warn the general public to mitigate exposure to harmful toxins. Identifying its nitrogen fixation abilities under various nutrient conditions will help predict its behavior in specific environmental nutrient scenarios. Understanding its nitrogen fixation capabilities is essential for improving nutrient modelling in the already nutrient-rich Chesapeake Bay and as global temperatures rise, *M. wollei* may increase in frequency and intensity so understanding their nutrient limitations can help develop adaptive strategies and mitigate their impact in a changing climate. Additionally, other emerging Cyanobacteria were also identified on the Flats, along with their associated microbial microbiomes, which underscores the complexity and diversity of the system, that deserves further investigation and elucidation.

Chapter 2: Molecular Identification of Filamentous Cyanobacteria at the Susquehanna Flats

Abstract

The Susquehanna Flats harbors a biodiverse and resilient submerged aquatic vegetation (SAV) bed just below the mouth of the Susquehanna River in the upper Chesapeake Bay. Therefore, the health of the Flats SAV remove nutrients and therefore protect the health of Chesapeake Bay. Nitrogen fixing and toxin producing filamentous Cyanobacteria have seasonally bloomed at the Susquehanna Flats. These include a Cyanobacterial mat with a woolly consistency, first observed in 2004, and a mat with a mucilaginous consistency, first observed in 2022. Morphological assessments suggested that the woolly mat was *Microseira* (*Lyngbya*) *wollei* while the mucilaginous one was *Oscillatoria sp.* However, species within the Oscillatoriaceae family, including both *Microseira* (*Lyngbya*) *wollei* and *Oscillatoria sp*., are difficult to morphologically identify because different species level groups are morphologically difficult or impossible to distinguish. Properly identifying Oscillatoriaceae mats is important because different species can produce different toxins. Additionally, new DNA sequencing technology provides tools to better identify these organisms, as well as their associated microbiota. However, such identification had not been done previously in the flats. Therefore, the filamentous Cyanobacteria at the Susquehanna Flats were identified using high-throughput sequencing of the full length of the 16S rRNA gene and *nifH* genes associated with the mucilaginous and woolly mats. The microbial diversity of the bacteria associated with the filamentous Cyanobacteria mats was also investigated. The woolly mat was shown to be a novel ecotype of *Microseira* (*Lyngbya*) *wollei*, and the mucilaginous mat was shown to be a novel species level group of from the genus

Phormidium, whose closest known relative produces the toxin microcystin. The *Microseira* (*Lyngbya*) *wollei* mats and *Phormidium sp*. mats also contain a diverse assemblage of bacteria, including other nitrogen fixing Cyanobacteria. The data from this study provide a better taxonomic understanding of the Cyanobacterial mats and suggest that future management efforts should consider that both are likely toxin producing. Furthermore, it suggests that much of the biogeochemical influence of the mats on the surrounding environment could be modified by their microbiota whose role should be further explored.

Introduction

Filamentous Cyanobacteria was first observed at the Susquehanna Flats in 2004. Experts morphologically identified it as *Microseira wollei* (*M. wollei*). In 2022, experts from University of Maryland Center for Environmental Science, St. Mary's College of Maryland, and Maryland Department of Natural Resources first observed another filamentous Cyanobacteria at the Susquehanna Flats and morphologically identified it as Oscillatoria sp. *Microseira wollei* and *Oscillatoria sp.* both belong to the Oscillatoriaceae family. Species in the Oscillatoriaceae family are notoriously difficult to differentiate morphologically because they often look similar and sometimes identical. Therefore, advanced molecular identification was required to accurately identify the filamentous Cyanobacteria at the Susquehanna Flats.

Oscillatoriaceae Taxonomy

Microseira (*Lyngbya*) *wollei* is a member of the Oscillatoriaceae family of Cyanobacteria only recently classified into the *Microseira* clade. Along with other filamentous Cyanobacteria in the

Oscillatoriaceae family *M. wollei* and other members of this family, historically been phylogenetically identified using morphological and environmental characteristics (Farlow ex Gomont; Wolle, 1887; Speziale and Dyck, 1992; Ben-Porath and Zehr, 1994; McGregor & Sendall, 2015). However, morphology and habitat are ambiguous measurements, as many Oscillatoriaceae are morphologically similar. This ambiguity has led to inaccuracies and frequent revisions of the family Oscillatoriaceae, including different *M. wollei* populations (Speziale and Dyck, 1992; McGregor and Sendall, 2015). Misidentification can be problematic as many Oscillatoriaceae are toxic. However, different species produce different toxins. Thus, accurate species identification is crucial to ensure that managers can adapt best management practices for harmful Oscillatoriaceae mats when they appear in their particular regions. Fortunately, as new DNA sequencing technologies have become more readily available, the identification and taxonomy of Oscillatoriaceae has become more refined and organized (McGregor and Sendall, 2015).

Due to its morphological ambiguity*, M. wollei* has been reclassified several times and has historically been published as six different species in three genera (Speziale & Dyck 1992). In the 1870s and 1880s, *M. wollei* was identified as either *Plectonema wollei* (*P. wollei*) or *Lyngbya wollei* (*L. wollei*). Farlow (1877) originally published the species collected from Woburn, Massachusetts as *P. wollei*. Wolle (1887) identified a filamentous Cyanobacteria collected in New Jersey as *L. wollei*. While Farlow and Wolle soon agreed that both Cyanobacteria were the same organism, many publications continued to use *L. wollei* in publications until Farlow ex Gomont (1892) published that it should be identified as *P. wollei*.

In 1987, Silva et al. (1987) concluded that *L. wollei* was the correct identification due to the false branching that was first characterized by Wolle in 1887. This identification also resolved many identification conflicts and encompassed species that were previously improperly identified as other *Lyngbya spp.* (Speziale and Dyck, 1992). By sequencing the 16S rRNA gene from a population in Australia, McGregor and Sendall (2015) determined that what was historically thought of as *Lyngbya wollei* belongs in an entirely different genus. They determined that the *Lyngbya wollei* clade is evolutionarily distinct and genetically dissimilar from other *Lyngbya* and should be considered under a separate taxon within Oscillatoriaceae and was officially reclassified as *Microseira. wollei* (McGregor and Sendall, 2015).

Given that *Microseria* and *Lyngbya* have morphological similarities, the hypothesis that the prominent filamentous Cyanobacteria present at the Susquehanna Flats was *M. wollei* was tested in two summer field seasons in 2022 and 2023. Although the filamentous Cyanobacteria morphologically presented as *M. wollei*, due to the overhaul of Oscillatoriaceae species using molecular techniques, and availability of DNA sequencing technologies, identifying it as *M. wollei* using only morphological characteristics would have been unreliable. Therefore, advanced molecular methods were used to confirm the taxonomic identity of the Oscillatoriaceae mat. For clarification purposes, the mat that was hypothesized to be dominated by *M. wollei* will be referred to here as the "woolly mat" as it was uncertain what species was until the DNA results were obtained.

Filamentous algal mats can provide a substrate for attachment of bacteria and can provide protection against sunlight radiation and predation for the associated microbes (Byappanahalli et al., 2003; Chilton et al., 1986; Marks and Power, 2001; Rex et al., 1982; Taft, 1975). Mats of *M. wollei* have been found to act as a secondary host to fecal indicator bacteria (FIB), including *Escherichia coli* (*E. coli*), Enterococci, and *Clostrodium perfringens* (Vijayavel, 2013). However, besides these findings made by Vijayavel (2013), there is a lack of information on the *M. wollei* microbiome overall. The strongest method to investigate the *M. wollei* associated microbial community was through advanced molecular techniques.

Generally, the predominant Cyanobacteria observed on the Susquehanna Flats since its first sightings in the 2000s has been *M. wollei.* However, during this project, a second predominant Cyanobacteria mat was observed at the Flats. It was a bright green, mucilaginous, non-integrous mat at the benthos and surface of the Flats. This sample was morphologically identified as *Oscillatoria sp.*, but since this cyanobacterium had not been recorded prior to this observation, it was collected for sequencing as well. This mat will subsequently be referred to as the "mucilaginous mat" in reference to its morphology. (Image 2.1).

Thus, morphological assessments have been used to hypothesize taxonomy in the Flats: *M. wollei* and *Oscillatoria sp*. The *M. wollei* was morphologically identified, and *M. wollei* is a part of Oscillatoraceae is only a family level pattern. However, in other environmental systems, members of Oscillatoriaceae have been identified using molecular approaches (Joyner, 2007; Joyner et al., 2008; McGregor and Sendall, 2015; Engene et al., 2018). Furthermore, microbial

communities have been shown to affect the biogeochemistry of many Cyanobacterial mats (Grim et al., 2021; Brasell et al., 2015). However, molecular approaches have not previously been employed to identify either Cyanobacterial mat morphotype in the Chesapeake Bay. Furthermore, the microbial community has not previously been established for *M. wollei* in the Bay or elsewhere or for the mucilaginous mats. Therefore, high throughput sequencing of the 16S rRNA genes and *nifH* genes were carried out in order to identify the mats and their associated microbial community structure. The 16S rRNA genes would provide high resolution taxonomic information about all species while the *nifH* genes in particular would provide more information about the genotypes of the mat communities as well as their associated diazotrophs.

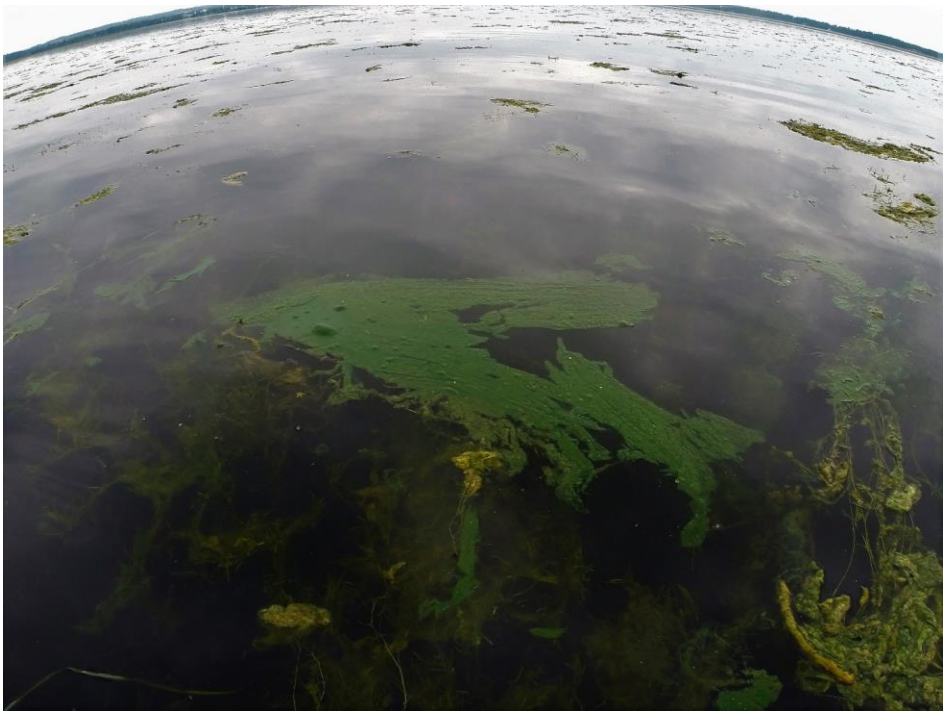

Image 2.1 Mucilaginous mat at the surface of the water column at the Susquehanna Flats. Photo taken by Maryland Department of Natural Resources (2022).

Background of the 16S rRNA Gene and Pacific Biosciences (PacBio) Sequencing

The 16S rRNA gene is universal to all bacteria (Woese et al., 1985; Woese, 1987) and widely used as a taxonomic barcode (Fox et al., 1980; Chaban and Hill, 2012; Woese and Fox, 1977; Woese et al., 1985). It is effective as a barcode gene due to its fragments ranging between totally conserved and variable, which allow researchers to link bacteria to distantly related and closely related ancestors (Baker et al., 2003). The 16S rRNA gene is ~1500 base pairs long (Clarridge, 2004). Since it is longer, the third generation Pacific Biological Sequencing (PacBio) was chosen to sequence the 16S rRNA gene as it can produce reads of upwards of 10 kb (Pacific Biosciences, 2023). Also, PacBio sequencing and bioinformatic programs can identify organisms to a species level and render an understanding of its microbial community structure (Callahan et al., 2019).

Because third generation long-read sequencing is pioneered by Pacific Biosciences (PacBio), and because the sequencer used was sold by PacBio, this paper will refer to it as PacBio sequencing (Rhoads and Au, 2015). Third generation long-read sequencing is the latest DNA sequencing technology. Although next-generation, or short-read sequencing, is highly accurate with low error rates, third-generation sequencing, distributed through PacBio, can produce much longer read lengths of upwards of 10 kb at a faster rate than the second-generation methods (Pacific Biosciences, 2023).

PacBio sequencing historically produced reads that had more errors than Next-generation sequencing (NGS) techniques, but the error rates have decreased with technological advances in

the molecular methodology and software analysis (Hu et al., 2021). PacBio sequences may still output reads with higher error rates than NGS. However, molecular and bioinformatic technology advances are able to correct the sequencing errors for higher accuracy.

The bioinformatics tool, DADA2, was used to learn and account for errors in the sequences. The DADA2 algorithm is able to learn error rates and accurately identify sequences of the original community even in the presence of errors in the sequences data (Callahan et al., 2019). Improved circular consensus sequencing and high-fidelity reads allows for highly accurate reads by repeatedly sequencing the same DNA molecule and then creating a consensus sequence from the multiple passes (Hon et al., 2020). This technique and the error-identifying program, DADA2, produce results that are reliable for analysis of long reads. Therefore, PacBio was used to sequence the long and complex 16S rRNA genes, and DADA2 corrected the errors in each sequence.

Background of the *nifH* Gene and Illumina MiSeq Paired End (Illumina) Sequencing

Nitrogen fixing Cyanobacteria, also known as diazotrophs, tend to coexist with each other (Ben-Porath & Zehr, 1994; McGregor & Sendall, 2015). Since *M. wollei* is a diazotroph and has been observed to entangle sediment, plant matter, and other Cyanobacteria in its mats, it was hypothesized that these mats harbor a complex and diverse microbial community. To specifically observe the diazotrophic bacteria, the *nifH* genes (which encode for the enzyme nitrogenase, responsible for the nitrogen fixation reaction), from the mat samples were sequenced.

The *nifH* genes from each sample were sequenced to molecularly identify the host Oscillatoriaceae organism and thoroughly investigate the complexity of the nitrogen fixing microbial community and identify the present diazotrophic microbes. The *nifH* gene was sequenced as it is the iron containing protein within nitrogenase, which is the enzyme that reduces N_2 to ammonium. Nitrogen fixing Cyanobacteria contain nitrogenase enzymes, which allows them to convert N_2 to NH_3 (Paerl and Zehr, 2000; Rascio and La Rocca, 2013). The *nifH* gene is highly conserved among bacteria, yet it exhibits sufficient variation to allow for the identification of unique *nifH* sequences from different bacterial species (Zehr, 1992; Zehr & McReynolds, 1989). This allows for a consistent and efficient way to study the nitrogen-fixing organisms in a diverse microbial community (Zehr, 1992; Zehr and McReynolds, 1989; Ben-Porath and Zehr; 1994).

As *nifH* sequences are shorter than 16S rRNA gene sequences, long read sequencing was not required and the less expensive higher depth of sequencing, Illumina MiSeq was used to capture the diversity of diazotrophic bacteria in the mats. Illumina sequencing is a short-read next generation sequencing approach that can capture around 250 base pairs in two directions for a total sequence length of up to around 500 bases technology, which succeeded the first-generation Sanger sequencing (Hu et al., 2021). The *nifH* gene is 886 base pairs long, so MiSeq sequencing can read the whole gene with some overlap. The Illumina technology performed paired-end sequencing and read each of part of the DNA fragment multiple times, which allowed for high-quality and accurate sequencing. Therefore, Illumina sequencing was used to sequence the short and highly conserved *nifH* genes (Hu et al., 2021; Tucker et al., 2009).

Associated Microbial Communities

The hypothesis proposed that the filamentous and mucilaginous mats harbored distinct yet diverse microbial communities, with microbial biodiversity varying by site. It was also anticipated that the microbial communities in rinsed and unrinsed filamentous samples would differ, with rinsed samples showing lower species relative abundance and, consequently, reduced biodiversity. This reduction in diversity was expected to result from the removal of sediment-associated microbes during rinsing, leading to lower microbe-to-host gene ratios. Additionally, it was hypothesized that the mucilaginous mat would exhibit less biodiversity than the filamentous mats due to its apparent lack of associated sediment and microenvironments. In contrast, the filamentous mats, which visibly trapped sediment particles and supported more fauna and microscale heterogeneity, were expected to demonstrate higher microbial diversity.

Methods

Field Collections

Samples were hand collected by snorkeling using gloves, so as to not contaminate the samples. Samples were taken on 6 -7 August 2023. This month showed the highest range of both woolly and mucilaginous mats relative to other months (June-July 2023) when the mat was observed. Samples of the woolly mats, which were previously morphologically identified as *M. wollei,* were collected from multiple sites at the Susquehanna Flats. The woolly mats had Cyanobacterial filaments with strong integrity that were observed on the benthos, growing on SAV and floating at the surface. Samples were also collected from the more recently observed mucilaginous Cyanobacterial mat, which was morphologically identified as *Oscillatoria sp*. The mucilaginous

mats were observed to have very little integrity with a mucilaginous characteristic, that broke apart very easily.

Two samples from each site with woolly mats were collected and separated between “rinsed” and “unrinsed” samples to detect whether sediment within the mat shaped the microbial community. The “rinsed” samples were rinsed as thoroughly as possible in the Susquehanna Flats water on site before placing in the preservative. The “unrinsed” samples were placed directly in the preservative in the field. Samples were collected from sites 17, 20, 23, and 25 (Figure 3.1), which were labeled 17C, 20C, 23C, and 25C for the “rinsed” (or "cleaned") samples and 17D, 20D, 23D, and 25D for the “unrinsed” (or "dirty") samples. Single samples of the mucilaginous mats were only collected from sites 12 and 17, which are labeled 12.Phm and 17.Phm respectively. The mucilaginous mats did not appear to be loaded with sediment so only unrinsed samples were collected.

Samples placed directly into a sterile test tube with 400 µL of Zymo DNA/RNA shield a preservative and nucleic acid stabilization solution that can preserve most DNA samples at room temperature (Trivedi et al., 2022). Sample temperature was maintained at seawater at ambient temperature in transit, and then placed into liquid nitrogen upon return to the field lab. Once back at Horn Point Laboratory, samples were stored in a -80°C freezer until they were processed for DNA extraction.

DNA Extraction

DNA was extracted from each sample over the course of a three-day period using an in-house phenol chloroform-based protocol. The protocol was modified from several previous protocols (Renshaw et al., 2015; Plough, 2018; Cram et al., 2024; Fowler et al., 2024). Before extraction began, forceps, and pestles were sterilized in 70% ethanol and placed in a Stratagene stratalinker 1800 Crosslinker, which emits 1800 lumens of UV light per minute in order to kill bacteria and crosslink DNA, for 10 minutes.

To lyse the cells and free the DNA in suspension, a small amount (about 100 µL, estimated by eye) of each sample was transferred to their respective 2 mL tubes. Leftover preservative was removed with a pipette, which made breaking down the sample easier. The tubes were then frozen using liquid nitrogen for 30 seconds or placed in the -80°C freezer for 10 minutes. Each frozen sample was ground with a Kimble Pellet pestle and 900 µL of Cetyltrimethylammonium bromide buffer (CTAB) and 10 µL of beta-mercaptoethanol added to each tube. Samples were vortexed for 5 seconds and placed in a bead-beater for 30 seconds. Samples were then incubated at 65°C for 20 minutes and vortexed for 3 seconds every five minutes.

To clean the DNA, 400 µL of phenol-chloroform-isoamyl alcohol (25:24:1 ratio) solution was added to each sample and inverted five times. A Sorvall Legend T Benchtop centrifuge was then used to spin the samples for two minutes at 15,000 G. The bottom phenol layer was discarded, and the process repeated with a phenol-chloroform wash. After discarding the subsequent bottom layer, 400 µL of chloroform-isoamyl alcohol solution (24:1 ratio) was added to each sample and

inverted five times. The samples were then spun in the centrifuge at 15,000 G for 3 minutes and the DNA top layer was transferred to a new 2 mL tube, leaving the interface behind. Ammonium acetate (10M) was added at 0.31 times the volume of the lysate as well as adding ethanol at 3.05 times the volume of the lysate and inverted five times. Finally, the samples were incubated in a 20°C freezer overnight to allow the DNA to precipitate.

After 16 hours in the freezer, the samples were spun at 15,000g at 4°C for 90 minutes centrifuge. The supernatant was gently poured out to reveal a pellet of DNA. Subsequently, 250 µL of cold 70% ethanol was added to each pellet and spun again at 15,000g in 4°C for 30 minutes after which the ethanol was poured out and the pellet was dried by hanging the tubes inverted in the hood. Once the tubes were completely dry the DNA pellet was resuspended in 25 µL of tellurium and incubated at 37°C for 90 minutes.

The DNA of each sample was quantified using an Invitrogen Qubit 4 Fluorometer Pub. No. MAN0017210 and using its procedure (Thermo Fisher Scientific, 2017) and samples were diluted to a common concentration of 10 ng/µl. Diluted samples were shipped to Molecular Research Laboratories. A Mock sample (bei Resources HM-782 Microbial Mock Community B) and two control samples were included for sequencing to check for accuracy and any sample contamination.

DNA Sequencing

Molecular Research Laboratories performed amplicon sequencing on the quantified DNA. Molecular Research Laboratories completed at least 10,000 reads per assay for the long read PacBio sequencing on the 16S rRNA gene and 20,000 reads per assay for the short-read Illumina sequencing on the *nifH* gene.

The specific primers chosen to amplify the 16S rRNA gene using long read PacBio sequencing (27F: AGRGTTYGATYMTGGCTCAG and 1492R: RGYTACCTTGTTACGACTT) cover most of the 16S rRNA gene and (Callahan et al., 2019) and amplify most bacteria including the family Oscillatoracaea which encompasses *Microseira* and its relatives (Klindworth et al., 2013). The primers used to amplify the *nifH* gene using short-read Illumina sequencing (primers *nifH*19F: GCIWTITAYGGNAARGGNGG and *nifH* -univ-463R: GCRTAIABNGCCATCATYTC) where chosen because they amplify most of the *nifH* genes in aquatic and marine environments (Gaby and Buckley, 2012).

Divisive Amplicon Denoising Algorithm (DADA2)

Molecular Research Laboratories returned demultiplexed FASTQ files which were filtered and organized using the FASTQ files using a custom DADA2 pipeline, modified from Lee (2019) and Callahan et al. (2016), described below. First, the forward and reverse complement of the reverse primer from each sequence was removed using "Cutadapt" (Martin, 2010). By removing these primers, the resulting data was more accurate for downstream analyses, such as alignment

and phylogenetic tree construction. This process was also performed on the reverse reads for the *nifH* sequences.

The DADA2 program pipeline first de-noised the *nifH* fastq files then merged the forward and reverse (paired-end) readings to ensure higher quality reads. The DADA2 program was used to first de-noise the *nifH* fastq files then merged the forward and reverse (paired-end) readings to ensure higher quality reads. The DADA2 pipeline then removed chimeras and collected sample sequences (Callahan et al., 2016). As the 16SrRNA sequences did not contain both forward and reverse reads, the paired-end DADA2 protocol for the 16S rRNA sequences were altered to disallow inclusion of a merge read function, which usually merges forward and reverse reads. The altered protocol also increased the truncating length as the 16S rRNA sequences were longer than the nifH sequences (Callahan et al., 2016).

Once DADA2 corrected errors and removed chimaeras, the sequences were available in a comma separated table. Naïve baysean classification, using the Silva 132 database (Quast, 2013) assigned the 16S rRNA taxonomy. The *nifH* v2.0.5 database was used to assign *nifH* taxonomy (Moynihan, 2020). The most abundant 16S rRNA and *nifH* sequences were entered into the National Center for Biotechnology Information (NCBI) Basic Local Alignment Search Tool (BLAST) to match to any registered sequences in the GenBank database. The searches did not include any uncultured/environmental sample sequences. The top match was used to identify the closest known relative of each 16S Amplicon Sequence Variant (sASV) and *nifH* Amplicon Sequence Variant (nASV).

Phylogenetic Trees

Two phylogenetic trees were constructed, one each for the sASVs and nASVs. Each set of ASVs were treed along with each ASV's closest sequenced relative in GenBank, as well as all of the 16S rRNA and *nifH* sequences, as appropriate, from McGregor and Sendall's (2015). The sequence alignment was performed using the MUSCLE algorithm, which accurately handles multiple sequence alignments (Edgar, 2004). Phylogenetic trees were then constructed using the maximum likelihood (ML) approach implemented in RAxML, a tool that provides robust tree-building capabilities (Stamatakis, 2014). To assess the reliability of the tree nodes, bootstrap analyses were conducted with 100 resampled data sets, providing a measure of confidence for each branch in the trees. Finally, the resulting phylogenetic trees were visualized and formatted using FigTree (Rambaut, 2010), a software tool designed for displaying and editing phylogenetic trees.

Ecological Analyses

The relative abundances of the top 20 16S rRNA ASVs and top 20 *nifH* ASVs were calculated to identify the host ASVs of each sample. The ASVs with the highest relative abundances were identified as the Cyanobacteria mat's host ASVs. The closest sequenced relatives of the ASVs were then searched for in GenBank through BLAST and used to identify the ASVs on a taxonomic level based on the identity match.

To analyze the associated microbial communities of the woolly mats and mucilaginous mats, a ratio of the non-host sASVs to the mat host sASVs (sASV 1 for the woolly mat and sASV 4 for

the mucilaginous mat) and the non-host nASVs to the mat host nASVs (nASV 2 for the woolly mat and nASV 3 for the mucilaginous mat) were calculated. The correlation between samples were also analyzed using a canonical correlation analysis (CCA), which was run on a table of squared root transformed microbial to host gene ratios. For all correlation analyses, ASVs believed to be host genes (in the case of 16S rRNA gene analysis) or *nifH* genes of the woolly mat or mucilaginous mat were excluded from the analysis. These included 16S sASVs 1-6 and 8-15, 19, and any lower abundance sASVs that that were thought to be a host gene, and *nifH* nASVs 1, 2, 5 and 7.

Results

Cyanobacteria Mat Host Identification

Amongst the woolly mat samples top 20 most abundant sASVs, sASVs 1-3 and 5-8 had variable yet high relative abundances. Given their high abundance, the sASVs are hypothesized to be host sASVs of the woolly mats (Figure 2.1). However, for the purposes of calculating non-host sASVs to host sASVs, sASV 1 was used as the host sASV. There were also multiple sASV that had an identity match to a strain of *M. wollei* in the NCBI GenBank database (Table 2.1). The closest known relative of sASV 1, identified through 16S rRNA gene sequencing, was *Microseira wollei* NIES-4236 (Yamaguchi et al., 2019 unpubl.) with a 98.21% identity match in the NCBI GenBank database. sASV 3, which had the third highest relative abundance in the woolly mats (Figure 2.1), had a 98.62% identity match to *Microseira wollei* str. Carmichael-Alabama (Kellmann et al., 2008) in NCBI Genbank (Table 2.1).

The most abundant *nifH* based "nASV" in the woolly mat samples was nASV 1, which had a 78.95% identity match to *Filamentous cyanobacterium ESFC-1* (Woebken et al., 2012) in the NCBI GenBank database. The second most abundant *nifH* ASV, nASV 2, had a 100% match with *Microseira sp.* in the Silva 132 (Quast, 2013) database and a 100% identity match to *M. wollei* in the NCBI GenBank database. (Table 2.2). It is hypothesized that nASV 1 and nASV 2 were both *nifH* genes belonging to each of the three *M. wollei* ASVs.

Within the mucilaginous mats, sASV 3 had the highest relative abundance and was hypothesized as the host sASV for the mucilaginous mats. Through 16S rRNA gene sequencing, the mucilaginous mat host organism had a 98.22% identity match with *Phormidium sp.* DVL1003c (Shishido et al., 2013) in the NCBI GenBank database, making it the mucilaginous host organism's closest sequenced relative (Table 2.1). It also matched with *Phormidium* IAM M-71 in the Silva 132 (Quast, 2013) database. nASV 3 and 5 had the highest relative abundances in the mucilaginous mat samples. Like the woolly mat, it is hypothesized that the nASV 3 and 5 belong to the host organism. However, for the purposes of calculating non-host nASV to host nASV, nASV 3 was used as the mucilaginous host nASV. Through *nifH* gene sequencing, nASV 3's closest sequenced relative was identified as *Tolypothrix sp.* PCC 7910 (Park and Song, 2020) with an 86.56% identity match in NCBI GenBank. However, Silva 132 (Quast, 2013) could only identify the organism to its class, *Cyanophyceae,* of which *Phormidium* and *Tolypothrix* are a part of. (Table 2.2).

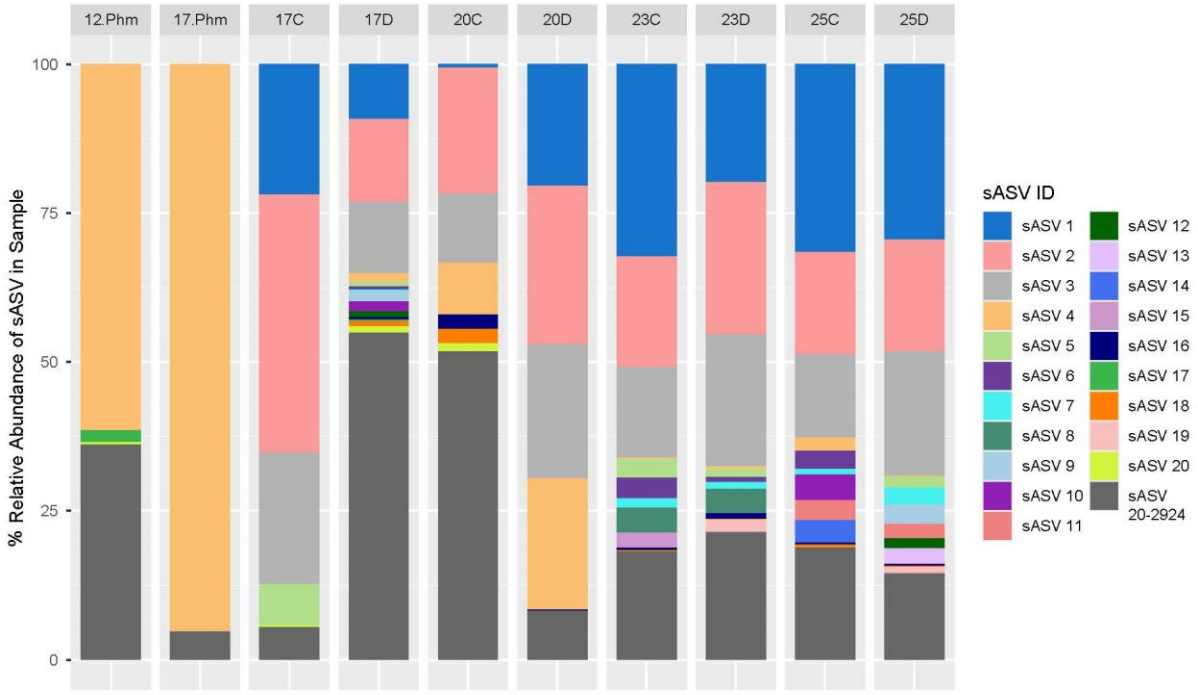

Figure 2.1 Stacked bar plot portrays the percent (%) relative abundance of the 20 most abundant sASVs in the samples collected from the Susquehanna Flats. The Figure combined sASVs 21-2924 for visualization purposes.

Table 2.1 sASV table of the top 20 most abundant 16S sASVs found in *M. wollei* mats collected from the Susquehanna Flats. The table consists of the sASV ID, the scientific name of the top NCBI GenBank closes known species match, the sASV and top match query cover (the percentage of the query (submitted) sequence that is aligned with the subject (documented) sequence), E-value, percent (%) identity of the sASV and top match, and the Accession number of the top match in NCBI GenBank.

sASV ID	Scientific Name	Query Cover (%)	E-value	% Identity	Accession
sASV 1	*Microseira wollei NIES-4236*	100	0	98.21	MK577503.1
sASV 2	*Microseira wollei NIES-4236*	100	0	98.29	MK577503.1
sASV 3	*Microseira wollei str. Carmichael/Alabama*	97	0	98.62	EU439567.1
sASV 4	*Phormidium sp. DVL1003c*	100	0	98.22	JQ771628.1
sASV 5	*Microseira wollei str. Carmichael/Alabama*	97	0	98.55	EU439567.1
sASV 6	*Microseira wollei str. Carmichael/Alabama*	97	0	98.69	EU439567.1
sASV 7	*Monilinema alkalinum CENA532*	100	0	96.07	KF246498.2
sASV 8	*Microseira wollei NIES-4236*	100	0	97.93	MK577503.1
sASV 9	*Microseira wollei NIES-4236*	100	0	98	MK577503.1
sASV 10	*Microseira wollei NIES-4236*	100	0	98.36	MK577503.1
sASV 11	*Microseira wollei NIES-4236*	100	0	97.93	MK577503.1
sASV 12	*Microseira wollei NIES-4236*	100	0	98.14	MK577503.1
sASV 13	*Microseira wollei NIES-4236*	100	0	97.93	MK577503.1
sASV 14	*Microseira wollei NIES-4236*	100	0	98	MK577503.1
sASV 15	*Microseira wollei NIES-4236*	100	0	98.08	MK577503.1
sASV 16	*Rhodanobacteraceae bacterium*	91	0	96.72	LC710947.1
sASV 17	*Haliscomenobacter hydrossis*	99	0	98.21	NR_074420.1
sASV 18	*Candida Roseilinea gracile*	96	0	91.29	KY937207.1
sASV 19	*Microseira wollei NIES-4236*	100	0	97.86	MK577503.1
sASV 20	*Aquincola sp.*	99	0	99.13	OK036958.1

The 16S rRNA phylogenetic tree revealed clusters of organisms grouped according to their evolutionary similarity. (Figure 2.2). In the tree, the only sASV that did not form a monophyletic group with *Micrsoeira wollei* and *Microseira wollei* Carmichael-Alabama (Kellmann et al., 2008) was sASV 4, which had the closest sequenced relative *Phormidium sp.* DVL1003c (Shishido et al., 2013). These tree placements infer that the nASVs 1-3 and 5-10 are ecotypes of *Microseira wollei* with slight evolutionary distinction and nASV 4 was an ecotype of *Phormidium*. However, nASV 4 was also evolutionarily similar to *Lyngbya martensiana*, which was unexpected. (Figure 2.2).

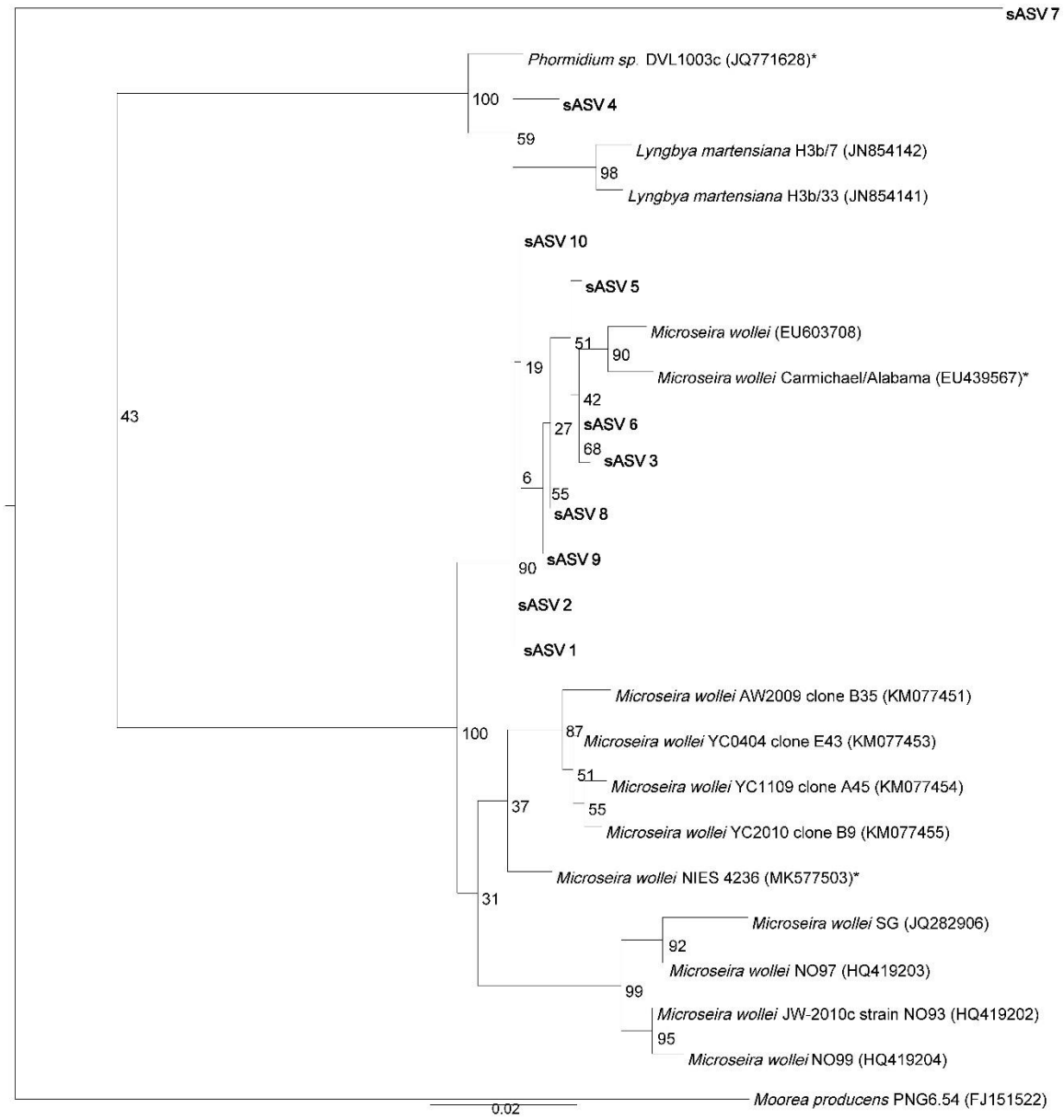

Figure 2.2 Phylogenetic tree of the 10 most relatively abundant sASVs from all samples. sASVs from the Susquehanna Flats are in bold and the closest sequenced relatives have an asterisk (*). 16S rRNA sequences from McGregor and Sendall (2015) are not bold, nor do they have an asterisk. Note that *Microseira wollei* Carmichael/Alabama was a closest sequenced relative and a 16S rRNA sequence from McGregor and Sendall's (2015) phylogenetic tree. GenBank accession numbers are in parenthesis for all ecotypes that are documented in GenBank. Bootstrap values are shown at the nodes of the phylogenetic tree, representing the percentage of 100 resampled datasets that support the given branching pattern. Higher values indicate stronger support for the evolutionary relationships depicted at each node. The scale bar (0.02) in the phylogenetic tree represents a 2% sequence divergence, meaning that the length of the branches corresponds to the amount of evolutionary change or difference in the aligned sequences. Branches of the tree that are 0.02 units long indicate a 2% difference in the nucleotide sequences analyzed.

The nASV 1 and nASV 2 were primarily present in the woolly mats while nASV 3 and nASV 5 were primarily present in the mucilaginous mat samples. The woolly mats contained more nASVs in each sample than the mucilaginous mats, but the sample microbial presence differed (Figure 2.3). A T-test revealed there was no significant difference in microbial structure between the rinsed and unrinsed samples for each site ($p < 0.05$). However, the mucilaginous samples had a distinct nASV composition compared to the rest, with lower dominance of nASV 1 and nASV 2 (Figure 2.3).

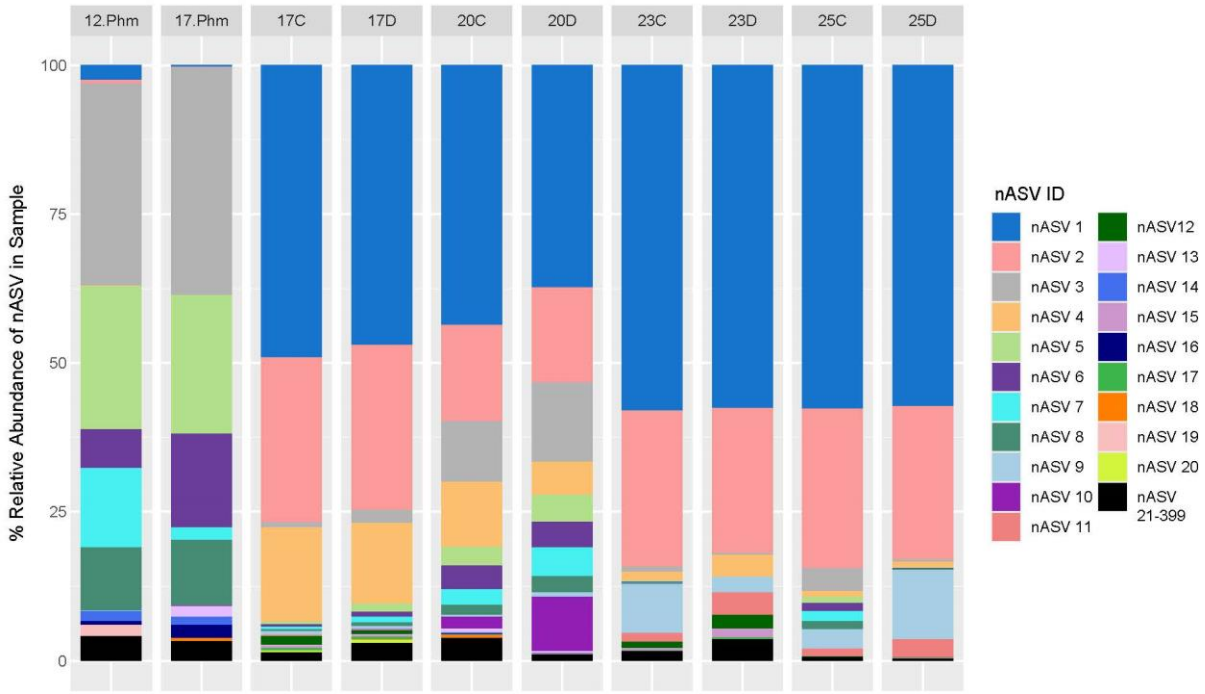

Figure 2.3 Stacked bar plot portraying the percent (%) relative abundance of the 20 most abundant nASVs in the samples collected from the Susquehanna Flats. The Figure combined nASVs 21-462 for visualization purposes.

Table 2.2 *nifH* ASV (nASV) table of the top 20 most abundant 16S nASVs found in *M. wollei* mats collected from the Susquehanna Flats. The table consists of the nASV ID, the scientific name of the top NCBI GenBank closes known species match, the nASV and top match query cover (the percentage of the query (submitted) sequence that is aligned with the subject (documented) sequence), E-value, percent (%) identity of the nASV and top match, and the Accession number of the top match in NCBI GenBank.

nASV ID	Scientific Name	Query Cover (%)	E-value	% Identity	Accession
nASV 1	*Filamentous cyanobacterium ESFC-1*	49	3.00E-26	78.95	JQ013030.1
nASV 2	*Microseira wollei*	76	2.00E-166	100	EF397782.1
nASV 3	*Tolypothrix sp. PCC 7910*	100	3.00E-125	86.56	CP050440.1
nASV 4	*Cylindrospermum stagnale PCC 7417*	50	3.00E-26	78.77	CP003642.1
nASV 5	*Tolypothrix sp. PCC 7910*	100	1.00E-128	87.03	CP050440.1
nASV 6	*Tolypothrix sp. PCC 7712*	100	1.00E-123	86.29	CP06378.1
nASV 7	*Tolypothrix sp. PCC 7910*	100	7.00E-127	86.79	CP050440.1
nASV 8	*Nostoc sp. PCC 7107*	100	7.00E-122	85.99	CP003548.1
nASV 9	*Leptothermofonsia sichuanensis E412*	100	2.00E-111	84.65	CP072600.1
nASV 10	*Pseudanabaena sp. PCC 9016*	96	9.00E-101	83.78	KP221667.1
nASV 11	*Methylomonas methanica MC09*	99	2.00E-131	87.23	CP002738.1
nASV 12	*Methylomonas sp. LL1*	100	3.00E-130	87.03	CP064653.1
nASV 13	*Zehria sp. KO68DGA*	99	5.00E-113	84.89	AB293988.1
nASV 14	*Allocoleopsis franciscana PCC 7113*	100	1.00E-108	84.12	CP003630.1
nASV 15	*Methylomonas methanica*	100	3.00E-115	84.98	AF484672.1
nASV 16	*Allocoleopsis franciscana PCC 7113*	100	3.00E-105	83.65	CP003630.1
nASV 17	*Methylomonas methanica MC09*	100	3.00E-130	87.03	CP00278.1
nASV 18	*Leptothermofonsia sichuanensis E412*	98	2.00E-132	97.74	CP072600.1
nASV 19	*Allocoleopsis franciscana PCC 7113*	99	1.00E-114	85	CP003630.1
nASV 20	*Methylomonas methanica MC09*	100	7.00E-127	85.56	CP002738.1

A phylogenetic of *nifH* gene evolutionary similarityrevealed that *Microseria wollei* formed a monophyletic group, with nASV 2 being part of this group. There were virtually no nucleotide differences between nASV 2 and *Microseira wollei* clone gnif-1 (EF397782) (Joyner et al., 2008), a pattern also reflected in McGregor and Sendall's (2015) *nifH* phylogenetic tree of *Microseria wollei*. Additionally, nASVs 3, 5, 6, 7, and 9 formed another monophyletic group, though with varying bootstrap support values, indicating differing levels of confidence in these relationships. The closest sequenced relative for nASVs 3, 5, 6, and 7 was *Tolypothrix sp. PCC 7910.* However, the tree showed that these sequences were evolutionarily distinct from one another, despite their close relationship. A similar pattern was observed for nASV 9, which was related to *Leptothermofonsia sichuanensis* E412 (Tang et al., 2022), yet remained distinct in the

tree. nASVs 11, 12, 16, and 18 were grouped with methanotrophs, suggesting that these nASVs were more likely to be methanotrophs rather than Cyanobacteria. nASV 1 was shown to be evolutionarily distinct from *Filamentous cyanobacterium* ESFC-1 (Woebken et al., 2012). Although ESFC 1 was the closest sequenced relative to nASV 1, their placement far apart on the tree indicated that they may not be related at the genus level, which was also reflected in their percent identity. Additionally, nASVs 4 and 13 were grouped with nASV 1, indicating a closer evolutionary similarity among these sequences. (Figure 2.4).

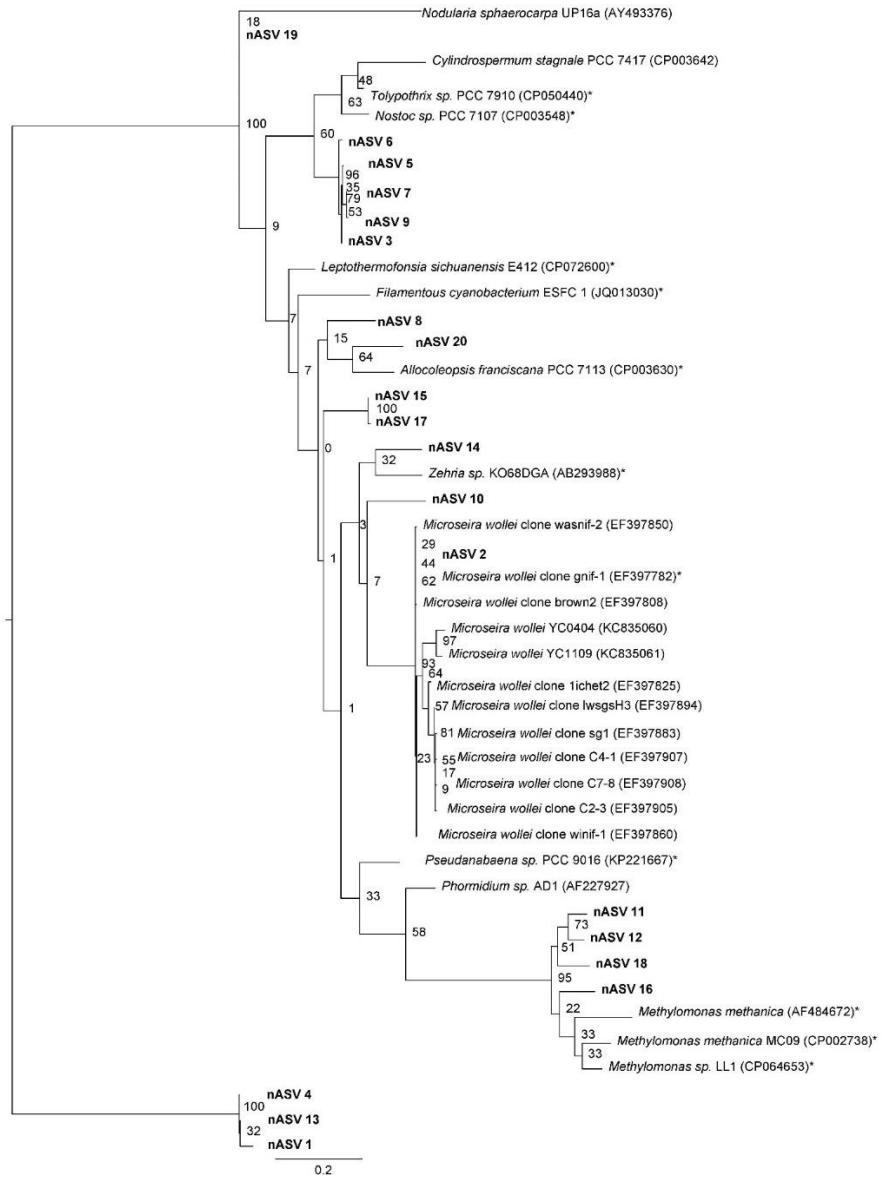

Figure 2.4 Phylogenetic tree of the 10 most relatively abundant sASVs from all samples. sASVs from the Susquehanna Flats are in bold and the closest sequenced relatives have an asterisk (*). 16S rRNA sequences from McGregor and Sendall (2015) are not bold, nor do they have an asterisk. Note that *Microseira wollei* Carmichael/Alabama was a closest sequenced relative and a 16S rRNA sequence from McGregor and Sendall's (2015) phylogenetic tree. Note that *Microseira wollei* clone gnif-1 (EF397782) is also a sequence in the McGregor and Sendall (2015) phylogenetic tree. GenBank accession numbers are in parenthesis for all ecotypes that are documented in GenBank. Bootstrap values are shown at the nodes of the phylogenetic tree, representing the percentage of 100 resampled datasets that support the given branching pattern. Higher values indicate stronger support for the evolutionary relationships depicted at each node. The scale bar (0.02) in the phylogenetic tree represents a 2% sequence divergence, meaning that the length of the branches corresponds to the amount of evolutionary change or difference in the aligned sequences. Branches of the tree that are 0.02 units long indicate a 2% difference in the nucleotide sequences analyzed.

Associated Microbial Communities

A correspondence analysis (CA) showed that the microbial community structure varied between sites (Figure 2.5). The ratios of the sample's host sASV to non-host sASVs were calculated to analyze the dissimilarity of microbial make-up between samples. The microbiome of the mucilaginous mat samples were most dissimilar from those of the woolly samples, those the two mucilaginous mat samples microbiota were also dissimilar from each other. Among the woolly mat samples, 17D and 20C's were most dissimilar from the other samples' microbial communities. Sample 23D's associated microbial community was more similar to 20C's and 25D's associated microbial communities than any other samples. (Figure 2.5).

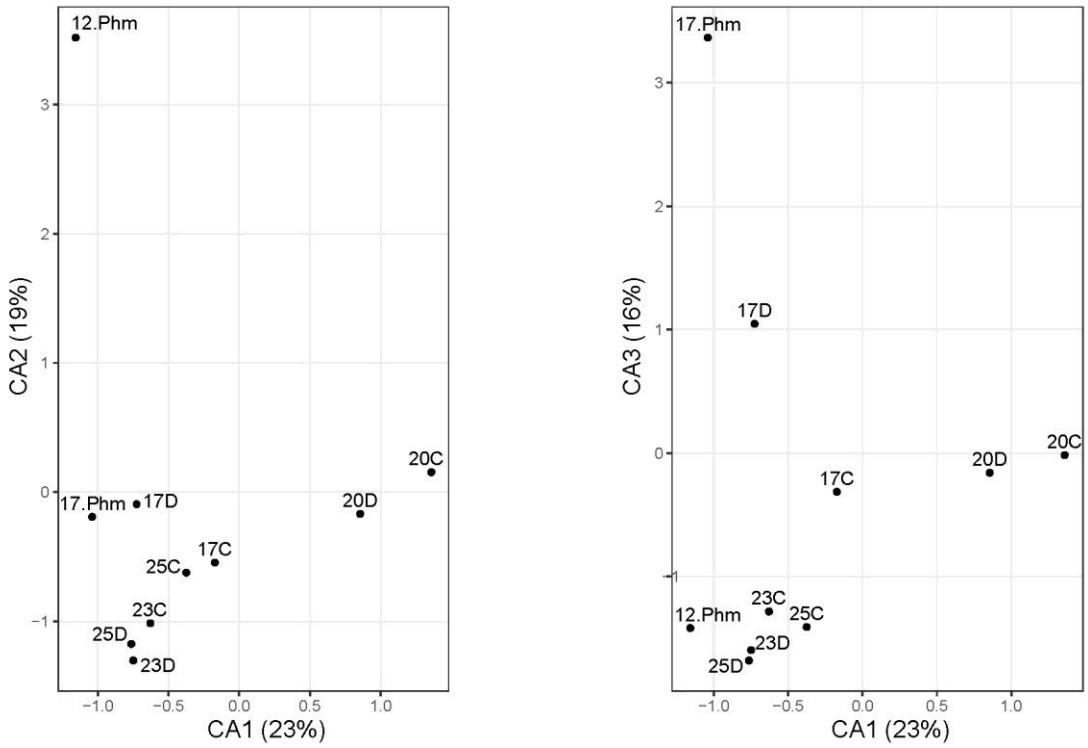

Figure 2.5 Canonical correlation analysis of the microbial communities (defined as the squared-root of non-host sASV counts to sASV host counts) sequenced by their 16S rRNA genes. Each point represents a sample's microbiome and with all other sASVs that are believed to be host-related sASVs removed. The distance between points represents the Chi Squared distance in community composition between those samples, with closer points having more similar community structure. CA1, CA2, and CA3 represent the primary axes of inertia and explaining 23%, 19% and 16 % of the total inertia respectively.

The *nifH* genes were used to analyze the correlation between samples' nitrogen fixing microbial communities. The ratios of the sample's host nASV to non-host nASVs were calculated to analyze the dissimilarity of microbial make-up between samples. The Correlation Analysis positioned samples 20C and 23D far from other samples, indicating a unique microbial community. The mucilaginous samples clustered, indicating less microbial community dissimilarity between the two samples. Samples 25C and 25D also clustered, indicating less microbial community dissimilarity between the two samples as well. Samples 17C, 17D, 23C,

25C, and 25D were less dissimilar to each other than other samples, inferring that their microbial communities was less dissimilar to each other than to other sample's microbial community. Samples12.Phm, and 20C samples were distinct, which suggests that their microbial makeup were each unique and dissimilar from the other samples. (Figure 2.6).

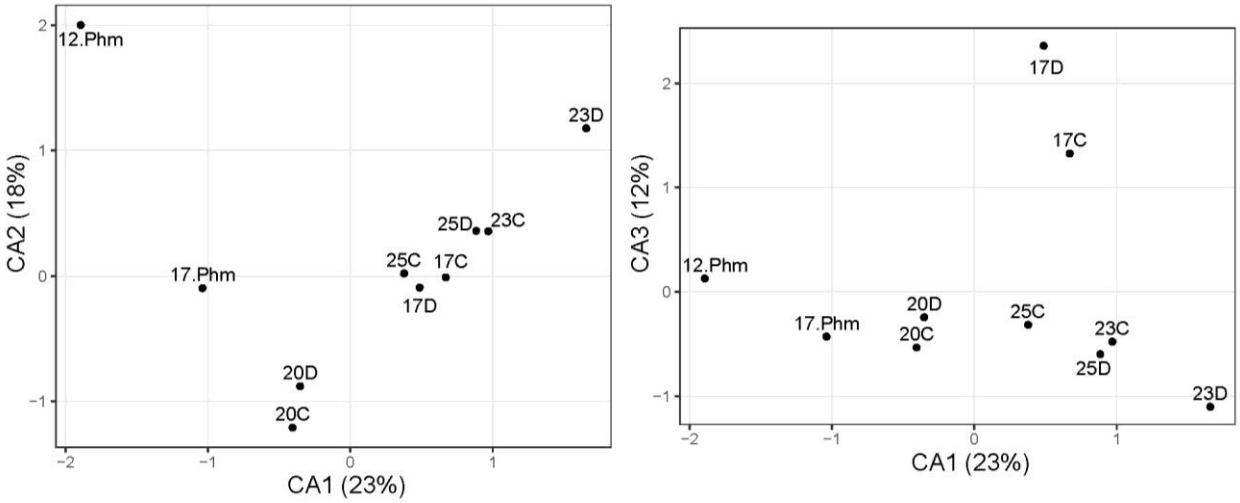

Figure 2.6 Canonical correlation analysis of the microbial communities (defined as the squared root of non-host nASV counts to nASV host counts) sequenced by their *nifH* genes. Each point represents a sample's microbiome and with all other nASVs that are believed to be host-related nASVs removed. "C" indicates that the sample was rinsed in the site water (clean) and "D" indicates that the sample was not rinsed in the site water (dirty). The distance between points represents the Chi Squared distance in community composition between those samples, with closer points having more similar community structure. CA1, CA2, and CA3 represent the primary axes of inertia and explaining 23%, 19% and 16 % of the total inertia respectively.

The ratios of the sample's host sASV to non-host sASVs were calculated to analyze the mucilaginous and woolly mat associated microbial communities. The mucilaginous mat (samples 12.Phm and 17.Phm) host sASV was sASV 4 (closet relative *Phormidium IAM M-71*) and the woolly mat (17C/D, 20C/D, 23C/D, and 25C/D) host sASV was sASV 3 (closest relative *Microseira Carmichael-Alabama*). Sample 12.Phm had a higher total microbial to host gene ratio

than sample 17.Phm, indicating that 12.Phm had a more dominant associated microbial presence and 17.Phm was made up of mainly the host, sASV 3. Samples 17C and 23C had similar microbe to host ratios with ~6 non-host microbes for every host microbe. Samples 17D, 20C, and 20D had higher ratios of ~60-90 non-host microbes for every host count. Samples 23D, 25C, and 25D had ~10-40 non-host microbes for every host microbe (Figure 2.7).

The samples' associated microbial communities varied at the phylum level (Figure 2.8). Among the dominant microbial phyla, Armatimonadetes, Omnitrophicaeota, and Spirochaetes exhibited low ratios in most samples. Cyanobacteria presence was variable with low presence in 17C and high presence in 20C and 20D. Gammaproteobacteria, Deinococcus-Thermus, and Plantomycetes were variable with a low proportion in the 17.Phm sample. Alphaproteobacteria presence was variable as well, with low microbial counts in samples 17.Phm and 20D. Overall, sample 17.Phm had a more microbial presence than 12.Phm.

Amongst the mucilaginous mat samples, 12.Phm had a higher presence of associated microbes than 17.Phm. Associated Cyanobacteria had a high presence in both samples, with a higher presence of *Leptolyngbya* BN43 in 17.Phm, and a higher presence of *Microseira* Carmichael-Alabama, *Oscillatoria* PCC-10802 and *Phormidium* ETS-05 in 12.Phm. (Figure 2.9). There were also variable genera present within the Cyanobacteria phylum. *Microseira* Carmichael-Alabama, the closest known relative to sASV 3, had low presence in sample 17.Phm and an even lower presence in sample 12.Phm. *Phormidium* IAM M-71, the closest known relative to sASV 4, had

variable presence in the filamentous samples. *Oscillatoria* PCC-10802 and *Phormidium* ETS-05 had low ratios in all samples with the highest ratio in the 12.Phm sample. (Figure 2.9)

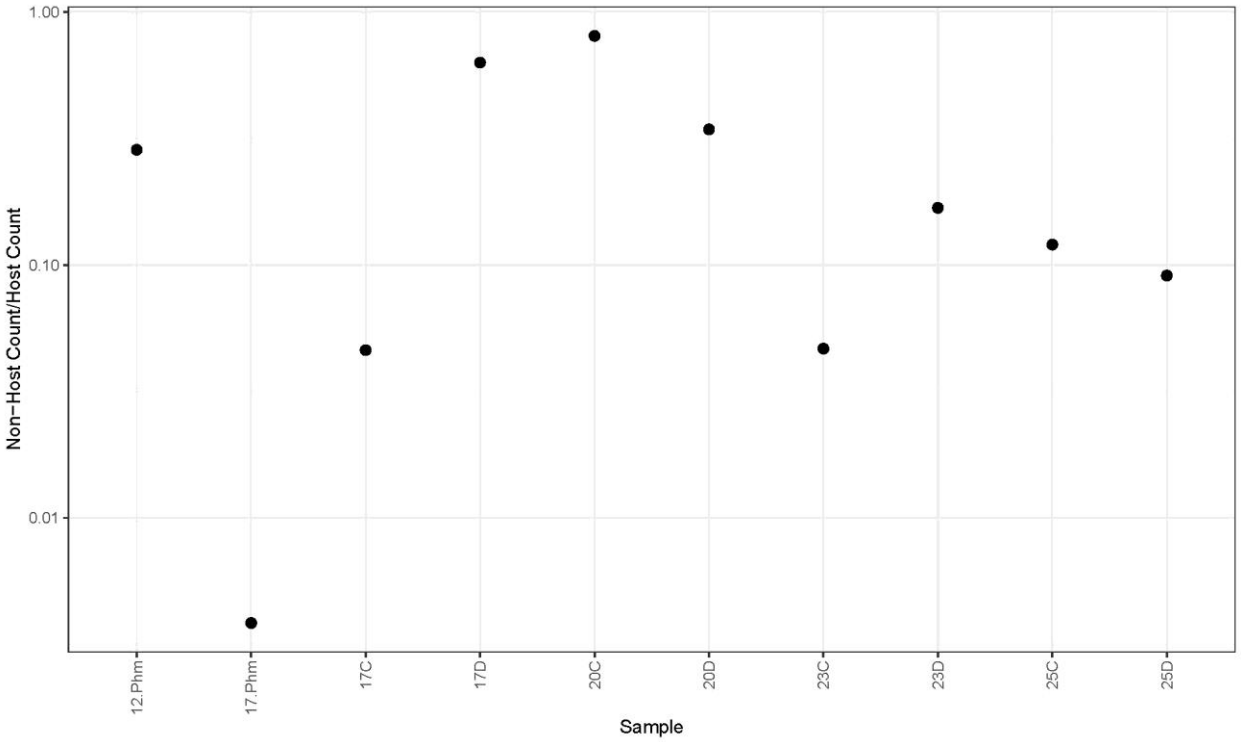

Figure 2.7 Ratios of the sample's non-host sASV microbial count to the host microbial count of each sample (along a $\log_{10}$ scaled axis) on the y-axis. The sample is portrayed on the x-axis. "C" indicates that the sample was rinsed in the site water (clean) and "D" indicates that the sample was not rinsed in the site water (dirty). The samples of the mucilaginous mat, 12.Phm and 17.Phm, host sASV was sASV 4 and the woolly mat host sASV was sASV 3.

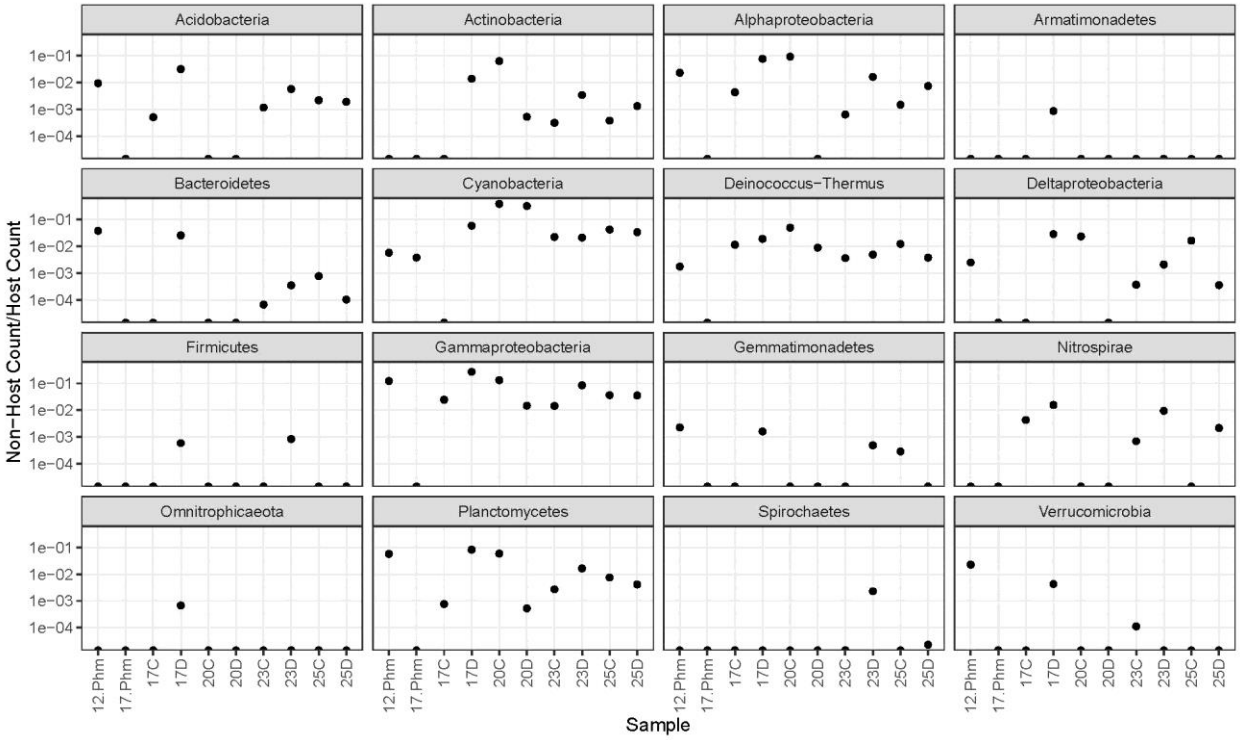

Figure 2.8 Scatter plots portraying the ratio (along a $\log_{10}$ scaled axis) of each non-host phylum count to the host phylum count. The ratio is portrayed on the y-axis. "C" indicates that the sample was rinsed in the site water (clean) and "D" indicates that the sample was not rinsed in the site water (dirty). The mucilaginous mat samples', 12.Phm and 17.Phm, host sASV was sASV 4 (*Phormidium* IAM M-71) and the woolly mat host sASV was sASV 3 (*Microseira* Carmichael-Alabama).

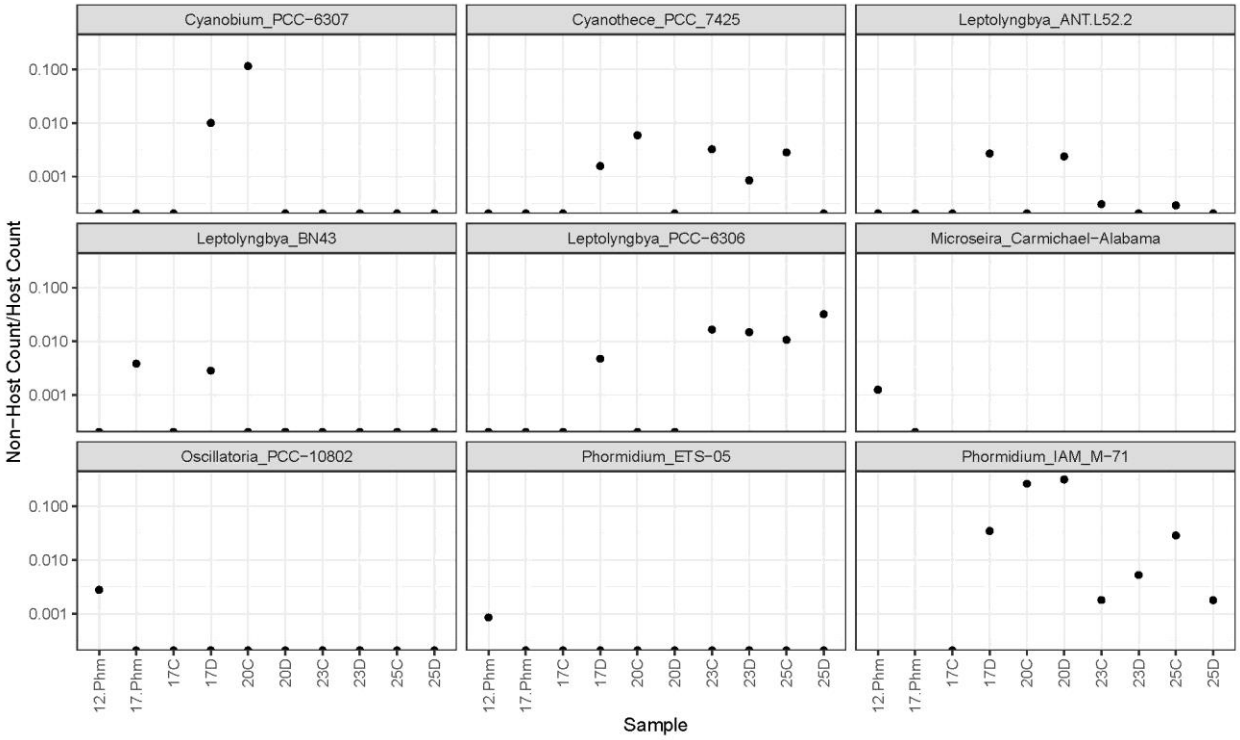

Figure 2.9 Scatter plots of the sASV ratio (along a $\log_{10}$ scaled axis) of each non-host genus count to the host genus count within the Cyanobacteria phylum. The ratio is portrayed on the y-axis. "C" indicates that the sample was rinsed in the site water (clean) and "D" indicates that the sample was not rinsed in the site water (dirty). The mucilaginous mat samples', 12.Phm and 17.Phm, host sASV was sASV 4 (*Phormidium* IAM M-71) and the woolly mat host sASV was sASV 3 (*Microseira* Carmichael-Alabama).

Associated Nitrogen Fixing Microbial Community

The *nifH* gene sequences revealed a diverse and complex microbial community associated with the woolly and mucilaginous mats. There were >350 *nifH* Amplicon Sequence Variants (nASV) sequenced from the samples collected at the Susquehanna Flats.

Among the nASVs, the mucilaginous mat samples (12.Phm and 17.Phm) had smaller ratios of non-host microbial count to host microbial count than the filamentous samples with 20C and

20D exhibiting the highest ratios of non-host microbial count to host microbial counts. (Figure 2.10). Cyanobacteria, Pseudomonadota, and Thermodesulfobacteriota were among the most dominant phyla present. The mucilaginous samples had lower phyla richness, mainly made up of up Cyanobacteria and Pseudomonadota presence in sample 17.Phm. (Figure 2.11).

Among the Cyanobacteria phylum, *Leptolyngbya*, *Leptothermofonsia*, and *Tricormus* were the most dominant genera, although the latter was not found in the mucilaginous samples (Figure 2.12). The *Microseira nifH* genes were found in the mucilaginous samples. *Pseudomonadota* genera containing methanotroph *nifH* genes were present across samples; however, counts were variable, which may be due to the different environmental conditions the mats were in. Thus, different environmental conditions may influence the associated microbial communities of the filamentous Cyanobacteria mats.

The presence of Thermodesulfobacteria and Pseudomonadota indicate anerobic conditions and methane sources within the woolly mats. Among the Pseudomonadota phylum, methanotrophs had variable presence. *Methylococcus* had a higher presence in the samples collected from sites 17 and 20. *Methylomonas* had variable presence, with low presence in sample 12.Phm and samples from site 20. (Figure 2.13).

Among Thermodesulfobacteriota, of which sulfate-reducing genera were present, *Desulfobulbus* and *Geobacter* were the most dominant genera (Vick et al., 2009; Jeanthon et al., 2002). Both of these phyla are associated with anaerobic conditions, indicating anaerobic conditions within the

woolly mats (Suzuki et al., 2007). *Geobacter* was also considered one of the predominant Fe (III)-reducing microorganisms in sediment (Lovley et al., 2011). (Figure 2.14).

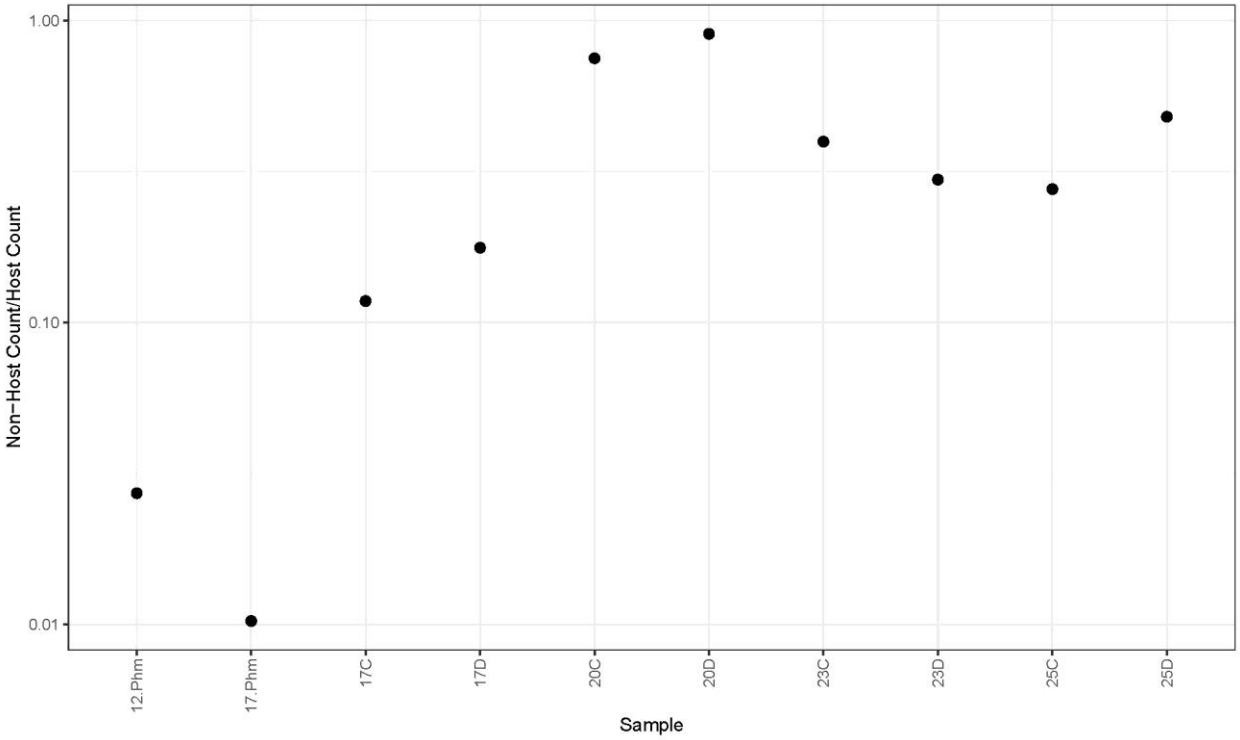

Figure 2.10 Scatter plot portraying the ratio of the sample's non-host nASV microbial count to the host microbial count of each sample on the y-axis (along a $\log_{10}$ scaled axis). The sample is portrayed on the y-axis. "C" indicates that the sample was rinsed in the site water (clean) and "D" indicates that the sample was not rinsed in the site water (dirty). The samples of the mucilaginous mat, 12.Phm and 17.Phm, host nASV was nASV 3 (*Tolypothrix sp.* PCC 7910) and the woolly mat host nASV was nASV 2 (*Microseira wollei*).

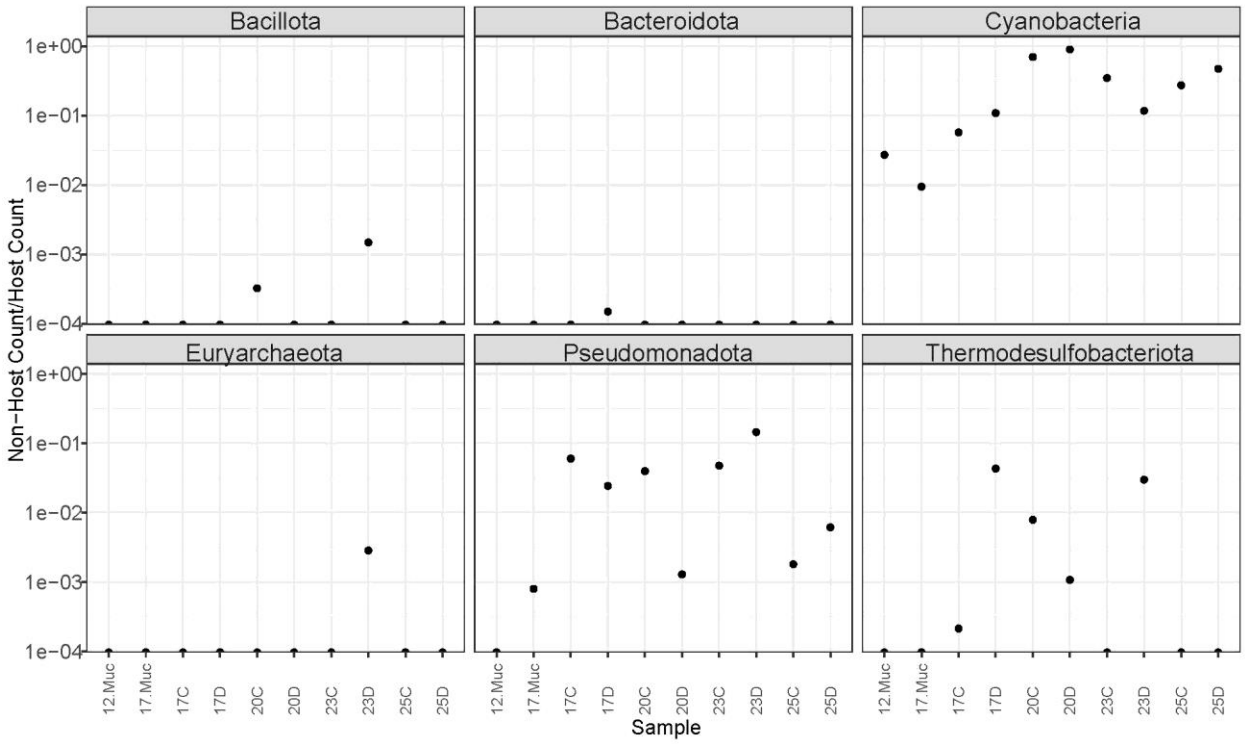

Figure 2.11 Scatter plots portraying the nASV ratio (along a $\log_{10}$ scaled axis) of each non-host phylum count to the host phylum count. The ratio is portrayed on the y-axis. "C" indicates that the sample was rinsed in the site water (clean) and "D" indicates that the sample was not rinsed in the site water (dirty). The mucilaginous mat samples', 12.Phm and 17.Phm, host nASV was nASV 3 (*Tolypothrix sp.* PCC 7910) and the woolly mat host nASV was nASV 2 (*Microseira wollei*).

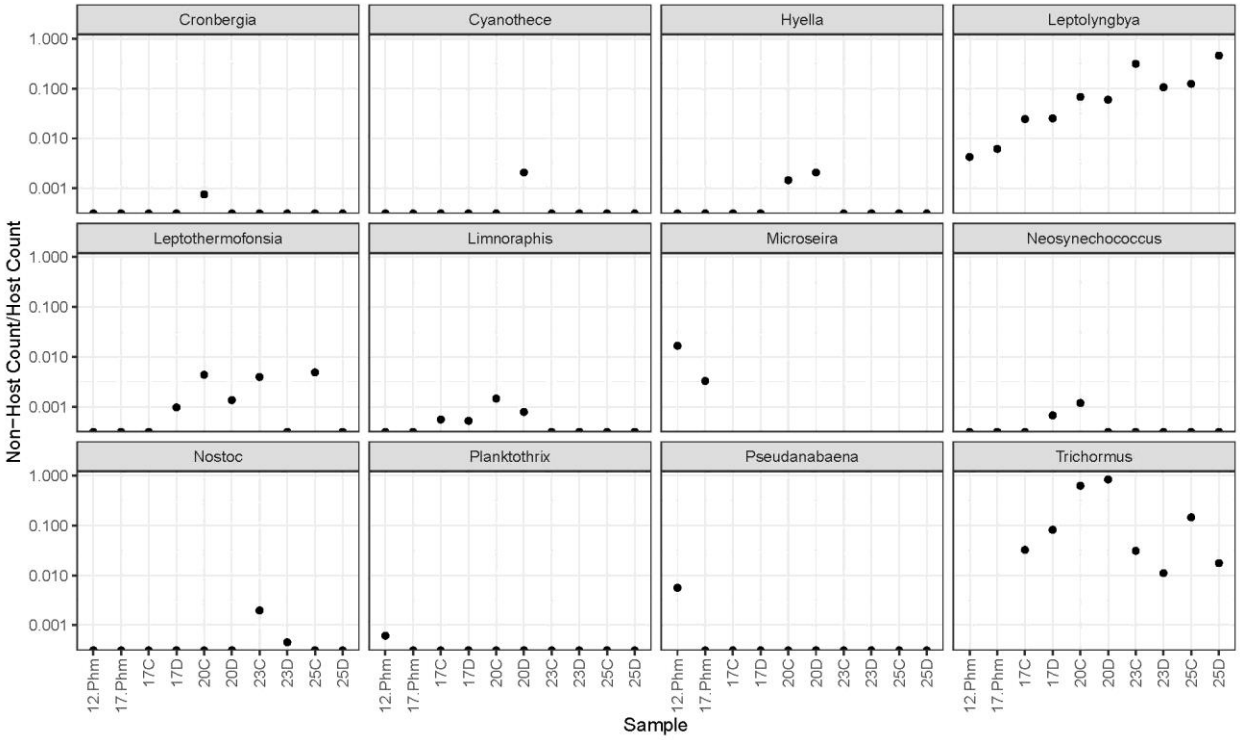

Figure 2.12 Scatter plots of the nASV ratio (along a $\log_{10}$ scaled axis) of each non-host genus count to the host genus count within the Cyanobacteria phylum. The ratio is portrayed on the y-axis. "C" indicates that the sample was rinsed in the site water (clean) and "D" indicates that the sample was not rinsed in the site water (dirty). The mucilaginous mat samples', 12.Phm and 17.Phm, host nASV was nASV 3 (*Phormidium* IAM M-71) and the woolly mat host nASV was nASV 2 (*Microseira wollei*).

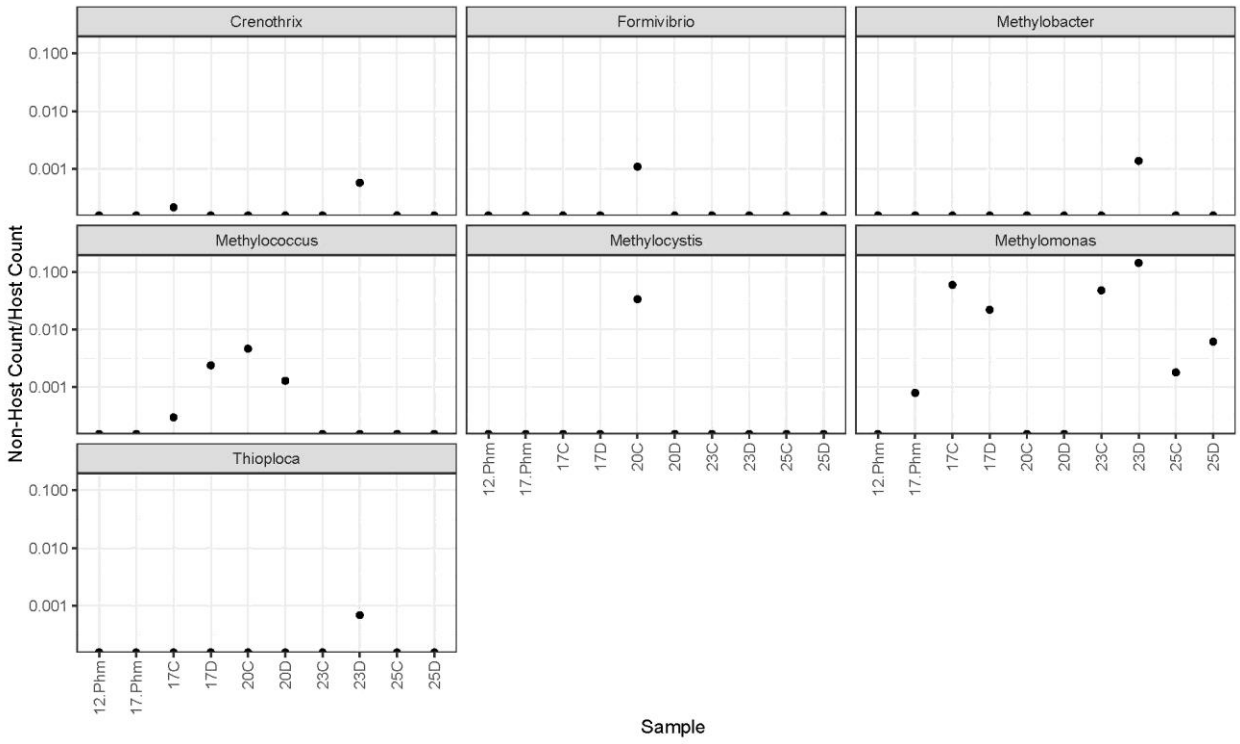

Figure 2.13 Scatter plots of the nASV ratio (along a $\log_{10}$ scaled axis) of each non-host genus count to the host genus count within the Pseudomonadota phylum. The ratio is portrayed on the y-axis. “C” indicates that the sample was rinsed in the site water (clean) and “D” indicates that the sample was not rinsed in the site water (dirty). The mucilaginous mat samples’, 12.Phm and 17.Phm, host nASV was nASV 3 and the woolly mat host nASV was nASV 2.

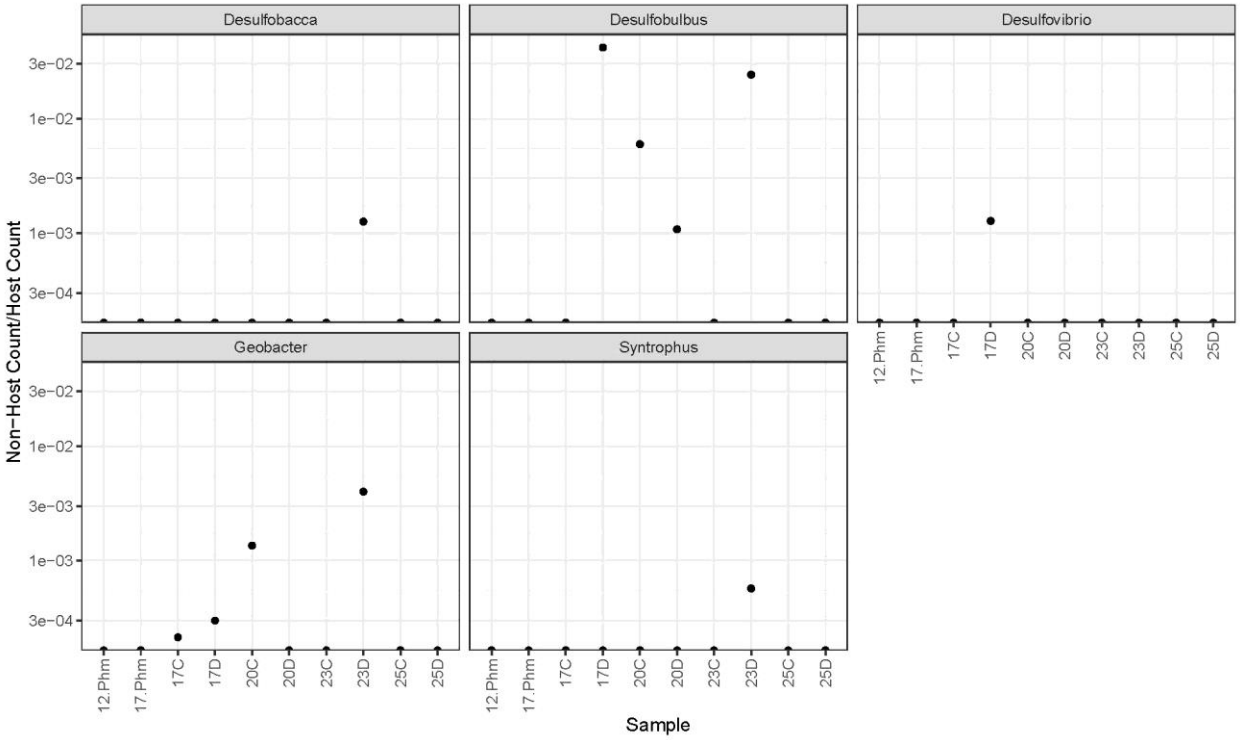

Figure 2.14 Scatter plots of the nASV ratio (along a $\log_{10}$ scaled axis) of each non-host genus count to the host genus count within the Thermodesulfobacteriota phylum. The ratio is portrayed on the y-axis. "C" indicates that the sample was rinsed in the site water (clean) and "D" indicates that the sample was not rinsed in the site water (dirty). The mucilaginous mat samples', 12.Phm and 17.Phm, host nASV was nASV 3 and the woolly mat host nASV was nASV 2.

Discussion

Woolly Mat Host- *Microseira wollei* Ecotype

For the purposes of this analysis, ASVs with a ≥98% and < 100% identity match to the closest sequenced relative in GenBank are considered the same species as the match, but of a different ecotype. If the ASV had a 95% to 98% identity match to the closest sequenced relative in GenBank, the ASV was considered to be of the same genus as the observed species (following Cheng et al., 2014).

The analyses indicated that within the woolly mat samples, 14 sASVs out of the 20 most abundant sASVs were all distinct ecotypes of the *M. wollei* species suggesting microdiversity within the *M. wollei* population. Within the top 20 most abundant sASVs, more than one *M. wollei* sASV was found in the mats at each site. sASV 1, 2, 8-15, and 19 had a ~98% (species level) identity match to *Microseira wollei* NIES-4236 (Yamaguchi et al., 2019 unpubl.), making them a novel ecotype of *M. wollei* with their closest relative being *Microseira wollei* NIES-4236 (Yamaguchi et al., 2019 unpubl.). sASV 3, 5, and 6 had a ~98.6% (species level) identity match to *Microseira wollei* str. Carmichael-Alabama (Kellmann et al., 2008), making them a novel ecotype of *Microseira wollei* with their closest relative being *Microseira wollei* str. Carmichael-Alabama (Kellmann et al., 2008). These sASVs had high yet variable relative abundances, which may be because they were all *M. wollei* ecotypes that coexist in the mats. (Figure 2.12.). Three of these sASVs (1, 2, and 3) were "dominant" comprising more than half of all *M. wollei* ASVs. The relative proportions of these dominant sASVs varied between sites, suggesting that environmental or historical effects may shape the structure within this population (Martiny et al., 2011).

Because two *nifH* gene ASVs (nASVs) were dominant in the woolly mat samples, and only the second most abundant of these mapped to *M. wollei*, it was hypothesized that both the first and second most abundant genes are actually from the same *M. wollei* with the first gene being novel. (Figure 2.13). While it is conceivable that the other *nifH* gene is from some other organism, its abundance, relative to that of nASV2 suggests that it is most likely from the dominant known diazotroph in the environment, with *M. wollei* having two *nifH* genes (nASV1 and nASV2). While it is conceivable, given the 16s rRNA gene microdiversity, that some nASVs harbor one

nifH gene and others harbor the other, the consistent 2-1 ratio of nASV1 to nASV2 across the different samples, in spite of different ratios of the dominant sASVs suggests that each ecotype harbors both *nifH* genes, in a common 2-1 ratio (Figure 2.1, 2.2). It is hypothesized that given its dissimilarity to other samples, the *nifH* gene corresponding to nASV1 is novel and currently unique to this site, while nASV2 has been documented in GenBank as having been found in Florida. (Table 2.2, Figure 2.13). However, note that the supplied GenBank reference (Joyner et al., 2008) did not refer to the accession number for this sequence so its distribution in Florida, aside from being associated with fresh and coastal environments is unknown to us and missing from the scientific literature.

Similar below species level for *M. wollei* have been previously documented by Joyner et al. (2008). Using 16S rRNA and *nifH* gene sequences, Joyner et al. (2008) identified three distinct "Operational taxonomic units" (OTUs), encompassing at least two different *Lyngbya wollei* species (since reclassified as *M. wollei*). Joyner et al.'s (2008) OTUs are similar to the Susquehanna Flats ASVs but were determined from clone libraries with a separate informatics protocol. Given the OTUs phylogenetic differences, Joyner et al. (2008) contended one of the OTUs should be considered a different species from the other two. These OTUs coexisted across 21 river and spring sites in Florida. However, it was found that different sites tended to be dominated by different, single, OTUs. This is in contrast to the Susquehanna Flats sites, where the ASVs tend to co-occur with their proportions varying between sites (Figure 2.1). They also found a direct 1-1 mapping in abundance between 16S rRNA genes and *nifH* genes, suggesting that each OTU harbored a particular *nifH* gene in their site, in contrast to the Susquehanna Flats where it appears that each sample harbors the same nASVs.

Conversely, Engene et al. (2010) suggest caution when observing microdiversity in Cyanobacterial mats. These authors also observed OTU level microdiversity amongst *Lyngbya spp.* but concluded that 16S rRNA sequencing can be unreliable to identify ecotypes of *Lyngbya* because *Lyngbya* can often contain multiple copies of the 16S rRNA gene, leading to an overestimation of *Lyngbya* microdiversity. However, this interpretation might not apply at the Susquehanna Flats because the proportions of the different sASVs vary between sites, a pattern that would not occur if each organisms harbored all of the same set of 16s ASV genes. Indeed, it is possible that there are different species with different combinations of 16s ASV genes, in which case the patterns could be more complicated than is articulated here, but in which there would still need to be more than one ecotype with different ratios or combinations of the observed 16s rRNA genes. Further investigation using metagenomics would allow researchers to identify which 16S rRNA genes and *nifH* genes are present in which organisms and provide a more wholistic picture of the within population diversity in the Susquehanna flats.

Associated Microbial Community of *Microseira wollei* Dominated Mats

The woolly mats harbored complex and diverse associated microbial communities that exhibited spatial differences amongst samples. The woolly mats contained various phyla, including Acidobacteria, Actinobacteria, Alphaproteobacteria, Cyanobacteria, Deinococcus-Thermus, Gammaproteobacteria, and Planctomycetes. These phyla are common across aquatic soil and other environments and their presence in the mats is unsurprising (Kielak et al., 2016; Barka et al., 2015; Delgado-Baquerizo et al., 2018; Sheng et al., 2016; Röske et al., 2012; Zhang et al., 2015).

nifH sequencing revealed a diverse nitrogen fixing microbial community associated with the *M. wollei* mats. Cyanobacteria, Pseudomonadota, and Thermodesulfobacteriota were among the most commonly detected nitrogen fixing phyla across samples. Within Pseudomonadota, methanotrophs were detected in the mats and within Thermodesulfobacteriota, sulfate-reducers were detected in the mats. The different genera of nitrogen fixing bacteria indicate that diazotrophs associated with the woolly mats have the potential to carry out a range of biogeochemical processes.

It was unexpected that the "rinsed" *M. wollei* samples, did not have any significant differences with the "unrinsed" samples' associated microbial communities ($p < 0.05$) as it was clear that the rinsing process removed a lot of sediment, and it was suspected that the sediment would harbor its own microbiota. This nondifference suggests that the woolly mats effectively "trap" their associated microbial communities or that the sediment that was rinsed away harbored relatively few organisms relative to the mats. The observation that the rinsed and unrinsed communities harbored similar proportions of *M. wollei* preclude that the similarity could be from the sediment having the same microbial community since the mats visually have more *M. wollei* than sediment. Though, that most microorganisms in *M. wollei* mats are tightly bound to their hosts suggests an opportunity for close ecological associations between *M. wollei* and its associated microbial community, which should be taken into consideration future explorations of *M. wollei* mat biogeochemistry. Sequencing the attached sediment that is rinsed off would also further reveal the associated microbial communities that are more associated with the filamentous Cyanobacteria mats and those that are more associated with the sediment.

The high-level microbial patterns seen in the samples from the Susquehanna Flats mirror those seen elsewhere. For instance, associated microbial communities of *Lyngbya spp*. collected from Papua New Guinea, Curaçao, and Jamaica, found similar phyla to the Susquehanna Flats sites including Alphaproteobacteria, Betaproteobacteria, c-proteobacteria, and Bacteroidetes (Engene et al., 2010).

The spatial variability of the associated microbial communities may reflect differences in environmental factors, such as location, depth, water clarity, and water column nutrient make-up (Gurbisz, 2016; Nguyen et al., 2021). Therefore, abiotic factors and the microbiome of filamentous and *M. wollei* mats should be taken into consideration when making management decisions.

The presence of fecal indicator bacteria, *Pseudomonas,* as well as human pathogens, Legionella and Bacteroides, were detected. This finding mirrors observations of *M. wollei* dominated mats in Lake St. Clair (Vijayavel et al., 2013) which also trapped fecal indicator bacteria and pathogens.

Mucilaginous Mat Host- *Phormidium* Ecotype

In contrast to the *M. wollei* mat, the mucilaginous mats had only one sASV (sASV) 4, which had a 98.22% (species level) identity match to *Phormidium sp*. DVL1003c. This partial match

suggests that sASV 4 is a novel ecotype of *Phormidium* with its closest sequenced relative being *Phormidium sp.* DVL1003c (Shishido et al., 2013). (Figure 2.12). The most abundant *nifH* gene in the mat was nASV 3, which had an 86.56% (< genus level) identity match to its closest sequenced relative, *Tolypothrix sp.* PCC 7910. This lack of identity suggests that this gene is novel. Any similarity to *Tolypothrix sp.* PCC 7910 (Park and Song, 2020) suggests that the gene may share a common ancestor with one found *Tolypothrix sp.* PCC 7910 (Park and Song, 2020) and that the gene arrived in *Phormidium* due to horizontal gene transfer. (Figure 2.13). With only a 98.22% identity match to the *Phormidium sp.* DVL1003c (Shishido et al., 2013) 16S rRNA gene and an 86.56% identity match to the *Tolypothrix sp. nifH gene,* it is hypothesized that the *Phormidium* species at the Flats is a novel ecotype of *Phormidium* that has not been sequenced elsewhere.

Phormidium taxonomic classification has changed over time, with molecular and morphological approaches sometimes contradicting each other (Marquardt and Palinska, 2007; Palinska and Marquardt, 2008; Palinska et al., 2011). *Phormidium* is not a monophyletic genus and morphological identification does not reveal the associated microbial communities as well (McAllister et al., 2016; Marquardt and Palinska, 2007). Therefore, it is highly suggested that information provided by molecular studies such as this one should take precedence over morphological approaches.

The Susquehanna Flats is unlike other environments in which *Phormidium* has been previously detected – in those other environments, water flow tends to be moderate with higher dissolved

inorganic nitrogen (>0.1 mg L^{-1}) than seen at the Susquehanna Flats sites (Heath, 2009; Heath et al., 2016. Thus, this new *Phormidium* species level group appears to be found outside the environmental range of previously discovered *Phormidium*, warranting additional study into its physiology and ecology. However, the flats does share some features with other *Phormidium* dominated environments – in particular dissolved reactive phosphorus is low in both other *Phormidium* dominated sites (>0.01 mg L^{-1}) (McAllister et al., 2016; Heath et al., 2011) and in this study. Similarly, both the other *Phormidium* waters (McAllister et al., 2016; Heath et al., 2011) and the Flats has warm summer waters, reaching >22 °C in August 2023 (measured with a Hydrolab HL4) when the *Phormidium* dominated mats were present.

Phormidium dominated mats in other environments have been found to produce cyanotoxins (Gugger et al., 2005; Teneva et al., 2005; Wood et al., 2007; Borges et al., 2015), including anatoxin-a (ATX), homoanatoxin-a (HTX) (Quiblier et al., 2013), saxitoxins and microcystins (Teneva et al., 2005). Animal deaths have been linked to *Phormidium* dominated mat outbreaks in France, Netherlands, New Zealand, and the United States (Gugger et al., 2005; Wood et al., 2007; Puschner et al., 2008; Faassen et al., 2012). Thus, it is recommended that the scientific community prioritize testing the *Phormidium* dominated mats in the Susquehanna Flats for these and other toxins.

Associated Microbial Community of *Phormidium sp.* Dominated Mats

Phormidium at site 12 had a higher presence of non-*Phormidium* microbial species compared *Phormidium* mats at site 17. However, both samples exhibited a high presence of non-

Phormidium Cyanobacteria. The results mirror microbial analyses of other *Phormidium* dominated mats which have been found to contain bacteria, Cyanobacteria, and some eukaryotic algae (McAlister et al., 2016). These microorganisms have been shown to exhibit symbiotic relationships with one-another and the *Phormidium* (Hart et al., 2013; Brasell et al., 2015) and so similar interactions may occur in the Susquehanna Flats as well.

While only one survey of the *Phormidium* was conducted during one point during the summer, observations elsewhere suggest mats are temporally dynamic with *Phormidium*-dominated mats progress through three distinct phases of microbial community composition (Brasell et al., 2015). In the first phase, the microbial community is primarily composed of eukaryotic diatoms, Alphaproteobacteria, and Betaproteobacteria. The second phase sees a shift, with the microbial community dominated by Alphaproteobacteria, Betaproteobacteria, Sphingobacteria, and Flavobacteria, along with a significant presence of diatoms. During this phase, *Phormidium* is present but in lower abundance, mainly using the substrate for growth. The final phase is dominated by Cyanobacteria, Sphingobacteria and Flavobacteria, with minimal diatom presence. This phase consists of species that recycle nutrients, supporting and stabilizing the mat's structure. Because the study focused on amplifying the 16S rRNA and *nifH* genes, the presence of eukaryotic diatoms was not detected. However, the dominance of *Phormidium* in the samples and presence of Cyanobacteria suggests that the mats observed were likely in the final, stable, nutrient-cycling phase. (Figure 2.1, 2.2, 2.6).

Management Implications

While the *M. wollei* dominated mats at the Flats produce saxitoxins (Wazniak et al., 2022 unpubl.) the *Phormidium* dominated mats at the Flats have not been tested for toxins. Like *M. wollei,* different *Phormidium* species can produce various toxins, so following molecular identification, toxin analysis is essential to understand the possible toxin impact on human and environmental health (Mitsui et al., 1987; Lilleheil et al., 1997; Anagnostidis and Komarek, 1988; Baker et al., 2001; Teneva et al., 2005).

The novel 16S ASVs suggesting microdiversity within the *M. wollei* mats would not have been discovered without long read PacBio long-sequencing. Future studies should use metagenomics to confirm and identify the multiple ecotypes in the bay. Furthermore, metagenomics has the potential to better characterize the genetic potential of the microbial communities associated with the mat samples.

Metagenomic sequencing would allow researchers to confidently identify the ecotype of *M. wollei* and *Phormidium* at the Flats and their potentially different microbiomes, which would enhance the understanding of microbial diversity in *M. wollei* and *Phormidium* mats in comparable aquatic ecosystems. Identifying the microbes present in the mats is crucial, as some of these microbes may be sources of toxins or play significant roles in biogeochemical fluxes, which may alter the surrounding environment's nutrient fluxes. Uncovering dominant microbes, allows better understanding of biogeochemical processes, and possible toxin-producers, which is

crucial for implementing effective management decisions, especially in nutrient-loaded environments.

Chapter 3: *Microseira* (*Lyngbya*) *wollei* Ecophysiology

Abstract

Just below the mouth of the Susquehanna River at the head of the Chesapeake Bay lies a recovering submerged aquatic vegetation (SAV) bed at the Susquehanna Flats. The Susquehanna Flats plays a crucial role in nutrient removal, situated at the confluence where the Susquehanna River, the largest tributary of the Chesapeake Bay, flows into the Bay. The SAV bed was decimated by the devastating effects of Hurricane Agnes in 1972 but has since recovered to be the most abundant and biodiverse SAV bed in the Chesapeake Bay. However, a filamentous cyanobacterium, molecularly identified as *Microseira* (*Lyngbya*) *wollei*, has bloomed consistently on an annual basis since the early 2000s. However, its ecophysiology and affects it may have on the recovering SAV bed has not been investigated. To investigate the basic nutrient requirements and preferences of the *Microseira* (*Lyngbya*) *wollei*, studies taking a three-prong approach of field, laboratory and modelling approaches, were initiated to study its role in the environment. This study focused on the field and laboratory approaches to provide the necessary information for a model simulation. Field studies included measuring *Microseira* (*Lyngbya*) *wollei* abundance and nitrogen oxides, ammonium, and soluble reactive phosphorus, at various sites at Flats. Laboratory experiments included nutrient bioassays and acetylene reduction assays to assess the *Microseira* (*Lyngbya*) *wollei* growth rates and nitrogen fixation rates. Nutrient bioassay experiments were conducted in which *Microseira* (*Lyngbya*) *wollei* samples received different nutrient additions of either nitrate (NO_3^-), phosphate (PO_4^{3-}), $NO_3^- + PO_4^{3-}$, or ammonium (NH_4^+). The growth response of *Microseira* (*Lyngbya*) *wollei* was measured over a six-day period and compared to the growth of control samples with no nutrient additions. The

growth rates were variable in both 2022 and 2023 but were stimulated by nutrient additions. The nitrogen fixation experiments were held over a 24-hour period and the *Microseira* (*Lyngbya*) *wollei* group that received daily PO_4^{3-} treatments had the highest nitrogen fixation rates. Although the growth rates were variable, a seasonal growth and nitrogen fixation pattern emerged, showing that the *Microseira* (*Lyngbya*) *wollei* nitrogen fixation rates are higher in the early summer months when growth rates are low, and the nitrogen fixation rates are lower in the late summer months when growth rates are higher. It is further hypothesized that *Microseira* (*Lyngbya*) *wollei* allocates energy to nitrogen fixation in the early summer months to produce potential anti-grazing toxins for protection. Later in the summer, it may recycle the nitrogen within its mats, reducing the need for continued nitrogen fixation. The *Microseira* (*Lyngbya*) *wollei* can then focus energy into growth, completing the seasonal pattern.

Introduction

The filamentous Cyanobacteria *Microseira* (*Lyngbya*) *wollei* is a non-heterocystous diazotroph, capable of converting N_2 gas dissolved in the water into ammonia (NH_3) for its own cellular use (Phlips et al., 1992). Gaseous N_2 comprises ~78% of the atmosphere and is available to nitrogen fixing prokaryotes, also known as diazotrophs, in the dissolved form in surface seawater. Only very specific groups of some heterotrophic bacteria and Cyanobacteria (diazotrophs) possess the enzyme nitrogenase, that catalyzes the reaction of nitrogen fixation (Paerl and Zehr, 2000). The very stable triple bond in N_2 makes nitrogen (N) fixation a very energetically demanding reaction; despite the energy cost, diazotrophs can have a competitive advantage over other non-diazotrophic eukaryotes in nitrogen-limited waters by N_2 into bioavailable ammonia. (Gallon,

1992; Paerl and Zehr, 2000; Deutsch et al., 2007; Schmittner et al., 2008). The biological nitrogen fixation reaction is as follows:

$$N_2 + 8H^+ + 8e^- + 16ATP \xrightarrow{\text{(nitrogenase)}} 2NH_3 + H_2 + 16ADP + 16P_i \quad \text{(Equation 1)}$$

During biological N fixation, N_2 is reduced to NH_3 by the enzyme nitrogenase. The process uses 8 hydrogen ions and 8 electrons to reduce the N_2 to NH_3 and the hydrolysis of 16 adenosine triphosphate (ATP) to 16 adenosine diphosphate (ADP) + $16P_i$ supplies the reaction with the required energy to split the N_2 triple bond. Hydrogen gas (H_2) and ammonia (NH_3) are the byproducts of the reaction. The NH_3 then accepts a proton (H^+) from water (H_2O), which results in the formation of ammonium (NH_4^+) for its own cellular needs. (Equation 1). Upon death or decay of the N fixing organisms, it releases the newly fixed nitrogen to the environment as bioavailable NH_4^+, which is then available to other non-nitrogen fixing organisms (Paerl and Zehr, 2000).

N_2 fixing organisms, such as *M. wollei*, require certain environmental and nutrient conditions to fix nitrogen due to the energetically demanding process (Phlips et al., 1992). Previous studies have shown that higher levels of Phosphorus (P) in aquatic environments can promote Cyanobacteria harmful algal bloom formation (cHAB) (Schindler et al., 2008), with diazotrophic capacity alleviating N limitation. Consequently, P is likely the limiting nutrient for *M. wollei* growth, and *M. wollei* requires sufficient access to P, through the water column or P-rich sediments, as energy for nitrogenase activity (Hamilton et al., 2016). However, diazotrophic Cyanobacteria are efficient at halting their N_2 fixation when ample levels of readily assimilable

N, such as ammonium are available (Watkinson et al., 2005; Paerl et al., 2008). Consequently, diazotrophic Cyanobacteria can adapt to variable nutrient conditions, allowing them to thrive in both nutrient-rich and low-N waters. They can establish themselves initially through P uptake and N fixation, while non-diazotroph biomass is in low nitrogen environments (Elser et al., 2009; Lewis et al., 2020).

Because *M. wollei* is not N-limited like many eukaryotic phytoplankton (Paerl and Zehr, 2000), it can thrive in low N environments, such as those that occur seasonally within the submerged aquatic vegetation (SAV) beds at the Susquehanna Flats. Dissolved inorganic nitrogen (DIN) has been demonstrated to be substantially reduced at the center of the Flats SAV bed where SAV biomass was higher (Gurbisz et al., 2016). This occurs because SAV beds with their large seasonal biomass, such as the one on the Flats, reduce wave and current energy, causing suspended sediment and other particles that may contain nutrients to settle and are subsequently taken up by growing SAV biomass from the sediments (Ward et al., 1985; Gambi et al., 1990; Granata et al., 2001; Peterson et al., 2004). The lower DIN and dissolved inorganic phosphorus (DIP) in the water column limits the phytoplankton and epiphyte growth, which allows sufficient light to reach the benthos and allows for SAV photosynthesis (Moore, 2004; Gurbisz et al., 2016). The limitation of phytoplankton and epiphyte growth contributes to increasing water clarity at the center of the SAV bed. SAV also takes up DIN in the water column and may enhance denitrification, which may also account for lower levels of DIN at the center of the SAV bed at Susquehanna Flats during the summer months (Gurbisz and Kemp, 2014). The combination of increased water clarity and lower water column DIN levels provides an open niche for *M. wollei* to thrive as a diazotroph.

Therefore, the lower DIN levels at the Susquehanna Flats center (Gurbisz et al., 2016) likely selects for *M. wollei* growth, given its diazotrophic capacity. However, *M. wollei* growth requires ample access to phosphorus as well, for nitrogen fixation. This suggests that the *M. wollei* growth could be stimulated by available DIP and/or sediment P availability (Watkinson et al. 2005; Ahern et al., 2007). It is hypothesized that *M. wollei* establishes itself on the benthos at the center of the Flats where the sediment is rich in legacy P. The integrity of *M. wollei's* filaments effectively traps the fine-grained sediment particles as they overtop SAV plants and shade the benthos. As they get access to light and rapidly photosynthesize, the oxygen bubbles get trapped within the filaments and cause the Cyanobacteria to float to the surface in dense tangled mats (Albert et al., 2005). Once they create these mats, they then can utilize the P from the trapped sediment particles entrained within its filaments as well as DIP from the water column. Therefore, it is also hypothesized that there are lower water column DIN and DIP levels where *M. wollei* is most prevalent.

To develop an understanding of *M. wollei* nutrient limitation, optimum growth and conditions that promote nitrogen fixation, nutrient bioassay growth and nitrogen fixation experiments were carried out during the summer seasons of 2022 and 2023. It was hypothesized that *M. wollei* growth rates would be higher among the groups that received a nitrogen + phosphate treatment since the *M. wollei* would not be N or P limited. Additionally, it was anticipated that higher nitrogen fixation rates would be measured among the samples that received phosphate treatments, as they would experience nitrogen-limited conditions and because phosphate acts as an enzyme in the nitrogen fixation process. Experiments were also designed to investigate sediment nitrogen fixation under aerobic and anaerobic conditions to address nutrient availability

for the *M. wollei* and confirm whether most nitrogen fixation occurs within the sediment microbiome or with the *M. wollei* and its associated microbial community.

Methods

Study Site and Sample Collection

Microseira wollei samples were collected on June 14-15 and July 26-27 in 2022 and June 5-6 and August 7 in 2023. Core samples were taken by hand while snorkeling, for *M. wollei* and SAV biomass, and nutrients and other water quality parameters from the Susquehanna Flats at sites along 2 crisscrossing transects (Figure 3.1). Percent cover of SAV and Cyanobacteria was estimated in four random 0.25 m^2 quadrats at each site, using a one to four scale, with one being 0-25% and four being 75-100% cover (Duarte and Kirkman, 2001). Samples of *M. wollei* for laboratory experiments were also collected directly from benthos by snorkeling. In 2022, most samples were collected from sites 22 and 23. In 2023, most samples were collected from sites 17, 23, and 27. (Figure 3.1). Samples were transported in coolers with site water, to the laboratory, where samples were subsequently cleaned of other material (e.g. SAV, invertebrates, detritus). Aerators kept samples from going anaerobic.

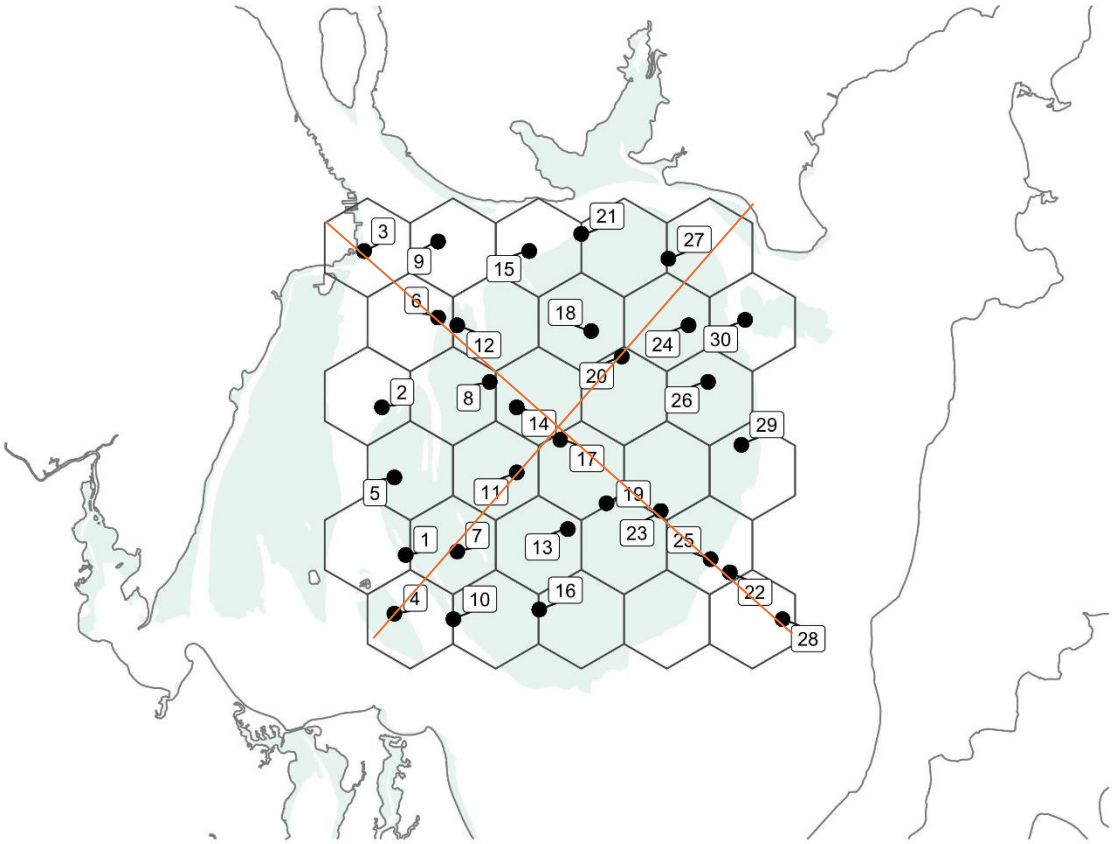

Figure 3.1 Map of the Susquehanna Flats site numbers and location relative to the SAV bed. Black points represent sites, and the red cross represents the two transects.

Nutrient Bioassay Growth Experiment

Samples for nutrient bioassays were rinsed with filtered site water back at the lab, and forceps were used to remove any remaining organisms, such as invertebrates and SAV. Subsamples of volumetrically measured (5 mL) *M. wollei* in 3L wide-mouthed polycarbonate jars containing 700 mL of GF/F filtered (nominal pore size of 0.7 µM) site water in triplicate treatments of: 10 µM NO_3^-, 5 µM PO_4^{3-}, 10 µM NO_3^- + 5 µM PO_4^{3-}, and 10 µM NH_4^+, and controls with no

nutrient additions (Table 3.1, Figure 3.2). Nutrients were added daily at ~12:00-13:00 h, and lightly stirred to ensure even distribution.

Before the initial addition of nutrient treatments, samples were maintained in an incubation chamber at ambient temperature and 12h light/dark cycle at ~ 50 µE light (using a Waltz UM-500 light meter) (under 2 layers of neutral density screening) for two to four days to acclimate; and then subsequently wet-weight obtained for initial biomass. Wet weight of biomass samples were obtained every two to three days and the experiment terminated after ~six days, at which time cumulated biomass was calculated to determine growth rate. In 2022, excess water was uniformly blotted from the samples, before each weighing. In 2023, samples were wrapped in a filter to contain the filaments and were spun in a salad spinner in a consistent manner, to remove excess weight from water, before each weighing, which yielded more reproducible results (Image 3.1).

Table 3.1. Nutrient bioassay growth rate experiment samples, sample number, and assigned nutrient treatments.

Sample	**Nutrient Treatment**
1-3	Control
4-6	+ 10 µM NO_3^-
7-9	+ 5 µM PO_4^{3-}
10-12	+ 10 µM NO_3^- + 5 µM PO_4^{3-}
13-15	+ 10 µM NH_4

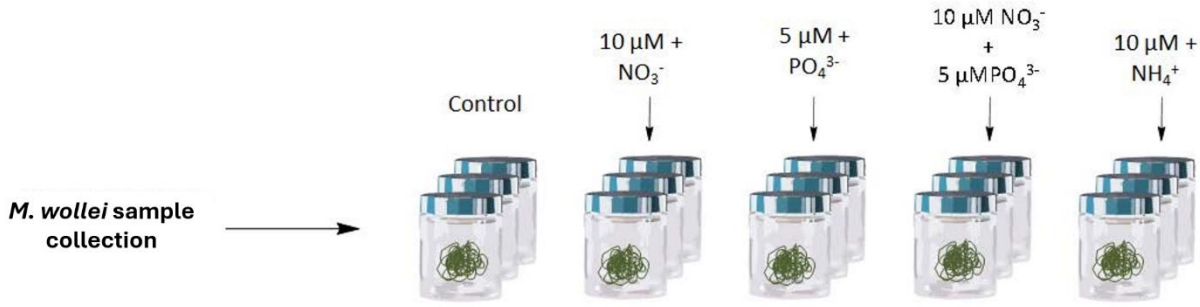

Figure 3.2: Nutrient bioassay growth experimental set-up in triplicate. Three control samples, three samples that received a daily nitrate (+ NO_3^-) treatment, three samples that received a daily phosphate treatment (+ PO_4^{3-}), three samples that received a daily nitrate + phosphate treatment (+ NO_3^- + PO_4^{3-}), and three samples that received a daily ammonium (+ NH_4^+) treatment (Graphic: A. Vader, UMCES).

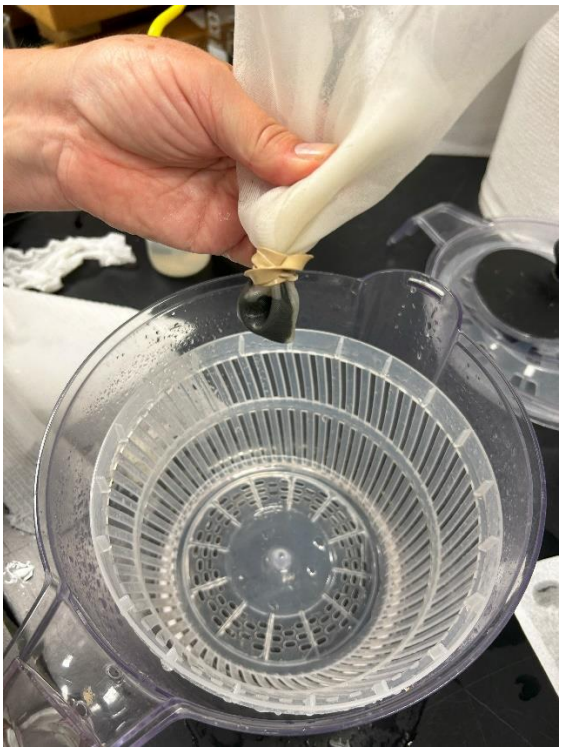

Image 3.1 Removal of excess water from *M. wollei* samples with use of salad spinner, to provide more consistent measurement of biomass wet weights among all samples.

Microseira (*Lyngbya*) *wollei* Nitrogen Fixation Experiments

Subsamples of *M. wollei* from the nutrient bioassay experiment were used for N fixation experiments using the acetylene reduction assay (ARA) method (Hardy et al., 1968, Capone, 1993). (Equation 2).

$C_2H_2 + 2e^- + 2H^+ \rightarrow C_2H_4$ (Equation 2)

Subsamples consisting of 0.5 mL of *M. wollei* and 30 mL of filtered site water were placed in 50 mL Erlenmeyer flasks with gas-tight suba-seal caps. Acetylene gas, generated from reacting calcium carbide and water, was then added to the flasks at a volume equal to 15% gas phase volume of the flask. These samples were then measured immediately for acetylene reduction, taking several time points over a 24h period. This method uses acetylene as a triple bonded substrate analog for nitrogen gas, and the enzyme nitrogenase preferentially reduces the weaker triple bond of acetylene to ethylene (rather than the stronger triple bond of dinitrogen to ammonium). (Equation 2). Ethylene production was measured by injecting 100 µL subsamples of the headspace of each flask with a gas-tight syringe into a Shimadzu gas chromatograph GC-8A with a Flame Ionization Detector (FID). Acetylene reduction rates were determined by the ethylene peak heights recorded on a Chromatopac Integrator (C-R8A) and compared to the peak heights of 100 ppm ethylene standards. These measurements were normalized to the dry weight of the Cyanobacteria samples and flask headspace volume. The acetylene reduction rates were converted to nitrogen fixation rates using a standard 3:1 ratio of acetylene to nitrogen reduced (Hardy et al., 1968; Goldsborough and O'Neil, 2016; Capone, 1993; Montoya et al., 1996; Postgate, 1998).

Sediment Nitrogen Fixation Experiments

To test whether the majority of N fixation was produced either by *M. wollei* or sediment microbes, sediment N fixation experiments were also conducted. Sediment samples were collected using 250 ml cut-off syringes to sample the top ~5cm of the sediment along North-South (N-S) and East-West (E-W) transects. Cores were maintained in an upright position in coolers until processed at Horn Point Laboratory (O'Neil and Capone, 1989). The experimental flasks were sampled for ethylene production approximately four times over a ~24 h period. Samples of 20 ml of sediment and 40 ml of site water were added to 250 ml flasks with the gas tight seal product, suba-seal, in duplicate treatments of either aerobic or anaerobic (flushed with nitrogen gas) headspace conditions in the dark, to measure nitrogen fixation rates to test whether rates were primarily heterotrophic or autotrophic in nature, along an anaerobic to aerophilic gradient. After ethylene analysis, the dry weights were then taken to normalize the ARA results. (Montoya et al., 1996; Postgate, 1998)

Results

Susquehanna Flats Bottom Nutrients and *Microseira wollei* Abundance

Microseira wollei was most abundant in the southeast part of the Flats in both 2022 and 2023, which generally corresponded to lower bottom water concentrations of SRP, NO_x, and NH_4^+. In June 2022, the bottom NH_4, NO_x, and SRP levels were negatively correlated with *M. wollei* abundance ($p < 0.05$). The July 2022 bottom NH_4, NO_x, and SRP levels were not significantly correlated with *M. wollei* abundance. (Table 3.3; Figure 3.3, 3.4, 3.5, 3.6).

In June 2023, the Flats experienced an anomalous high tide at the time of sampling, which may have caused enhanced water column mixing and increasing inputs from the surrounding Chesapeake Bay water (Table 3.2). The bottom NH_4 and NOx levels had low negative correlation with *M. wollei* abundance and the bottom SRP levels had a moderate positive correlation with *M. wollei* abundance. In August 2023, the bottom NH_4 levels had no correlation with *M. wollei* abundance and NO_x levels had moderate negative correlations with *M. wollei* abundance and the bottom SRP levels had a low positive correlation with *M. wollei* abundance. In 2023, the correlations between nutrient levels and *M. wollei* abundance were not significant. (Table 3.3; Figure 3.3, 3.4, 3.5, 3.6).

Table 3.2 High (H) and low (L) tide levels (m) at Havre de Grace, Maryland on June 6 in 2021-2024 and the time of each tide measurement. Asterisk (*) represents the sampling time at the Flats during the anomalous high tide event (NOAA Tide Predictions, 2021-2024).

Date	Time	Tide (m)	High/Low
2021	1:56 AM	0.15	L
	8:07 AM	0.75	H
	3:08 PM	0.15	L
	8:32 PM	0.6	H
2022	3:28 AM	0.6	H
	9:20 AM	0.19	L
	3:14 PM	0.76	H
	10:13 PM	0.12	L
2023	12:05 AM	0.55	H
	5:59 AM	0.11	L
	11:55 AM	0.92*	H
	7:35 PM	0.07	L
2024	4:01 AM	0.1	L
	10:06 AM	0.91	H
	5:43 PM	0.05	L
	10:55 PM	0.57	H

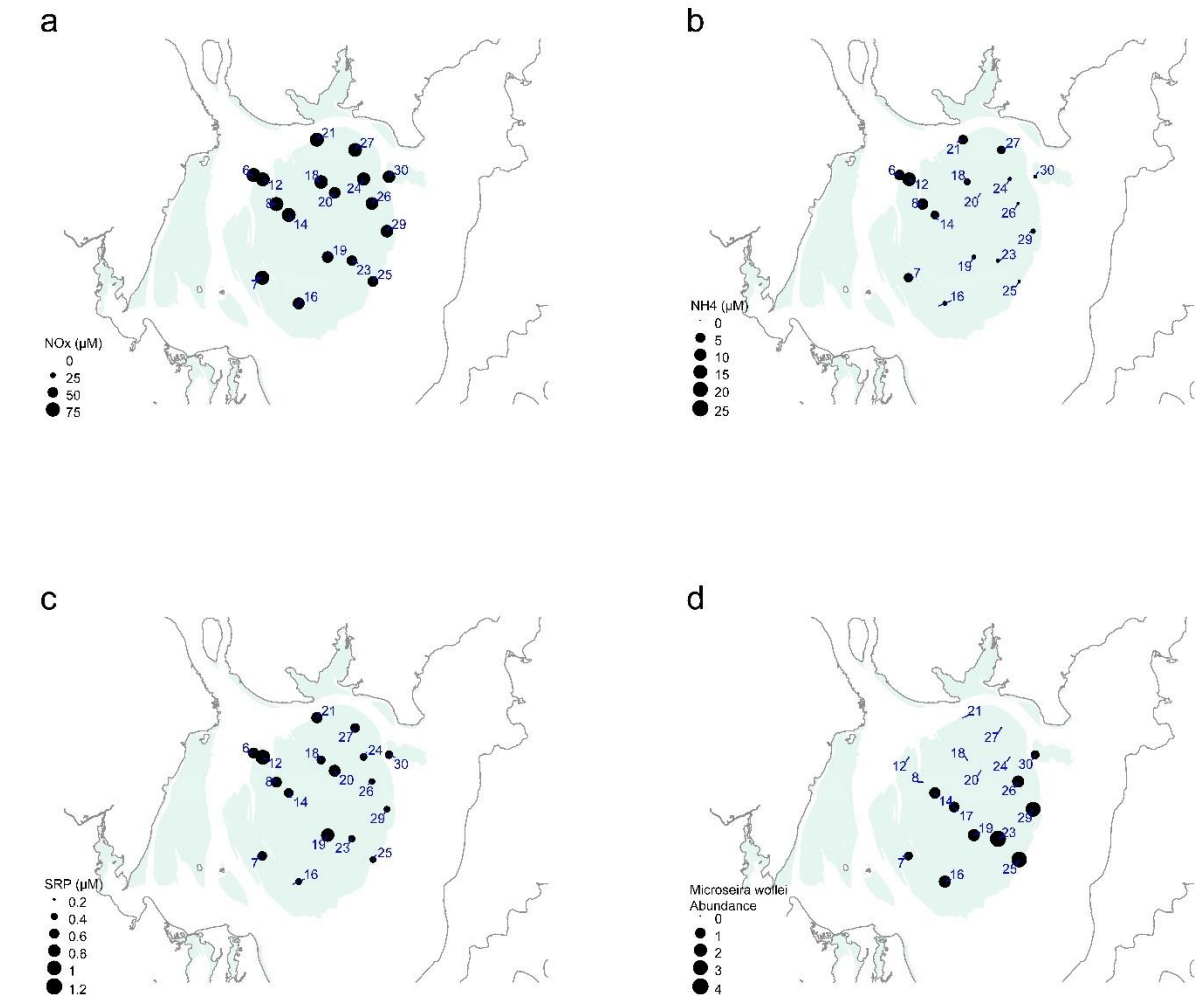

Figure 3.3 Figure presents the spatial distribution of nutrient concentrations and the abundance of *M. wollei* at the Flats on 14-15 June 2022. The varying sizes of circles represent different concentration levels, and the numbers represent the site number. A. NO_x (µM) b. NH_4 (µM) c. SRP (µM) d. *M. wollei* abundance (0 = 0% quadrat cover, 1 = 1-25% quadrat cover, 2 = 26-50% quadrat cover, 3 = 51-75% quadrat cover, 4 = 76-100% quadrat cover).

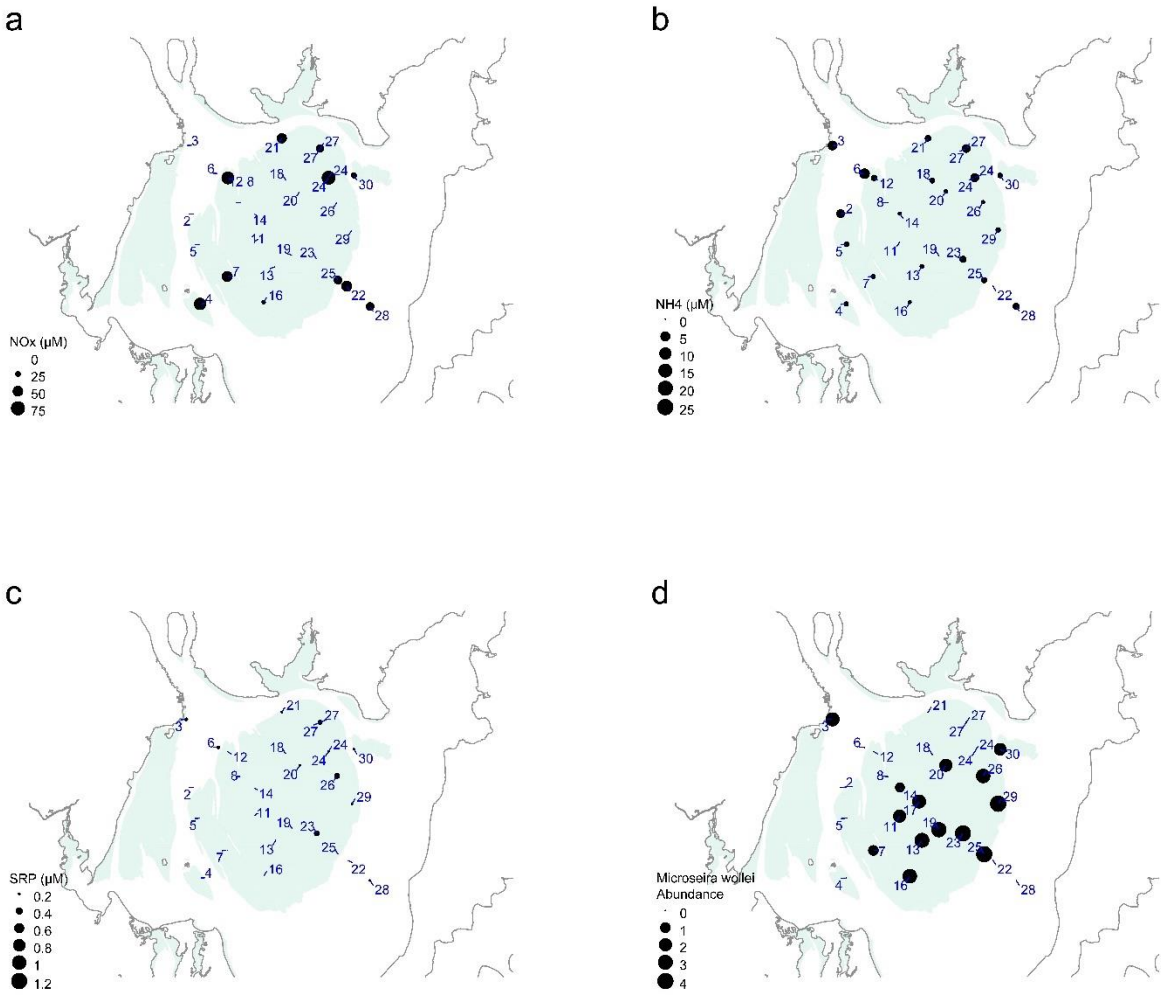

Figure 3.4 Figure presents the spatial distribution of nutrient concentrations and the abundance of *M. wollei* at the Flats on 26-27 July 2022. The varying sizes of circles represent different concentration levels, and the numbers represent the site number. A. NO_x (µM) b. NH_4 (µM) c. SRP (µM) d. *M. wollei* abundance (0 = 0% quadrat cover, 1 = 1-25% quadrat cover, 2 = 26-50% quadrat cover, 3 = 51-75% quadrat cover, 4 = 76-100% quadrat cover).

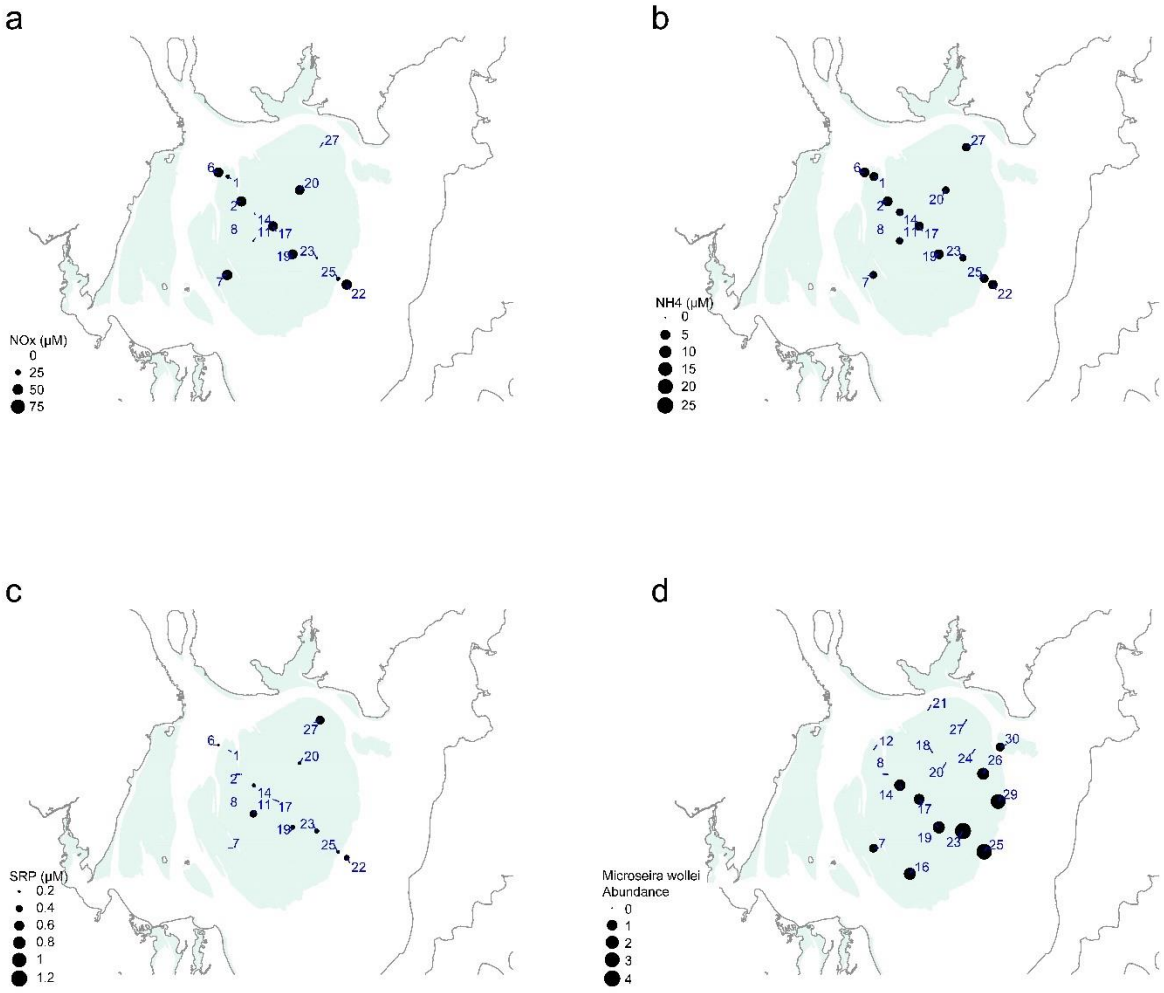

Figure 3.5 Figure presents the spatial distribution of nutrient concentrations and the abundance of *M. wollei* at the Flats on 5-6 June 2023. The varying sizes of circles represent different concentration levels, and the numbers represent the site number. A. NO_x (µM) b. NH_4 (µM) c. SRP (µM) d. *M. wollei* abundance (0 = 0% quadrat cover, 1 = 1-25% quadrat cover, 2 = 26-50% quadrat cover, 3 = 51-75% quadrat cover, 4 = 76-100% quadrat cover).

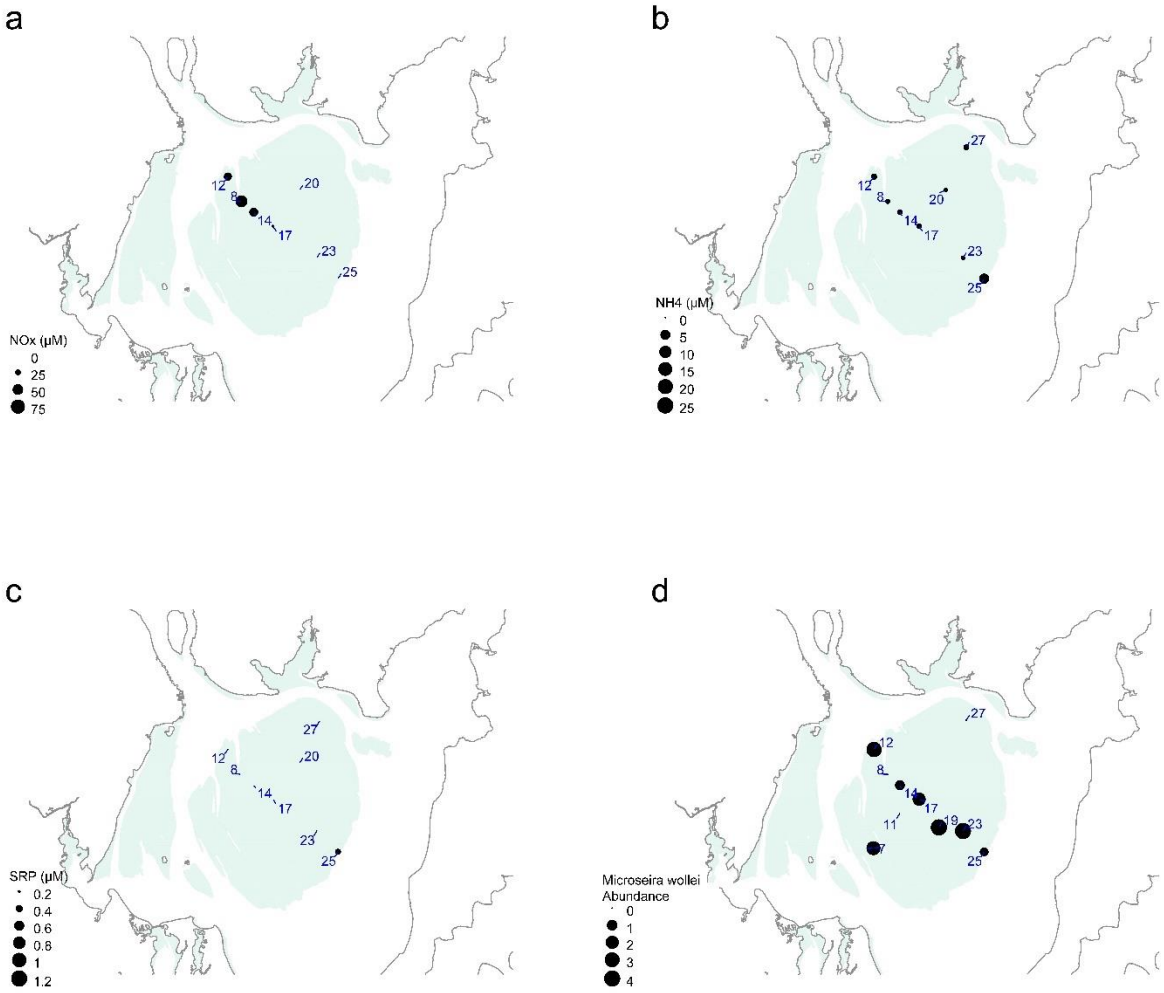

Figure 3.6 Figure presents the spatial distribution of nutrient concentrations and the abundance of *M. wollei* at the Flats on 6-7 August 2023. The varying sizes of circles represent different concentration levels, and the numbers represent the site number. A. NO_x (µM) b. NH_4 (µM) c. SRP (µM) d. *M. wollei* abundance (0 = 0% quadrat cover, 1 = 1-25% quadrat cover, 2 = 26-50% quadrat cover, 3 = 51-75% quadrat cover, 4 = 76-100% quadrat cover).

Table 3.3 Pearson values and *p*-values of *Microseira wollei* abundance and NH_4, NO_x, and SRP levels (µM) taken from the water column bottom and surface in June and July 2022 and June and August 2023. Significant *p*-values ($p < 0.05$) are labeled with an asterisk (*).

Month/Year	Bottom/Surface	Nutrient	Pearson r-value	*P*-value
June 2022	Bottom	NH_4	-0.63	0.007*
		NOx	-0.65	0.005*
		SRP	-0.6	0.01*
	Surface	NH_4	-0.4	0.123
		NOx	0.18	0.52
		SRP	0.23	0.39
July 2022	Bottom	NH_4	-0.29	0.15
		NOx	-0.37	0.06
		SRP	0.25	0.21
	Surface	NH_4	-0.41	0.03*
		NOx	-0.31	0.12
		SRP	-0.03	0.87
June 2023	Bottom	NH_4	-0.22	0.54
		NOx	-0.15	0.68
		SRP	0.35	0.32
	Surface	NH_4	-0.36	0.3
		NOx	0.01	0.99
		SRP	-0.01	0.99
August 2023	Bottom	NH_4	0	1
		NOx	-0.45	0.31
		SRP	0.24	0.57
	Surface	NH_4	-0.83	0.01*
		NOx	-0.58	0.13
		SRP	0.62	0.1

Nutrient Bioassay Growth Rates

Growth rates were highly variable in both 2022 and 2023 for the control samples and the experimental groups that received daily nitrate treatment and phosphate treatment. Filamentous Cyanobacteria is difficult to work with as each filament is made up of hundreds of cells and there

is no uniform way to measure it, and because it can trap so much organic material (McGregor and Sendall, 2015; Engene et al., 2018). This may have caused variability in the results. In 2022, the samples with added nitrate had the highest mean growth rate (0.098 grams/day (g/d)) and the samples with added nitrate + phosphate had the lowest mean growth rate (0.009 g/d). The group with added nitrate and the group with added phosphate, had higher mean growth rates than the control group, but with higher standard errors. The group that received nitrate + phosphate and the group that received ammonium treatments had lower mean growth rates than the control group and had lower standard errors. Methods were being developed in 2022, which account for only one replicate of the experiment and may account for inconclusive results. It is unclear why the group that received the nitrate + phosphate treatment and the group that received the ammonium treatment had lower growth rates than the control group (Figure 3.3).

The 2023 nutrient bioassay growth rate experiments included experiments in June, July, and August. Thus, each experiment will be referred to by the month it was held in. In 2023, all mean growth rates were lower in June than in July and August. The control group exhibited the highest mean growth rate in June (0.062 g/d). However, in July, the group that received the nitrate + phosphate treatment had the highest growth rate (0.150 g/d) and in August, the groups that received the nitrate treatment and nitrate + phosphate treatment had the highest growth rates (0.125 g/d). (Figure 3.4).

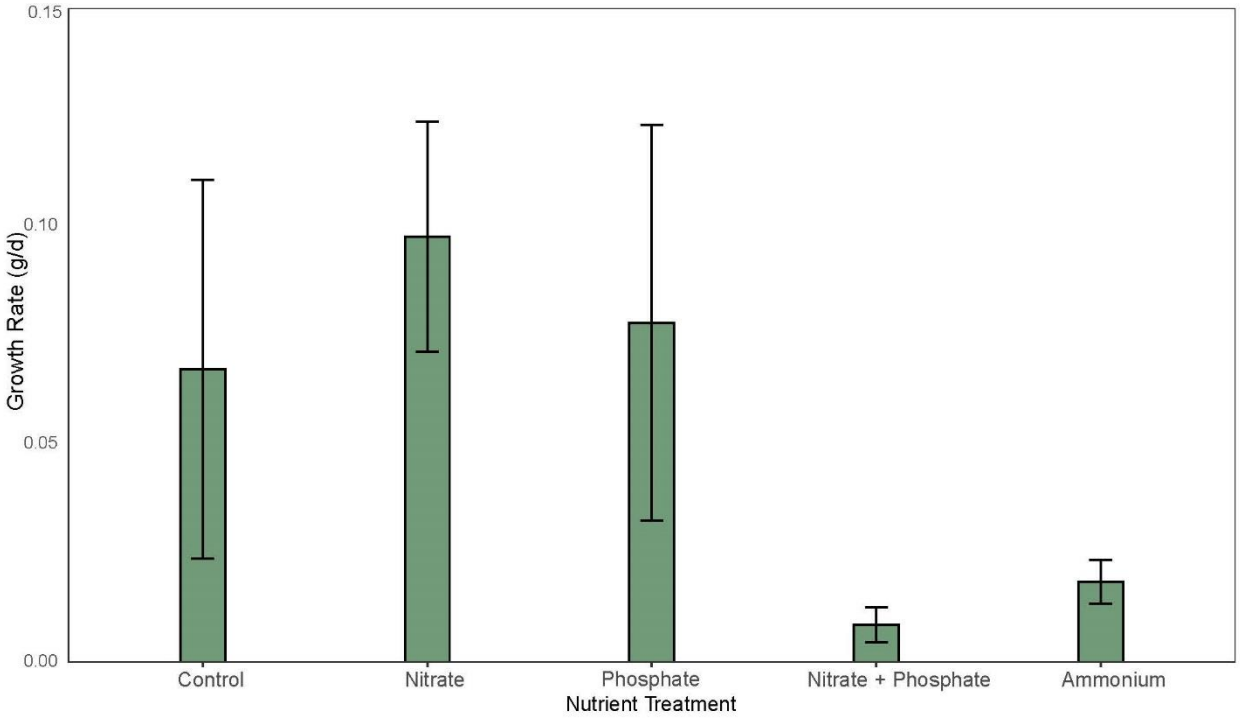

Figure 3.3 Nutrient bioassay mean growth rates of *M. wollei* samples collected from the Susquehanna Flats in July 2022. The experiment was conducted over a 6-day period in August 2022. The x-axis denotes the various nutrient treatments, including Control, Nitrate, Phosphate, Nitrate + Phosphate, and Ammonium, while the y-axis represents the growth rate in grams per day (g/d). Each bar represents the mean growth rate of the samples that received the respective treatment, with error bars indicating the standard error of the mean.

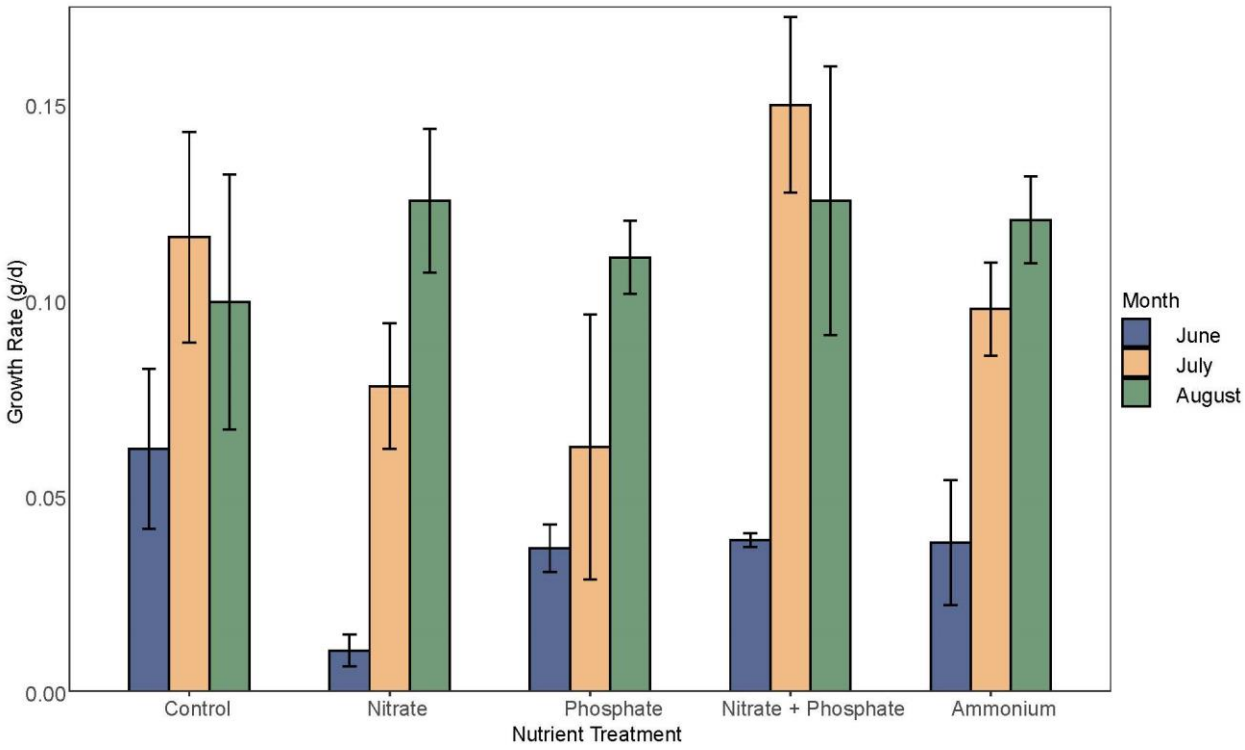

Figure 3.4 Nutrient bioassay mean growth rates of *M. wollei* samples collected from the Susquehanna Flats in June, July, and August 2023. The experiment was held over a six-day period during the respective months in 2023. The x-axis denotes the various nutrient treatments, including Control, Nitrate, Phosphate, Nitrate + Phosphate, and Ammonium. The y-axis represents the growth rate in grams per day (g/d). Blue signifies the mean growth rate in June for each nutrient treatment, pink signifies the mean growth rate in July for each nutrient treatment, and green signifies the mean growth rate in August for each nutrient treatment. Error bars represent the standard error of the mean.

Microseira (*Lyngbya*) *wollei* and Sediment Nitrogen Fixation Rates

Microseira wollei nitrogen fixation rates in 2023 were higher in July than in August. The only increase in rates over control were in experimental group that received phosphate treatments starting 20 July 2022, although due to high variability, was not statisitcally significant. The experimental group that received phosphate treatments also had a higher mean nitrogen fixation rate than the control group. N_2 fixation declined and all samples exhibted little to no nitrogen fixation rates at the beginning of August. (Figure 3.5).

In 2023, the N_2 fixation rates were higher in June before dropping off considerably in July and August. The group that received daily phosphate treatments had the highest mean nitrogen fixation rates in both June experiments. The group that received ammonium treatments had the lowest mean nitrogen fixation rates during the experiment that began on 15 June 23 and the group that received the nitrate + phosphate treatment had the lowest nitrogen fixation rates during the experiment that began on 22 June 2023. N_2 fixation rates dropped considerably to minimal levels that were considered to be zero nitrogen fixation or background fixation rates in July and August. (Figure 3.6).

The sediment collected from the N-S E-W transects had lower nitrogen fixation rates than the *M. wollei* samples by two to three orders of magnitude. The nitrogen fixation rates were not significantly different between the aerobic and anaerobic samples collected in June and July 2022 and June and August 2023. (Table 3.4 and 3.5).

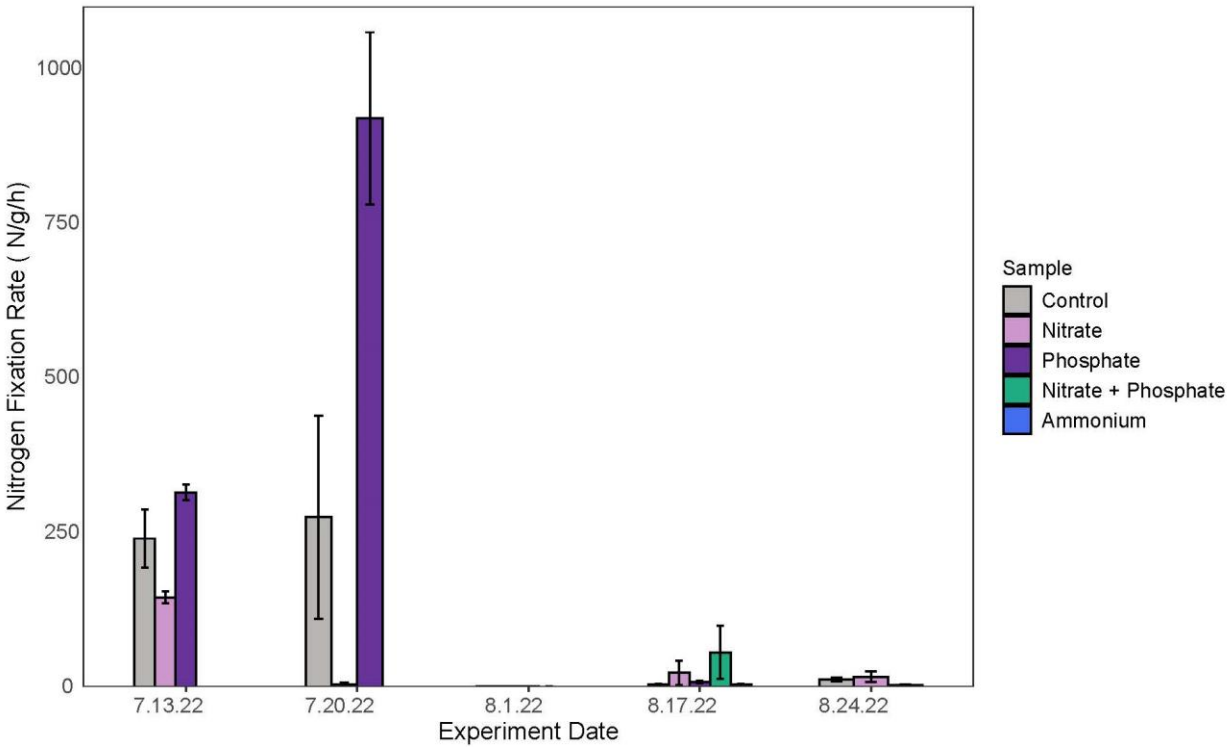

Figure 3.5 Average nitrogen fixation rates for different nutrient treatments (Control, Nitrate, Phosphate, Nitrate + Phosphate, Ammonium) from 2022. The x-axis denotes the start date of each experiment and the y-axis represents the nitrogen fixation rate in nitrogen/grams/hour (N/g/h). The error bars represent the standard error of the mean. Gray bars represent the control samples, pink represents the samples that received the nitrate treatment, purple represents the samples that received the phosphate treatment, green represents the samples that received the nitrate + phosphate treatment, and the blue bars represent the samples that received the ammonium treatment.

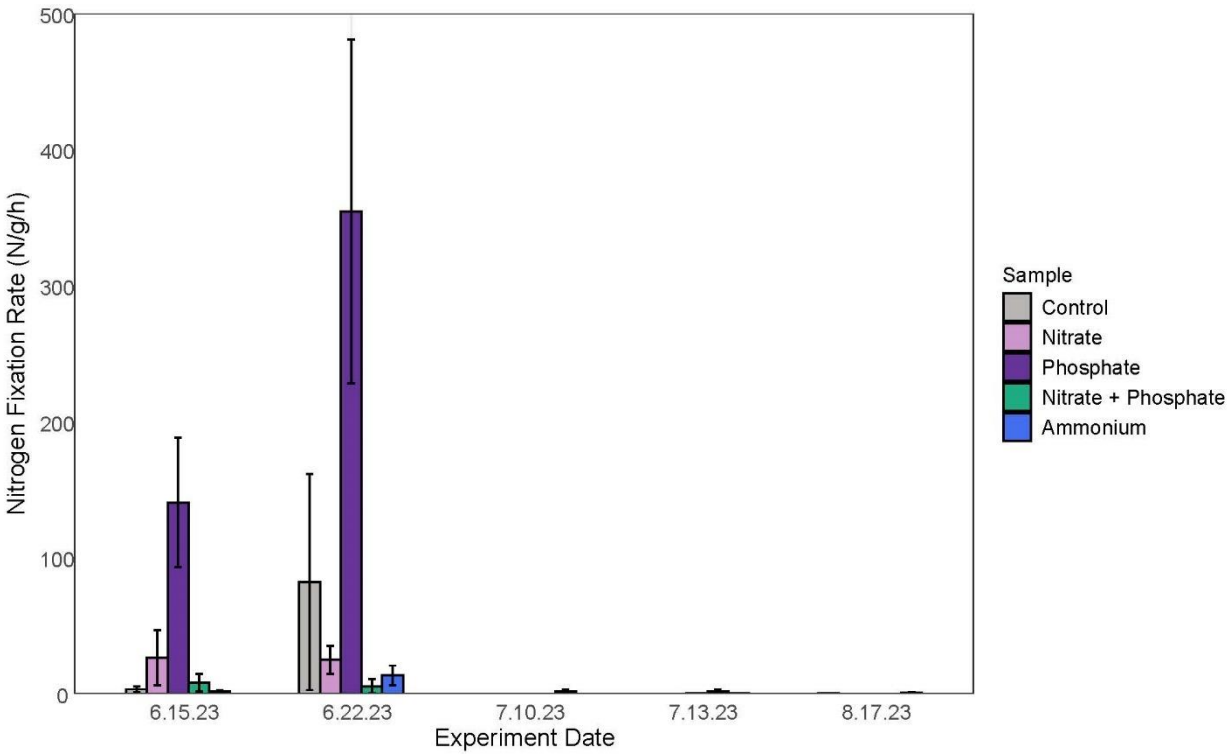

Figure 3.6 Mean average nitrogen fixation rates for different nutrient treatments (Control, Nitrate, Phosphate, Nitrate + Phosphate, Ammonium) from 2023. The x-axis denotes the start date of each experiment and the y-axis represents the nitrogen fixation rate in nitrogen/grams/hour (N/g/h). The error bars portray the standard error of the mean. Gray bars represent the control samples, pink represents the samples that received the nitrate treatment, purple represents the samples that received the phosphate treatment, green represents the samples that received the nitrate + phosphate treatment, and the blue bars represent the samples that received the ammonium treatment.

Table 3.4 Nitrogen fixation rates (N/g/h) from sediment samples collected in June and July 2022. Each row represents a sample identified by its number, which corresponds with the site the sample was collected from and its nitrogen fixation rate under anaerobic or aerobic conditions.

Month	Condition	Sample	Nitrogen Fixation Rate (N/g/h)
June	Aerobic	8	0.001
		12	0.338
		14	0
		17	0.001
		19	0.001
		23	0.002
		25	0.0004
	Anaerobic	8	0.0002
		14	0.002
		17	0.0004
		19	0.0002
		23	0.002
		25	0.002
July	Aerobic	7	0.266
		8	0.123
		11	0.029
		12	0.114
		14	0.055
		17	0.06
		19	7.532
		20	0.078
		22	0
		23	0.011
		25	0.021
		27	0.044
	Anaerobic	7	0.052
		8	0.050
		11	0.049
		12	0.069
		14	0.0913
		17	0.1
		19	5.064
		20	0.086
		22	0
		23	0.109
		25	0.068
		27	0.038

Table 3.5 Nitrogen fixation rates (N/g/h) from sediment samples collected in June 2023. Each row represents a sample identified by its number, which corresponds with the site the sample was collected from and its nitrogen fixation rate under anaerobic or aerobic conditions.

Month	Condition	Sample	Nitrogen Fixation Rate (N/g/h)
June	Aerobic	7	0.002
		8	0.002
		11	0.001
		12	0.029
		14	0.002
		17	0.002
		19	0.001
		20	0.002
		23	0.003
		25	0.001
		27	0.001
	Anaerobic	7	0.003
		8	0.001
		11	0.001
		12	0.001
		14	0.002
		17	0.003
		19	0.001
		23	0.002
		25	0.001
		27	0.000

Discussion

During most sampling trips, *M. wollei* abundance was significantly negatively correlated with NH_4, NO_x, and SRP bottom water nutrient levels in June 2022. *Microseira wollei* abundance also had a significant negative correlation with surface NH_4 in July 2022 and August 2023. (Table 3.3). These findings agree with the hypothesis that higher *M. wollei* abundance would occur with lower DIN and DIP levels because the lower DIN levels would limit phytoplankton and epiphyte growth and provide a niche for *M. wollei*. It was hypothesized that the DIP levels were generally

lower with higher *M. wollei* abundance because the *M. wollei* was utilizing the available DIP along with the particulate phosphorus to stimulate N_2 fixation in the early summer months and growth in the later summer months.

In August 2022, the nutrient bioassay experimental group that received the nitrate treatments had the highest mean growth rate, of 0.098 g/d. This could have occurred as the *M. wollei* had enough N and used energy for growth instead of investing in the energetically demanding process of fixing N_2. The control samples exhibited the highest mean growth in June 2023 of 0.062 g/d. This may imply that the *M. wollei* had adequate nutrients for growth from within its own mats and were not nutrient limited when collected. They could also have also been allocating the additional nutrients to saxitoxin production (which is a compound high in N) instead of growth. However, this was the only month this trend occurred. Overall, the samples in June 2023 exhibited the lowest mean growth rates and highest N fixation rates across sampling months. (Figure 3.11). Saxitoxin measurements were also higher in the early summer months than the later summer months (Wazniak et al., 2022 unpubl.). It is hypothesized that *M. wollei* was expending energy to fix N_2 and allocate the nitrogen into saxitoxin production rather than growth in the early summer months as they are not protected by the canopy of SAV growth, and they could be using the saxitoxins as an anti-grazing defense mechanism.

The samples exhibited higher growth rates and low to zero N_2 fixation in July and August 2023. (Figure 3.11) Measured $\delta^{15}N$ levels collected later in the summer 2023 and maintained in the lab had values of 10 ‰ which indicated highly recycled nitrogen (Rejmánková et al., 2004). It is

hypothesized that after *M. wollei* has fixed sufficient nitrogen for ample biomass, the mats begin to recycle the N internally, in the form of ammonium, which is more readily taken up in the later summer months and no longer need to fix N_2, which is energetically costly. They can recycle the N within its mats and use it for growth. This is also an indication that the mats are a consortium of microbes that create a mini ecosystem with biogeochemical processes occurring just within the mats.

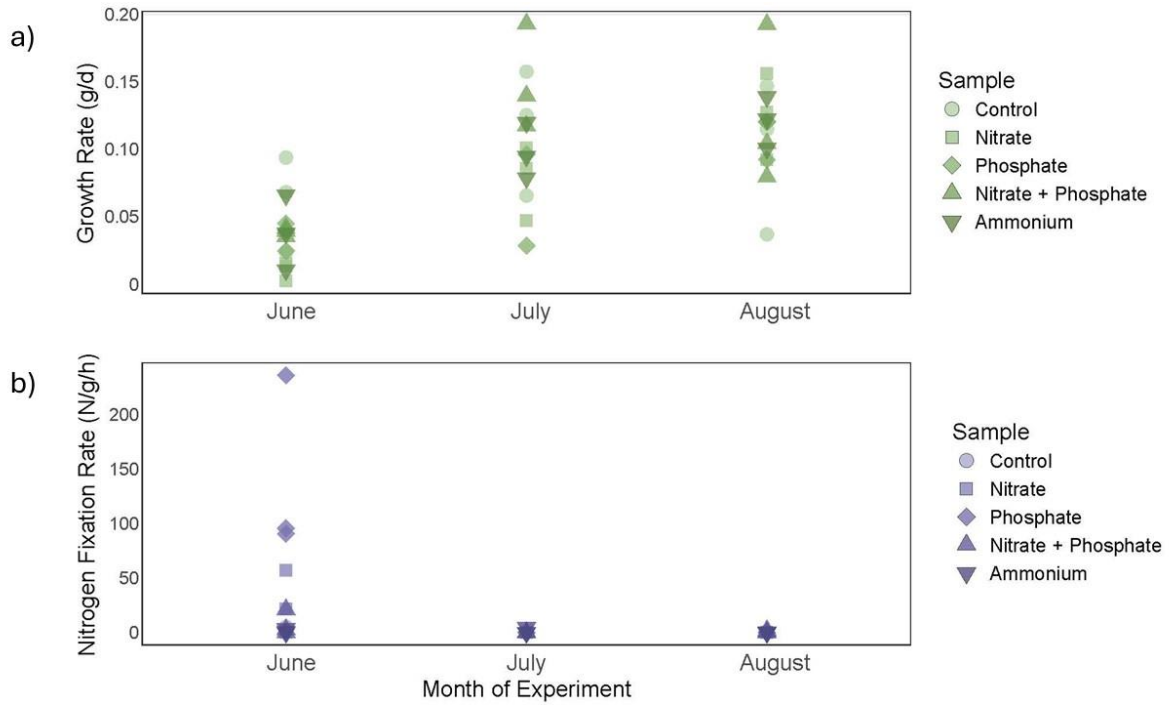

Fig 3.11 a) Scatter plot of the 2023 mean nutrient bioassay growth rates normalized to gram per day (g/d) from experiments held in June, July, and August. Each green shape represents a nutrient treatment group. b) Scatter plot of the 2023 mean nitrogen fixation rates normalized to nitrogen/gram/day (N/g/d) from experiments held in June, July, and August.

Microseira wollei may adopt a seasonal growth strategy to fix nitrogen and establish itself at the Flats during the early summer months when the area is nitrogen limited, which allows them to gain a foothold in the environment. Once it has fixed sufficient nitrogen and established itself, it uses recycled nitrogen within its mats, conserving energy that would otherwise be expended on nitrogen fixation for cellular needs and saxitoxin production. This energy could then be focused into growth.

The nutrient bioassay growth stimulation from both nitrogen and phosphorus additions were expected and were similar to the results reported by Yin et al. (1997), where they also found that nitrate and phosphate additions stimulated *M. wollei* growth. When Ahern et al. (2006) investigated *Moorea producens* (formerly *Lyngbya majuscula*), a marine filamentous Cyanobacteria, in Moreton Bay, Australia, they found similar results to the July 2022 experiment that nitrate and phosphate additions stimulated growth. Ahern et al. (2006) also found that phosphorus stimulated growth more often than nitrogen additions. The same result was produced only in the June 2023 experiment. Watkinson et al. (2005) also found that phosphorus additions stimulated photosynthesis in *Moorea producens* collected from Moreton Bay, Australia. Although biomass was not measured, productivity as measured by photosynthesis in these experiments, are analogous to potential growth rates. These studies suggest that the growth of filamentous Cyanobacteria, including *M. wollei*, is primarily stimulated by phosphorus, with nitrogen also promoting growth, albeit to a lesser extent than phosphorus. Given the variable results observed for *M. wollei* at the Flats in this study, it is recommended that additional nutrient

bioassay growth experiments be conducted specifically on *M. wollei* populations present at the Flats.

Samples that received the phosphate treatments had higher nitrogen fixation rates in the first two experiments conducted in 2022 and 2023. This supports results of previous studies on Cyanobacteria in general, and *M. wollei* specifically in this case, fixes nitrogen when they are nitrogen limited and have access to available P (Howarth et al., 1988; Paerl, 1990; Vitousek and Howarth, 1991). For example, at the beginning of summer, when N is limited, *M. wollei* forms mats on the benthos where the sediment is rich in P, which allow it to establish itself in nitrogen-depleted waters. They then have ample access to P to fix N_2 efficiently. This behavior might also explain why *M. wollei* traps P-laden sediment in its filaments and keeps it when forming surface mats.

Mann and Steinke (1993) observed a similar seasonal trend in nitrogen fixation with the Cyanobacteria *Lyngbya confervoides* C.Ag. ex Gomont, *Oscillatoria limosa* Ag. ex Gomont, and *Microcoleus chthonoplastes* Thuret ex Gomont at Beachwood Mangrove Nature Reserve II, South Africa. They found that N_2 fixation rates were higher during the early summer months and significantly decreased ($p < 0.05$) during the non-summer months. Paerl et al. (1993) demonstrated that dissolved organic carbon (DOC) stimulated nitrogenase activity in marine *Lyngbya spp.* dominated mats, with significantly higher nitrogenase activity observed in these samples compared to controls. Interestingly, the addition of N and P did not enhance nitrogenase

activity, although nitrogen did stimulate photosynthetic activity. Paerl et al. (1993) hypothesized that DOC stimulates nitrogenase activity, while nitrogen stimulates photosynthetic activity, indicating a strong interdependence between these two processes that supports the growth of the mats.

Although DOC additions were not directly incorporated into the bioassays, molecular analyses (Chapter 2) revealed that *M. wollei* mats harbor a diverse associated microbial community, and amphipods among other organic material was plentiful in the mats. It is hypothesized that these factors lead to complex biogeochemical processes and potentially create a self-sustaining ecosystem within the mats. With the results from the experiments on *M. wollei* from the Flats, and the experiments led by Mann and Steink (1993) and Paerl et al (1993), it can be hypothesized that the effects of DOC and nutrient additions appear to vary among different populations of filamentous Cyanobacteria, depending on the specific environmental and nutrient conditions they encounter.

The variability in growth rates prevented drawing concrete conclusions, which are essential for modeling the Susquehanna Flats and understanding the behavior of *M. wollei* in this environment. To reduce this variability and gain a clearer understanding of seasonal growth patterns, additional replications of nutrient bioassays are needed. Further investigation into the seasonal patterns of growth and nitrogen fixation is also necessary, as these may be influenced by factors such as light availability, nutrient levels, or SAV growth. These seasonal patterns likely create varying conditions at the Flats throughout the year.

Conducting nitrogen fixation experiments across the full seasonal cycle of *M. wollei* abundance from May through September (or later, if it persists) would provide deeper insights into these patterns, aiding in the development of a model for the Flats and informing targeted, month-specific management strategies. While nutrient bioassays have been conducted, nutrient uptake rates remain unclear. Performing nutrient uptake experiments during the summer could reveal more about *M. wollei's* seasonal growth strategies. Additionally, nutrient bioassays focused on saxitoxin production should be conducted to identify which nutrients may trigger saxitoxin production, offering valuable information for management strategies. Regular monthly measurements of δ15N levels and saxitoxin production should also be taken to compare with growth, nutrient uptake, and nitrogen fixation rates. This comprehensive approach will enhance understanding of *M. wollei's* seasonal strategy and contribute to the development of a model for the Susquehanna Flats, ultimately guiding management strategies to support the growth of submerged aquatic vegetation (SAV).

Overall Conclusions

The recovering SAV beds on Susquehanna Flats play a key role in intercepting nutrients from the Susquehanna River basin, providing a valuable ecosystem service for the Chesapeake Bay. The low nutrient levels at the southeast part of the Flats, as compared to outside, indicate that the SAV beds are effective at sequestering incoming nutrients from the Susquehanna River. Although *M. wollei* and *Phormidium sp*. continue to bloom at the Flats seasonally, at ~11,000 acres, the SAV beds are continuing to grow and expand (Chesapeake Bay Program, 2024) and the filamentous Cyanobacteria mats do not seem to be affecting the SAV recovery efforts to date.

Microseira wollei may just be a "side effect" of reduced nutrient levels and the resurgence of SAV. The nitrogen limited waters are leaving an open niche for *M. wollei* and *Phormidium sp*. to bloom, but this should not halt SAV recovery efforts. Efforts to reduce nutrient levels, particularly phosphorus, should continue in the Chesapeake Bay, as the availability of phosphorus allows *M. wollei* to thrive as they can fix their own nitrogen. Additionally, measures to reduce sediment pollution should be maintained, and monitoring for *M. wollei* blooms should be implemented.

The molecular identification of *M. wollei* and *Phormidium sp*. and their 16S rRNA and *nifH* sequences will be entered into in NCBI GenBank for further reference. Toxin analysis of *M. wollei* at the Flats will continue and toxin analysis of *Phormidium sp*. at the Flats should also take priority. By documenting the sequences and the toxins produced by the filamentous Cyanobacteria at the Flats will provide information for other scientists who may encounter the same ecotype. This can allow for more collaboration and management efforts to hopefully reduce toxin impacts on animals and humans.

Further investigation into the microbial communities associated with filamentous Cyanobacteria should be conducted in various environments. As observed at the Flats, the microbial communities linked to *M. wollei* and *Phormidium sp*. are complex and may form a somewhat self-contained ecosystem, with biogeochemical cycles occurring within the mats. Therefore, when studying filamentous Cyanobacteria, it is important to consider their associated microbial

communities, as *M. wollei* was found to effectively traps these microbes, making it a host of many diverse microbes that interact with one another.

Creating an ecosystem model with the use of parameters measured in this study could provide crucial information about the upper Chesapeake Bay SAV community processes and help implement effective management programs. These studies can also help policymakers to identify how to implement monitoring and management programs for similar areas experiencing *M. wollei* or other Cyanobacterial blooms. A model can also be valuable to predict environmental changes of the Flats in a changing climate, as well as forecasting how these changes will affect the growth of *M. wollei* and SAV.

Microseira wollei and the newly observed, *Phormidium sp*. blooms need to be reported and investigated as *M. wollei* does produce saxitoxins, which can cause paralytic shellfish poisoning, and *Phormidium sp.* have been found to produce cyanotoxins (Gugger et al., 2005; Teneva et al., 2005; Wood et al., 2007; Borges et al., 2015). Colleagues at the Maryland Department of Natural Resources and the Boyer Lab at State University of New York Environmental Science Forestry confirmed, as part of this study, that the saxitoxins produced do enter amphipods that are living amongst, and presumably grazing on the *M. wollei* filaments (Wazniak et al., 2022 unpubl.). This is the first account of significant saxitoxin levels at the Susquehanna Flats and the largest values recorded to date in the Chesapeake Bay. Since much of the water quality and economy relies on

filter feeding shellfish, i.e. the eastern oyster (*Crassostrea virginica*), efforts to monitor these blooms and mitigate contamination need to be a priority.

Works Cited

Ahern, K., Ahern., C., Udy, J. 2006. Nutrient additions generate prolific growth of *Lyngbya majuscula* (Cyanobacteria) in field and bioassay experiments. *Harmful Algae, 6(1)*, 134-151. https://doi.org/10.1016/j.hal.2006.08.004.

Albert, S., O'Neil, J.M., Udy, J.W., Ahern, K.S., O'Sullivan, C.M., Dennison W.C. 2005. Blooms of the cyanobacterium *Lyngbya majuscula* in coastal Queensland, Australia: disparate sites, common factors. *Marine Pollution Bulletin, 51*, 428-437.

Anagnostidis, K., Komarek, J., 1988. Modern approach to the classification system of cyanophites. 3-Oscillatorisales. *Arch. Hydrobiol., 80*, 1988, 50–53.

Ashton, P.J. 1981. Nitrogen Fixation and the Nitrogen Budget of a Eutrophic Impoundment. *Water Research, 15(7),* 823-833. https://doi.org/10.1016/0043-1354(81)90136-6.

Baker, GC., Smith, J.J., Cowan, D.A. 2003. Review and re-analysis of domain-specific 16S primers. *J Microbiol Methods, 55*, 541–555.

Baker, P.D., Steffensen, D.A., Humpage, A.R., Nicholson, B.C., Falconer, I.R., Lanthois, B., Fergusson, K.M., Saint, C.P. 2001. Preliminary evidence of toxicity associated with the benthic cyanobacterium *Phormidium* in South Australia. *Environ. Toxicol., 16*, 506–511.

Barka, E. A., Vatsa, P., Sanchez, L., Gaveau-Vaillant, N., Jacquard, C., Meier-Kolthoff, J. P., Klenk, H. P., Clément, C., Ouhdouch, Y., & van Wezel, G. P. (2015). Taxonomy, Physiology, and Natural Products of Actinobacteria. Microbiology and molecular biology reviews: *MMBR, 80(1)*, 1–43. https://doi.org/10.1128/MMBR.00019-15.

Bartoli, M., D. Nizzoli, G. Castaldelli, and P. Viaroli. 2008. Community metabolism and buffering capacity of nitrogen in a *Ruppia cirrhosa* meadow. *Journal of Experimental Marine Biology and Ecology, 360*, 21–30. https://doi.org/10.1016/j.jembe.2008.03.005.

Batiuk, R., Brownson, K., Dennison, W., Ehrhart, M., Hanson, J., Hanmer, R., Landry, B., Reichert-Nguyen, J, Soueidan, J., Tassone, S., Vogt,B. 2023. Rising Watershed and Bay Water Temperatures: Ecological Implications and Management Responses – A STAC Workshop. STAC Publication Number 23-001. Edgewater, MD. (505 pages)

Bayley, S., V.D. Stotts, P.F. Springer, and J. Steenis. 1978. Changes in submerged aquatic macrophyte populations at the head of Chesapeake Bay, 1958–1975. *Estuaries, 1*, 171–182.

Ben-Porath, J., Zehr, J.P. 1994. Detection and characterization of Cyanobacterial *nifH* genes. *Appl Environ Microbiol., 60(3)*, 880-887. https://doi.org/10.1128/aem.60.3.880-887.1994.

Borges, H., Branco, L., Martins, M., Lima, C., Barbosa, P., Lira, G., Bittencourt, Oliveira, M., Molica, R. 2015. Cyanotoxin production and phylogeny of benthic Cyanobacterial strains isolated from the northeast of Brazil. *Harmful Algae, 43*, 46–57.

Boyd, C.E., Davis, J.A., Johnston, E. 1978. Die-offs of the blue-green alga, *Anabaena variabilis*, in fish ponds. *Arch. Hydrobiologia 74*, 129-133.

Brasell, K.A., Heath, M.W., Ryan, K.G., Wood, S.A. 2015. Successional change in microbial communities of benthic *Phormidium*-dominated biofilms. *Microb. Ecol., 69(2)*, 254–266.

Briand, J.F., Leboulanger, C., Humbert, J.F., Bernard, C., Dufour, P. 2004. *Cylindrospermopsis raciborskii* (Cyanobacteria) invasion at mid-latitudes: selection, wide physiological tolerance, or global warming. *J. Phycol., 40*, 231–238.

Brooks, B. W., Lazorchak, J. M., Howard, M. D. A., Johnson, M. V., Morton, S. L., Perkins, D. A. K., Reavie, E. D., Scott, G. I., Smith, S. A., & Steevens, J. A. 2017. In some places, in some cases, and at some times, harmful algal blooms are the greatest threat to inland water quality. *Environmental toxicology and chemistry*, *36*(5), 1125–1127. https://doi.org/10.1002/etc.3801.

Butler, A., Thomas, C., Calomeni, A., McQueen, A., & Slack, W. 2023. *Microseira wollei* (*M. wollei*) blooms in freshwater ecosystems in Lake St. Clair (Michigan, USA)–impacts and possible management approaches. *Engineer Research and Development Center (U.S.)*. https://doi.org/10.21079/11681/47648.

Byappanahalli, M., Shively, D., Nevers, M., Sadowsky, M., Whitman, R. 2003. Growth and survival of *Escherichia coli* and enterococci populations in the macro-alga *Cladophora* (Chlorophyta). *FEMS Microbiology Ecology, 26(2)*, 203-211. https://doi.org/10.1016/S0168-6496(03)00214-9.

Caffrey, J. M., Kemp, W. M. 1992. Influence of the submersed plant, *Potamogeton perfoliatus*, on nitrogen cycling in estuarine sediments. *Limnol. Oceanogr., 37*, 1483–1495. https://doi.org/10.4319/lo.1992.37.7.1483.

Callahan, B., McMurdie, P., Rosen, M., Han, A., Johnson, A., Holmes, S. 2016. DADA2: High-resolution sample inference from Illumina amplicon data. *Nature Methods, 13(7)*, 581-583. https://doi.org/10.1038/nmeth.3869.

Callahan, B.J., Wong, J., Heiner, C., Oh, S., Theriot, C.M., Gulati, A.S., McGill, S.K., Dougherty, M.K. 2019. High-throughput amplicon sequencing of the full-length 16S rRNA gene with single-nucleotide resolution. *Nucleic Acids Res*., *47*, e103.

Canale, R.P., Vogel, A.H. 1974. Effects of temperature on phytoplankton growth. *J. Environ. Eng. Div. ASCE, 100*, 229–241.

Capone, E. G. 1983. Benthic nitrogen fixation. In E. J. Carpenter & D. G. Capone (Eds.) *Nitrogen in the marine environment*, pp. 105–137.

Capone, E. G. 1993. Determination of nitrogenase activity in aquatic samples using the acetylene reduction procedure. In P. F. Kemp, B. F. Sherr, E. B. Sherr, & J. J. Cole (Eds.) *Handbook of methods in aquatic microbial ecology*, pp. 621–631.

Carmichael, W. 2001. Health Effects of Toxin-Producing Cyanobacteria: "The CyanoHABs". *Human and Ecological Risk Assessment, 7*, 1393-1407. https://doi.org/10.1080/20018091095087.

Carmichael, W.W. 1997. The Cyanotoxins. J.A. In: Callow, J.A. (Ed.). *Advances in Botanical Research*, *47,* 211-255.

Carmichael, W.W. 1998. Microcystin concentrations in human livers, estimation of human lethal dose-lessons from Caruaru, Brazil. In Proceedings of the 4th International Conference on Toxic Cyanobacteria, Beaufort, NC, September 1998. Paerl, H.W. and Carmichael, W.W., Eds.

Carmichael, W.W. 2008. A world overview — One-hundred-twenty-seven years of research on toxic Cyanobacteria — Where do we go from here? In H. K. Hudnell (Ed.), Cyanobacterial harmful algal blooms: *State of the science and research needs*, *619*. https://doi.org/10.1007/978-0-387-75865-7_4.

Carmichael, W.W., Azevedo, M.F.O., An, J.S., Molica, R.J.R., Jochimsen, E.M., Lau, S., Rinehart, K.L., Shaw, G.R., Eagelsham, G.K. 2001. Human fatalities from Cyanobacteria: chemical and biological evidence for cyanotoxins. Environ. *Health Perspect., 109(7),* 663-668.

Carmichael, W.W., Boyer, G. 2016. Health impacts from Cyanobacteria harmful algae blooms: Implications for the North American Great Lakes. *Harmful Algae, 54*, 194-212. https://doi.org/10.1016/j.hal.2016.02.002.

Carmichael, W.W., Evans, W.R., Yin, Q.Q., Bell, P. Moczydlowski, E. 1997. Evidence for paralytic shellfish poisons in the freshwater cyanobacterium *Lyngbya wollei* (Farlow ex Gomont) comb.nov. *J. Appl. Envir. Microbiol., 63(8),* 3104-3110.

Casamatta, D., Johansen, J., Vis, M., Broadwater, S. 2005. Molecular and morphological characterization of ten polar and near-polar strains with the Oscillatoriales (Cyanobacteria). *Journal of Phycology, 41*, 421 - 438. 10.1111/j.1529-8817.2005.04062.x.

Chaban, B., Hill, J.E. 2012. A ‘universal’ type II chaperonin PCR detection system for the investigation of Archaea in complex microbial communities. *ISME J, 6*, 430–439. https://doi.org/10.1038/ismej.2011.96.

Cheng, C., Sun, J., Fen, Z., Kuihai, W., Yongyu, R. 2014. Molecular identification of clinical "difficult-to-identify" microbes from sequencing 16S ribosomal DNA and internal transcribed spacer 2. *Annals of Clinical Microbiology and Antimicrobials, 13(1).* https://doi.org/10.1186/1476-0711-13-1.

Chesapeake Bay Program. 2024, July 31. *Underwater grasses in the Chesapeake Bay continue upward climb*. Chesapeake Bay Program. https://www.chesapeakebay.net/news/pressrelease/underwater-grasses-in-the-chesapeake-bay-continue-upward-climb?fbclid=IwZXh0bgNhZW0CMTEAAR3RrO53Ln-6PrxBOuRve3G3k3Li448es4-CPMdCZiegZI3poNNAnmtHv9Q_aem_tNTr9oJG9tDKL7_8itqCaw.

Chilton, E.W., Lowe, R.L. and Schurr, K.M. 1986. Invertebrate communities associated with *Bangia atropurpurea* and *Cladophora glomerata* in western Lake Erie. *J. Great Lakes Res., 12*, 149-153.

Chorus, I., Bartram, J. (Eds.). 1999. Toxic Cyanobacteria in Water: A Guide to Their Public Health Consequences, Monitoring and Management. *World Health Organization*, EandFN Spon, Routledge.

Clarridge JE III. 2004. Impact of 16S rRNA gene sequence analysis for identification of bacteria on clinical microbiology and infectious diseases. *Clin. Microbiol. Rev., 17*, 840–862.

Codd, G.A. and Bell, S.G. 1996. The Occurrence And fate of Blue-Green Algal Toxins in Freshwaters. *R & D Report, 29*, National Rivers Authority.

Cram, J.A., Hollins, A., McCarty, A.J., Martinez, G., Cui, M., Gomes, M.L., Fuchsman, C.A. 2024. Microbial diversity and abundance vary along salinity, oxygen, and particle size gradients in the Chesapeake Bay. *Environmental Microbiology, 26(1)*, e16557. https://doi.org/10.1111/1462-2920.16557.

De Boer, W.F. 2007. Seagrass–sediment interactions, positive feedbacks and critical thresholds for occurrence: a review. *Hydrobiologia, 591*, 5–24.

Delgado-Baquerizo, M., Oliverio, A. M., Brewer, T. E., Benavent-González, A., Eldridge, D. J., Bardgett, R. D., Maestre, F. T., Singh, B. K., & Fierer, N. 2018. A global atlas of the dominant bacteria found in soil. *Science*, *359(6373)*, 320–325. https://doi.org/10.1126/science.aap9516.

Deutsch, C., Sarmiento, J. L., Sigman, D. M., Gruber, N., & Dunne, J. P. 2007. Spatial coupling of nitrogen inputs and losses in the ocean. *Nature, 445(7124)*, 163–167. https://doi.org/10.1038/nature05392.

Duarte, C., Kirkman, H. 2001. Methods for the measurement of seagrass abundance and depth distribution. *Global Seagrass Research Methods*, 141-153. https://doi.org/10.1016/B978-044450891-1/50008-6.

Edgar, Robert C. 2004. MUSCLE: multiple sequence alignment with high accuracy and high throughput. *Nucleic Acids Research 32(5),* 1792-1797.

Elenkin, A. A. 1938. Monographia algarum cyanophycearum aquidulcium et terrestrium in finibus USSR inventarum. *Sinezelenye vodorosli SSSR*, *1–2*, pp. 1–1908). Izd AN SSSR.

Elser, J. J., Andersen, T., Baron, J. S., Bergström, A. K., Jansson, M., Kyle, M., Nydick, K., Steger, L., Hessen, D. O. 2009. Shifts in lake N: P stoichiometry and nutrient limitation driven by atmospheric nitrogen deposition. *Science, 326(5954)*, 835-837.

Engene, N., Cameron, C., Gerwick, W. 2010. 16S rRNA Gene Heterogeneity in the Filamentous Marine Cyanobacterial Genus *Lyngbya. Journal of Phycology, 46(3)*, 591-601. https://doi.org/10.1111/j.1529-8817.2010.00840.

Engene, N., Choi, H., Esquenazi, E. 2018. Uncovering cryptic diversity of Lyngbya: the new tropical marine Cyanobacterial genus *Dapis* (Oscillatoriales). *Journal of Phycology, 54(4),* 435-446. https://doi.org/10.1111/jpy.12752.

Engene, N., Choi, H., Esquenazi, E., Rottacker, E. C., Ellisman, M. H., Dorrestein, P. C. & Gerwick, W. H. 2011. Underestimated biodiversity as a major explanation for the perceived rich secondary metabolite capacity of the Cyanobacterial genus *Lyngbya*. *Environ Microbiol, 13*, 1601–1610.

Engene, N., Rottacker, E. C., Kas tovsky , J., Byrum, T., Choi, H., Ellisman, M. H., Koma rek, J. & Gerwick, W. H. 2012. *Moorea producens* gen. nov., sp. nov. and *Moorea bouillonii* comb. nov., tropical marine Cyanobacteria rich in bioactive secondary metabolites. Int. *J. System. Evol. Microbiol. 62*, 1171–8.

Engene, N., Trongholn, A., Paul, V., De Clerck, O. 2018. Uncovering cryptic diversity of *Lyngbya*: the new tropical marine Cyanobacterial genus *Dapis* (Oscillatoriales). *Journal of Phycology, 54(4)*, 435-446.

Faassen, E.J., Harkema, L., Begeman, L., Lurling, M. 2012. First report of (homo) anatoxin-a and dog neurotoxicosis after ingestion of benthic Cyanobacteria in The Netherlands. *Toxicon, 60 (3)*, 378–384.

Fan, H., Sheng, S., Zhange, F. 2022. New hope for Parkinson's disease treatment: Targeting gut microbiota. *CNS Neuroscience & Therapeutics, 28(11),* 1675–1688. https://doi.org/10.1111/cns.13916

Farlow, W.G. 1877. Remarks on some algae found in the water supplies of the City of Boston. *Bull. Bussey Institution, 2*, 75-80.

Fogg GE. 1969. The physiology of an algal nuisance. *Proc R Soc London B. 173*, 175–189.

Foss, A.J., Phlips, E.J., Yilmaz, M., Chapman, A. 2012. Characterization of paralytic shellfish toxins from *Lyngbya wollei* dominated mats collected from two Florida springs. *Harmful Algae, 16*, 98-107.

Fourqurean J., Duarte, C., Kennedy, H., Marba, N. 2012. Seagrass ecosystems as a global carbon stock. *Nature Geoscience 5(7)*, 505–509. http://dx.doi.org/10.1038/ngeo1477.

Fowler, C.M., Ogburn, M.B., Aquilar, R., Heggie, K., Legett, H., Richie, K., Plough, L. 2024. Viability of high-frequency environmental DNA (eDNA) sampling as a fish enumeration tool. *Ecological Indicators, 166*. https://doi.org/10.1016/j.ecolind.2024.112384.

Fox, G.E., Stackebrandt, E., Hespell, R.B., Gibson, J., Maniloff, J., Dyer, T.A., … and Woese, C.R. 1980. The phylogeny of prokaryotes. *Science, 209*, 457–463.

Francis, G. 1878. Poisonous Australian Lake. *Nature, 18*, 11-12.

Fujiki, H., Suganuma, M., Hakii, H., Bartolini, G., Moore, R.E., Takayama, S., Sugimura, T. 1984. A two-stage mouse skin carcinogenesis study of lyngbyatoxin A. *J. Cancer Res. Clin. Oncol., 108*, 174-176.

Gaby, J., Buckley, D. 2012. A Comprehensive Evaluation of PCR Primers to Amplify the *nifH* Gene of Nitrogenase. *PLoS ONE, 7(7)*. https://doi.org/10.1371/journal.pone.0042149.

Gallon, J.R. 1992. Tansley Review No. 44/Reconciling the Incompatible: N_2 Fixation and O_2. *New Phytol. 122*, 571-609.

Gambi, M.C., Nowell, A.R.M., Jumars, P.A. 1990. Flume observations on flow dynamics in *Zostera marina* (eelgrass) beds. *Marine Ecology Progress Series, 61*, 159–169. https://doi.org/10.3354/meps061159.

Gao, Y; Cornwell, JC; Stoecker, DK; Owens, MS. 2014a. Influence of Cyanobacterial blooms on sediment biogeochemistry and nutrient fluxes. *Limnology & Oceanography, 59(3)*, 959-971. doi:10.4319/lo.2014.59.3.0959.

Gao, Y; O'Neil, JM; Stoecker, DK; Cornwell, JC. 2014b. Photosynthesis and nitrogen fixation during Cyanobacteria blooms in an oligohaline and tidal freshwater estuary. *Aquatic Microbial Ecology, 72(2)*, 129-144. doi:10.3354/ame01692.

Geitler, L. 1932. Cyanophyceae. In: Kryptogamen-Flora von Deutschland, Österreich und der Schweiz. Ed. 2. (Rabenhorst, L. Eds) Vol. 14, pp. 673-1196, i-[vi]. Leipzig: Akademische Verlagsgesellschaft.

Glibert, P. 2020. Harmful algae at the complex nexus of eutrophication and climate change. *Harmful Algae, 91*. https://doi.org/10.1016/j.hal.2019.03.001.

Goldsborough, H. and O'Neil, J.M. 2016. Nitrogen Fixation among Aquatic Grasses of the Chesapeake Bay: a Comparison. Final Report Maryland Sea Grant- REU Program, August 2016. http://www.mdsg.umd.edu/reu/students/heathergoldsborough-university-maryland-eastern-shore.

Gomont, M. 1892. Monographie des Oscillariées (Nostocacées homocystées). *Annales des Sciences Naturelles, Botanique, 7(15)*, 263-368.

Granata, T., Serra, T., Colomer, J., Casamitjana, X., Duarte, C.M., Gacia, E. 2001. Flow and particle distributions in a nearshore seagrass meadow before and after a storm. *Marine Ecology Progress Series, 218*, 95–106. https://doi.org/10.3354/meps218095.

Granéli, E., Carlsson, P., Olsson, P., Sundström, B., Granéli, W., Lindahl, O. 1989. From anoxia to fish poisoning: the last ten years of phytoplankton blooms in Swedish marine waters. In: Cosper EM, Bricelj VM, Carpenter EJ (eds) *Novel phytoplankton blooms: causes and impacts of recurrent brown tides and other unusual blooms*. Springer, Berlin Heidelberg New York, pp 407–427.

Grim, S. L., Voorhies, A. A., Biddanda, B. A., Jain, S., Nold, S. C., Green, R., & Dick, G. J. 2021. Omics-Inferred Partitioning and Expression of Diverse Biogeochemical Functions in a Low-O_2 Cyanobacterial Mat Community. *mSystems*, *6(6),* e0104221. https://doi.org/10.1128/mSystems.01042-21.

Gugger, M., Lenoir, S., Berger, C., Ledreux, A., Druart, J.-C., Humbert, J.-F., Guette, C., Bernard, C. 2005. First report in a river in France of the benthic cyanobacterium *Phormidium favosum* producing anatoxin-a associated with dog neurotoxicosis. *Toxicon, 45(7),* 919–928.

Gurbisz, C. 2016. Dynamics of a Large Submersed Plant Bed in Upper Chesapeake Bay. [Doctoral dissertation, University of Maryland Center for Environmental Science]. *ProQuest Dissertations & Theses Global*.

Gurbisz, C., Kemp, M., Sanford, L., Orth, R. 2016. Mechanisms of Storm-Related Loss and Resilience in a Large Submersed Plant Bed. *Estuaries and Coasts, 39*(*4*), 951-966. https://doi.org/10.1007/s12237-016-0074-4.

Gurbisz, C., Kemp, W.M. 2014. Unexpected resurgence of a large submersed plant bed in Chesapeake Bay: analysis of time series data. *Limnology and Oceanography, 59*, 482–494. https://doi.org/10.4319/lo.2014.59.2.0482.

Hallegraeff, G.M. 1993. A review of harmful algal blooms and their apparent global increase. *Phycologia, 32*, 79–99.

Hamilton, D. P., Salmaso, N., Paerl, H. W. 2016. Mitigating harmful Cyanobacterial blooms: strategies for control of nitrogen and phosphorus loads. *Aquatic Ecology, 50*, 351-366.

Hardy, R.W. F., Holsten, R. D., Jacskon, E. K., Bums, R. C. 1968. The acetylene-ethylene assay for N, fixation: laboratory and field evaluation. *Physiol., 43*, 1185-1207.

Harrington, P., Rose, A., Johnstone, R. 2016. The potential of benthic iron and phosphorus fluxes to support the growth of a bloom forming toxic cyanobacterium *Lyngbya majuscula*, Moreton Bay, *Australia Marine & Freshwater Research, 67(12)*, 1918-1927. https://doi.org/10.1071/MF15219.

Hart, D.D., Biggs, B.J., Nikora, V.I., Flinders, C.A. 2013. Flow effects on periphyton patches and their ecological consequences in a New Zealand river. *Freshw. Biol., 58(8),* 1588–1602.

Heath, M.W. 2009. Mat Forming Toxic Benthic Cyanobacteria in *New Zealand: Species Diversity and Abundance, Cyanotoxin Production and Concentrations*. School of Biological Science, Victoria University, Wellington, New Zealand, pp. 108.

Heath, M.W., Wood, S.A., Ryan, K.G., 2011. Spatial and temporal variability in *Phormidium* mats and associated anatoxin-a and homoanatoxin-a in two New Zealand rivers. *Aquat. Microb. Ecol., 64(1)*, 69–79.

Heath, M.W., Wood, S.A., Young, R., Ryan, K., 2016. The role of nitrogen and phosphorus in regulating Phormidium sp. (Cyanobacteria) growth and anatoxin production. *FEMS Microbiol. Ecol*. http://dx.doi.org/10.1093/femsec/fiw021.

Hon, T., Mars, K., Young, G., et al. 2020. Highly accurate long-read HiFi sequencing data for five complex genomes. *Sci. Data, 7*, 399.

Horne, A. J., & Viner, A. B. 1971. Nitrogen fixation and its significance in tropical Lake George, Uganda. *Nature, 232(5310)*, 417–418. https://doi.org/10.1038/232417a0.

Howarth, R. W, Cole, J. J. 1985. Molybdenum availability, nitrogen limitation, and phytoplankton growth in natural waters. *Science, 229*, 653-655.

Howarth, R.W., Marino, R., Lane, J., Cole, J.J. 1988. Nitrogen Fixation in Freshwater, Estuarine and Marine Ecosystems. 1. Rates and Importance. *Limnology and Oceanography, 33(2)*, 619-687.

Hu, T., Chitnis, N., Monos, D., Dinh., A. 2021. Next-generation sequencing technologies: An overview. *Human Immunology, 82(11),* 801-811. https://doi.org/10.1016/j.humimm.2021.02.012.

Hudnell, K. (Ed). 2008.Cyanobacterial Harmful Algal Blooms. Proceedings of the Interagency, International Symposium on Cyanobacterial Harmful Algal Blooms. *Adv. Exp. Med.Biol*. *Springer Science, 619*, 948.

Invitrogen Qubit 4 Fluorometer, (Thermo Fisher Scientific Inc., Multiple Life Technologies Corporation, Pub. No. MAN0017210).

Jeanthon, C., L'Haridon, S., Cueff, V., Banta, A., Reysenbach, A.L., Prieur, D. 2002. *Thermodesulfobacterium hydrogeniphilum* sp. nov., a thermophilic, chemolithoautotrophic, sulfate-reducing bacterium isolated from a deep-sea hydrothermal vent at Guaymas Basin, and emendation of the genus *Thermodesulfobacterium. International Journal of Systematic and Evolutionary Microbiology, 52(3)*. https://doi.org/10.1099/00207713-52-3-765.

Jiewen, C., Liu, X., Zou, Y., Gong, J., Ge, Z., et al. 2024. A high-fat diet promotes cancer progression by inducing gut microbiota–mediated leucine production and PMN-MDSC differentiation. *Proceedings of the National Academy of Sciences, 121(20).* https://doi.org/10.1073/pnas.2306776121.

Jochimsen, E. M., Carmichael, W. W., An, J. S., Cardo, D. M., Cookson, S. T., Holmes, C. E., Antunes, M. B., de Melo Filho, D. A., Lyra, T. M., Barreto, V. S., Azevedo, S. M., & Jarvis, W. R. 1998. Liver failure and death after exposure to microcystins at a hemodialysis center in Brazil. *The New England journal of medicine, 338(13)*, 873–878. https://doi.org/10.1056/NEJM199803263381304.

Joyner, J. J., Litaker, R. W., & Paerl, H. W. 2008. Morphological and genetic evidence that the cyanobacterium *Lyngbya wollei* (Farlow ex Gomont) Speziale and Dyck encompasses at least two species. *Applied and environmental microbiology, 74(12)*, 3710–3717. https://doi.org/10.1128/AEM.02645-07

Joyner, J.J. 2007. Molecular Identity and Nutrient Limitation of *Lyngbya wollei* Mat Communities in North Florida Freshwater Systems. [Doctoral dissertation (Marine Sciences), University of North Carolina, Chapel Hill. *Marine Ecology Progress Series, 394*, 101-110. https://doi.org/10.3354/meps08311.

Kellman, R., Mihali, T.K., Jeon, Y.J., Pickford, R., Francescp, P., Neilan, B. 2008. Biosynthetic intermediate analysis and functional homology reveal a saxitoxin gene cluster in Cyanobacteria. *Applied and Environmental Microbiology, 74(13),* 4044-4053.

Kielak, A.M., Barreto, C.C., Kowalchuk, G.A., van Veen, J.A., Kuramae, E.E. 2016. The ecology of Acidobacteria: moving beyond genes and genomes. *Front Microbiol., 7*, 744.

Kirpenko, Yu A., Sirenko, L.A., and Kirpenko, N.I. 1981. In "The Water Environment: Algal Toxins and Health". (W.W. Carmichael, ed.) pp. 257-269.

Klindworth, A., Pruesse, E., Schweer, T., Peplies, J., C., Horn, M., Glöckner, F. 2013. Evaluation of general 16S ribosomal RNA gene PCR primers for classical and next-generation sequencing-based diversity studies. *Nucleic Acids Research, 41(1)*. https://doi.org/10.1093/nar/gks808.

Knoll, Andrew. 2008. Cyanobacteria and Earth History.

Koch, E.W. 2001. Beyond light: Physical, geological, and geochemical parameters as possible submersed aquatic vegetation habitat requirements. *Estuaries, 24*, 1–17.

Komárek, J. 2018. Delimitation of the family Oscillatoriaceae (Cyanobacteria) according to the modern polyphasic approach (introductory review). *Brazilian Journal of Botany, 41(2)*, 449-546. https://doi.org/10.1007/s40415-017-0415-y.

Lee, M. 2019. Happy Belly Bioinformatics: an Open-Source Resource Dedicated to Helping Biologists Utilize Bioinformatics. *The Journal of Open Source Education.* https://doi.org/10.21105/jose.00053

Lefcheck, J., Hughes, B., Johnson, A., Pfirrmann, B., Rasher, D., Smyth, A., Williams, B., Beck, M., Orth, R. 2019. Are coastal habitats important nurseries? A meta-analysis. Conservation Letters, *a Journal of the Society for Conservation Biology, 12(4),* e12645. https://doi.org/10.1111/conl.12645.

Lefcheck, J.S., Wilcox, D.J., Murphy, R.R., Marion, S.R., Orth, R.J. 2017. Multiple stressors threaten a critical foundation species in Chesapeake Bay. *Global Change Biology*. https://doi.org/10.11.11/gbc.13623.

Lewis, A. S., Kim, B. S., Edwards, H. L., Wander, H. L., Garfield, C. M., Murphy, H. E., Poulin, N.D., Princiotta, S.D., Rose, K.C., Taylor, A.E., Weathers, C.R., Yokota, K., Richardson, D.C., Bruesewitz, D. A. 2020. Prevalence of phytoplankton limitation by both nitrogen and phosphorus related to nutrient stoichiometry, land use, and primary producer biomass across the northeastern United States. *Inland Waters, 10(1)*, 42-50.

Lilleheil, G., Andersen, R., Skulberg, O., Alexander, J. 1997. Effects of a Homoanatoxin-a containing extract from *Oscillatoria formosa* (Cyanophycea/Cyanobacteria) on neuromuscular transmission. *Toxicon, 35*, 1275–1289.

Lovley, D. R., Ueki, T., Zhang, T., Malvankar, N. S., Shrestha, P. M., Flanagan, K. A., Aklujkar, M., Butler, J. E., Giloteaux, L., Rotaru, A. E., Holmes, D. E., Franks, A. E., Orellana, R., Risso, C., & Nevin, K. P. 2011. Geobacter: the microbe electric's physiology, ecology, and practical applications. *Advances in microbial physiology, 59,* 1–100. https://doi.org/10.1016/B978-0-12-387661-4.00004-5.

Luhar, M., J. Rominger, and H. Nepf. 2008. Interaction between flow, transport and vegetation spatial structure. *Environmental Fluid Mechanics, 8*, 423–439. https://doi.org/10.1007/s10652-008-9080-9.

Mahoney, J. B., & Steimle, F. W., Jr. 1979. A mass mortality of marine animals associated with a bloom of *Ceratium tripos* in the New York Bight. In D. L. Taylor & H. H. Seliger (Eds.), *Toxic dinoflagellate blooms*, 225–230.

Mann, F., Steinke, T.D. 1993. Biological nitrogen fixation (acetylene reduction) associated with blue-green algal (Cyanobacterial) communities in the Beachwood Mangrove Nature Reserve II. Seasonal variation in acetylene reduction activity. *South African Journal of Botany, 59(1)*, 1-8. https://doi.org/10.1016/S0254-6299(16)30767-0.

Marks, J.C. and Power, M.E. 2001. Nutrient induced changes in the species composition of epiphytes on *Cladophora glomerata* Kutz (Chlorophyta). *Hydrobiologia, 450*, 187-196.

Marquardt, J., & Palinska, K. A. 2007. Genotypic and phenotypic diversity of Cyanobacteria assigned to the genus *Phormidium* (Oscillatoriales) from different habitats and geographical sites. *Archives of microbiology, 187(5)*, 397–413. https://doi.org/10.1007/s00203-006-0204-7.

Martin, M. 2011. Cutadapt removes adapter sequences from high-throughput sequencing reads. *EMBnet.journal 17(1)*, 10-12

Martiny, J. B., Eisen, J. A., Penn, K., Allison, S. D., Horner-Devine, M. C. 2011. Drivers of bacterial beta-diversity depend on spatial scale. *Proc. Natl. Acad. Sci. U. S. A., 108(19)*, 7850–7854. doi: 10.1073/pnas.1016308108.

Maryland Department of Natural Resources. Distribution of *Lyngbya* Blooms in MD (2000-2014) [Photograph]. https://dnr.maryland.gov/waters/bay/Pages/algal_blooms/Lyngyba-Distribution.aspx.

McAllister, T., Wood, S., Hawes, I. 2016. The rise of toxic benthic *Phormidium* proliferations: A review of their taxonomy, distribution, toxin content and factors regulating prevalence and increased severity. *Harmful Algae, 55*, 282-294. https://doi.org/10.1016/j.hal.2016.04.002.

McDevitt-Irwin, J. M., Iacarella, J. C., & Baum, J. K. 2016. Reassessing the nursery role of seagrass habitats from temperate to tropical regions: A meta-analysis. *Marine Ecology Progress Series, 557*, 133-143.

McGlathery, K.J., K. Sundbäck, and I.C. Anderson. 2007. Eutrophication in shallow coastal bays and lagoons: the role of plants in the coastal filter. *Marine Ecology Progress Series, 348*, 1–18. https://doi.org/10.3354/meps07132.

McGregor, G., Sendall, B. 2015. Phylogeny and Toxicology of *Lyngbya wollei* (Cyanobacteria, Oscillatoriales) from North-Eastern Australia, with a Description of *Microseira* Gen. *Journal of Phycology, 51(1)*, 109-119. https://onlinelibrary.wiley.com/doi/10.1111/jpy.12256.

Minello, T. J., Able, K. W., Weinstein, M. P., & Hays, C. G. 2003. Salt marshes as nurseries for nekton: Testing hypotheses on density, growth and survival through meta-analysis. *Marine Ecology Progress Series, 246*, 39–59.

Mitsui, A., Rosner, D., Goodman, A., Reyes-Vasquez, G., Kusumi, T., Kodama, T., Nomoto, K. 10-14, November 1987. Hemolytic toxins in marine cyanobacterium *Synechococcus* sp. *Proceedings International Red Tide Symposium*. Takamatsu, Japan.

Montoya, J. P., Voss, M., Kahler, P., & Capone, D. G. 1996. A simple, high-precision, high-sensitivity tracer assay for N (inf2) fixation. *Applied and environmental microbiology, 62(3)*, 986-993.

Moore, K., Wilcox, D., Orth, R. 2000. Analysis of the Abundance of Submersed Aquatic Vegetation Communities in the Chesapeake Bay. *Estuaries, 23(1)*, 115. https://doi.org/10.2307/1353229.

Moore, K.A. 2004. Influence of seagrasses on water quality in shallow regions of the lower Chesapeake Bay. *J. Coast. Res., 45*, 162–178, https://doi.org/10.2112/SI45-162.1.

Moore, K.A., Richard L. Wetzel, and Robert J. Orth. 1997. Seasonal pulses of turbidity and their relations to eelgrass (*Zostera marina* L.) survival in an estuary. *Journal of Experimental Marine Biology and Ecology, 215*, 115–134. https://doi.org/10.1016/S0022-0981(96)02774-8.

Moynihan, M.A. 2020. nifHdada2 GitHub repository. *Zenodo.* http://doi.org/10.5281/zenodo.3958370.

National Center for Biotechnology Information (NCBI)[Internet]. Bethesda (MD): National Library of Medicine (US), National Center for Biotechnology Information; [1988] – [cited 2024 Aug 15]. Available from: https://www.ncbi.nlm.nih.gov/

National Oceanic and Atmospheric Administration Tides and Currents. 2021-2024. Annual Prediction Tide Tables for Havre De Grace, MD (8574070). https://tidesandcurrents.noaa.gov/stationhome.html?id=8574070.

National Research Council (US) Subcommittee on Microbiological Criteria. An Evaluation of the Role of Microbiological Criteria for Foods and Food Ingredients. Washington (DC): National Academies Press (US); 1985. 5, Selection of Indicator Organisms and Agents as Components of Microbiological Criteria. Available from: https://www.ncbi.nlm.nih.gov/books.

Negri, A.P., Bunter, O., Jones, B., Llewellyn, L., 2004. Effects of the bloom-forming alga *Trichodesmium erythraeum* on the pearl oyster *Pinctada maxima*. *Aquaculture, 232*, 91–102.

Nguyen, J., Lara-Gutiérrez, J., & Stocker, R. 2021. Environmental fluctuations and their effects on microbial communities, populations and individuals. *FEMS microbiology reviews*, *45(4)*, fuaa068. https://doi.org/10.1093/femsre/fuaa068.

O'Neil, J.M., Davis, T.W., Burford, M.A., Gobler, C.J. 2012. The rise of harmful Cyanobacteria blooms: the potential roles of eutrophication and climate change. *Harmful Algae, 14*, 313–334.

O'Neil, J.M., Capone, D.G. 1989. Nitrogenase activity in tropical carbonate marine sediments. *Mar. Ecol. Prog. Ser*., *56*, 145-156.

Onodera, H., Satake, M., Oshima, Y., Yasumoto, T., & Carmichael, W. W. 1997. New saxitoxin analogues from the freshwater filamentous cyanobacterium Lyngbya wollei. *Natural toxins*, *5*(4), 146–151. https://doi.org/10.1002/1522-7189(1997)5:4<146::AID-NT4>3.0.CO;2-V

Orth, R.J., M.R. Williams, S.R. Marion, D.J. Wilcox, T.J.B. Carruthers, K.A. Moore, W.M. Kemp, W.C. Dennison, N. Rybicki, P. Bergstrom, and R.A. Bauiuk. 2010. Long-term trends in submersed aquatic vegetation (SAV) in Chesapeake Bay, USA, related to water quality. *Estuaries and Coasts, 33*, 1144–1163. doi:10.1007/s12237010-9311-4.

Pacific Biosciences. 2023. Uncover deep genomic insights with long-read HiFi sequencing. pp. 17.

Paerl, H. W., & Paul, V. J. 2012. Climate change: links to global expansion of harmful Cyanobacteria. *Water research, 46(5),* 1349–1363. https://doi.org/10.1016/j.watres.2011.08.002.

Paerl, H. W., Zehr, J. P. 2000. Marine Nitrogen Fixation. In D. L. Kirchman (Ed.), *Microbial Ecology of the Oceans* (2nd ed., Ser. Wiley Series in Ecological and Applied Microbiology, pp. 387–426). Wiley-Liss, Inc.

Paerl, H., Joye, S., Fitzpatrick, M. 1993. Evaluation of nutrient limitation of CO_2 and N_2 fixation in marine microbial mats. *Marine Ecology Progress Series, 101*, 297-306.

Paerl, H.W. 1988. Nuisance phytoplankton blooms in coastal, estuarine, and inland waters. *Limnology and Oceanography, 33(4.2),* 823-843. https://doi.org/10.4319/lo.1988.33.4part2.0823.

Paerl, H.W. 1990. Physiology Ecology and Regulation of N_2 Fixation in Natural Waters. *Advanced Microbial Ecology, 11*, 305-344.

Paerl, H.W., 2008. Nutrient and other environmental controls of harmful Cyanobacterial blooms along the freshwater-marine continuum. In: Hudnell, H.K. (Ed.) Cyanobacterial Harmful Algal Blooms: State of the Science and Research Needs. *Adv. Exp. Med. Biol., 619*, 217-237.

Paerl, H.W., Fulton, R., Moisander, P. 2001. Harmful Freshwater Algal Blooms, With an Emphasis on Cyanobacteria. *The Scientific World Journal, 1*, 76-113. https://doi.org/10.1100/tsw.2001.16

Paerl, H.W., Huisman, J. 2008. Blooms like it hot. *Science, 320*, 57–58.

Paerl, H.W., Huisman, J. 2009. Climate change: a catalyst for global expansion of harmful Cyanobacterial blooms. *Environmental Microbiology Reports, 1(1),* 27-37. https://doi.org/10.1111/j.1758-2229.2008.00004.x.

Paerl, H.W., Tucker, C. 1995. Ecology of Blue-Green Algae in Aquaculture Ponds. *J. World Aquacult. Society, 26,* 1-53.

Palinska, K. A., & Marquardt, J. 2008. Genotypic and phenotypic analysis of strains assigned to the widespread Cyanobacterial morphospecies *Phormidium autumnale* (Oscillatoriales*). Archives of microbiology, 189(4)*, 325–335. https://doi.org/10.1007/s00203-007-0323-9.

Palinska, K. A., Deventer, B., Hariri, K., & Lotocka, M. 2011. A taxonomic study on *Phormidium*–group (Cyanobacteria) based on morphology, pigments, RAPD molecular markers and RFLP analysis of the 16S rRNA gene fragment. *Fottea, 11(1)*, 41-55.

Park, Y., Song, J.Y. 2020. Genomic Survey of *Tolypothrix* PCC 7910 Phytochromes. *NCBI* direct submission. Unpublished.

Patrick, C.J. Weller, D. 2015. Interannual variation in submerged aquatic vegetation and its relationship to water quality in subestuaries of Chesapeake Bay. *Marine Ecology Progress Series, 537*, 121-135. https://doi.org/10.3354/meps11412.

Paul, V.J. 2008. Global warming and Cyanobacterial harmful algal blooms. In: Hudnell, H.K. (Ed.) Cyanobacterial Harmful Algal Blooms: State of the Science and Research Needs. *Adv. Exp. Med. Biol, 619*, 217–237.

Peperzak, L. 2003. Climate change and harmful algal blooms in the North Sea. *Acta Oecol. 24*, 139–144.

Peterson, C.H., R.A. Luettich Jr., F. Micheli, and G.A. Skilleter. 2004. Attenuation of water flow inside seagrass canopies of differing structure. *Marine Ecology Progress Series 268*, 81–92.

Phlips, E. J., Ihnat, J., Conroy, M. 1992. Nitrogen fixation by the benthic freshwater cyanobacterium *Lyngbya wollei*. *Hydrobiologia, 234(1),* 59–64. https://doi.org/10.1007/BF00010779.

Plough, L.V., Ogburn, M.B., Fitzgerald, C.L., Geranio, R., Marafino, G.A., Richie, K.D., 2018. Environmental DNA Analysis of River Herring in Chesapeake Bay: A Powerful Tool for Monitoring Threatened Keystone Species. *PLoS One 13(11),* e0205578.

Poirier-Larabie, S., Hudon, C., Poirier Richard, H.-P., & Gagnon, C. 2020. Cyanotoxin release from the benthic, mat-forming cyanobacterium *Microseira* (*Lyngbya*) *wollei* in the St. Lawrence River, Canada. *Environmental Science and Pollution Research, 27(24)*, 30285–30294. https://doi.org/10.1007/s11356-020-09290-2.

Postgate, J. R. 1998. Nitrogen fixation. *Cambridge University Press*.

Puschner, B., Hoff, B., Tor, E.R. 2008. Diagnosis of anatoxin-a poisoning in dogs from North America. *J. Vet. Diagnost. Investig., 20(1)*, 89–92.

Putnam, S. P., Smith, M. L., Metz, T. T., Womer, A. M., Sellers, E. J., McClain, S. J., Crandell, C. A., Scott, G. I., Shaw, T. J., & Ferry, J. L. 2022. Growth of the harmful benthic cyanobacterium *Microseira wollei* is driven by legacy sedimentary phosphorous. *Harmful Algae*, *117*, 102263. https://doi.org/10.1016/j.hal.2022.102263.

Quast, C., Pruesse, E., Yilmaz, P., Gerken, J., Schweer, T., Yarza, P., Peplies, J., Glöckner, F.O. 2013. The SILVA ribosomal RNA gene database project: improved data processing and web-based tools. *Nucl. Acids Res. 41(1)*, 590-596.

Quiblier, C., Wood, S., Echenique-Subiabre, I., Heath, M., Villeneuve, A., Humbert, J.F. 2013. A review of current knowledge on toxic benthic freshwater Cyanobacteria–ecology, toxin production and risk management. *Water Res. 47(15)*, 5464–5479.

Rambaut, A. 2018. FigTree v1.4.4. Institute of Evolutionary Biology, University of Edinburgh, Edinburgh. http://tree.bio.ed.ac.uk/software/figtree/.

Rascio, N. & La Rocca, Nicoletta. 2013. Biological Nitrogen Fixation. Reference Module in Earth Systems and Environmental Sciences. https://doi.org/10.1016/B978-0-12-409548-9.00685-0.

Rejmánková, E., Komárková, J., Rejmánek, M. 2004. δ15N as an indicator of N 2-fixation by Cyanobacterial mats in tropical marshes. *Biogeochemistry, 67(3)*, 353-368. https://doi.org/10.1023/B:BIOG.0000015790.28584.ed.

Renshaw, M.A., Olds, B.P., Jerde, C.L., McVeigh, M.M., Lodge, D.M., 2015. The Room Temperature Preservation of Filtered Environmental DNA Samples and Assimilation into a Phenol–Chloroform–Isoamyl Alcohol DNA Extraction. *Mol. Ecol. Resour. 15(1)*, 168–176. https://doi.org/10.1111/1755-0998.12281.

Rex, L.L., Rosen, B.H. and Kingston, J.C. 1982. A comparison of epiphytes on *Bangia atropurpurea* (Rhodophyta) and *Cladophora glomerata* (Chlorophyta) from northern Lake Michigan. *J. Great Lakes Res., 8*, 164-168.

Reynolds, C.S., Walsby, A.E. 1975. Water blooms. *Biol Rev, 50*, 437–481.

Rhoads, A., Au, K. F. 2015. PacBio sequencing and its applications. *Genomics Proteomics Bioinformatics, 13,* 278–289.

Risgaard-Petersen, N., L. Ditlev, and M. Ottosen. 2000. Nitrogen cycling in two temperate *Zostera marina* beds: seasonal variation. *Mar. Ecol. Prog. Ser., 198,* 93–107.

Röske, K., Sachse, R., Scheerer, C., Röske, I. 2012. Microbial diversity and composition of the sediment in the drinking water reservoir Saidenbach (Saxonia, Germany). *Systematic and applied microbiology, 35(1)*, 35-44.

Russ, E.R. and Palinkas, C.M. 2018. Seasonal-Scale and Decadal-Scale Sediment-Vegetation Interactions on the Subaqueous Susquehanna River Delta. *Upper Chesapeake Bay Estuaries and Coasts, 41(1).* https://doi.org/10.1007/s12237-018-0413-8.

Sav Acres and density Susquehanna Flats (CB1TF2). 2019, November. https://cast-content.chesapeakebay.net/documents/SAV_FactSheets/SusquehannaFlats(CB1TF2)_TT_11.11.19.pdf.

Schindler, D. W., Carpenter, S. R., Chapra, S. C., Hecky, R. E., & Orihel, D. M. 2016. Reducing phosphorus to curb lake eutrophication is a success. *Environmental science & technology, 50(17),* 8923-8929.

Schmittner, A., Oschlies, A., Matthews, H. D., & Galbraith, E. D. 2008. Future changes in climate, ocean circulation, ecosystems, and biogeochemical cycling simulated for a business-as-usual CO2 emission scenario until year 4000 AD. *Global biogeochemical cycles, 22(1)*.

Schubel, J.R., Pritchard, D.W. 1986. Responses of Upper Chesapeake Bay to Variations in Discharge of the Susquehanna River. *Springer Estuaries, 9(4)*, 236-249.

Sellner K.G. 1997. Physiology, Ecology, and Toxin Properties of Marine Cyanobacterial Blooms. *Limnology and Oceanography, 42*, 1089-1104.

Shapiro, J., Wright, D.I. 1990. Current beliefs regarding dominance by blue-greens: the case for the importance of CO_2 and pH. *Verh. IVTLAP, 24*, 38–54.

Sheng, P., Yu, Y., Zhang, G., Huang, J., He, L., Ding, J. 2016. Bacterial diversity and distribution in seven different estuarine sediments of Poyang Lake, China. *Environmental Earth Sciences, 75*, 1-9.

Shishido, T. K., Kaasalainen, U., Fewer, D. P., Rouhiainen, L., Jokela, J., Wahlsten, M., Fiore, M. F., Yunes, J. S., Rikkinen, J., Sivonen, K. 2013. Convergent evolution of [D-Leucine(1)] microcystin-LR in taxonomically disparate Cyanobacteria. *BMC evolutionary biology, 13*, 86. https://doi.org/10.1186/1471-2148-13-86.

Silva, P.C., Menez, E.G. & Moe, R.I. 1987. Catalog of the Benthic Marine Algae of the Philippines. *Smithsonian Contributions to the Marine Science 27*, 179.

Smith, V.H. 1990. Nitrogen, Phosphorus, and Nitrogen Fixation in Lacustrine and Estuarine Ecosystems. *Limnology and Oceanography, 35*, 1852-1859.

Smith, Z. J., Martin, R. M., Wei, B., Wilhelm, S. W., & Boyer, G. L. 2019. Spatial and Temporal Variation in Paralytic Shellfish Toxin Production by Benthic *Microseira (Lyngbya) wollei* in a Freshwater New York Lake. *Toxins*, *11*(1), 44. https://doi.org/10.3390/toxins11010044.

Speziale, B. J., Dyck, L.A. 1992. *Lyngbya* infestations: comparative taxonomy of *Lyngbya wollei* comb. nov. (Cyanobacteria). *Journal of Phycology, 28(5),* 693-706.

Stamatakis, A. 2014. RAxML version 8: a tool for phylogenetic analysis and post-analysis of large phylogenies. *Bioinformatics, 30(9),* 1312-1313. https://doi.org/10.1093%2Fbioinformatics%2Fbtu033.

Starmach, K. 1966. Cyanophyta—sinice. Flora Slodkow Polski, Panstw Wyd Nauk, Krakow.

Suzuki, D., Ueki, A., Amaishi, A. 2007. *Desulfobulbus japonicus* sp. nov., a novel Gram-negative propionate-oxidizing, sulfate-reducing bacterium isolated from an estuarine sediment in Japan. *International Journal of Systematic and Evolutionary Microbiology, 57(4).* https://doi.org/10.1099/ijs.0.64855-0.

Taft, C.E. 1975. History of *Cladophora* in the Great Lakes. *Cladophora in the Great Lakes (Shear, H. and Konasewich, D.E., Eds.),* 5-16. Great Lakes Research Advisory Board, International Joint Commission Regional O⁄ce, Windsor, ON.

Tang, J., Du, L., Shah, M., Yao, D., Zhao, K., Li, L., Li, M., Waleron, M.M., Waleron, M., Waleron, K.F. and Daroch, M. 2022. Polyphasic identification and genomic insights of *Leptothermofonsia sichuanensis* gen. nov., a novel thermophilic cyanobacteria within Leptolyngbyaceae. *Front. Microbiol*.

Teneva, I., Dzhambazov, B., Koleva, L., Mladenov, R., Schirmer, K. 2005. Toxic potential of five freshwater *Phormidium* species (Cyanoprokaryota). *Toxicon, 45(6),* 711-725. https://doi.org/10.1016/j.toxicon.2005.01.018.

Tiling, K. and Proffitt, C.E. 2017. Effects of *Lyngbya majuscula* blooms on the seagrass *Halodule wrightii* and resident invertebrates. *Harmful Algae, 62*, 104-112.

Trivedi, C., Keuschig, C., Larose, C., Rissi, D., Mourot, R., Bradley, J., Winkel, M., Benning, L. 2022. DNA/RNA Preservation in Glacial Snow and Ice Samples. *Frontiers in Microbiology, 13*. https://doi.org/10.3389/fmicb.2022.894893.

Tucker, T., Marra, M., Friedman, J. 2009. Massively Parallel Sequencing: the Next Big Thing in Genetic Medicine. *The American Journal of Human Genetics, 85(2)*, 142-154. https://doi.org/10.1016/j.ajhg.2009.06.022.

U.S. Environmental Protection Agency Region 3 Water Protection Division. 2016, January 21. Underwater Grass Comeback Helps Chesapeake Bay. *Stories of Progress in Achieving Healthy Waters*. https://www.epa.gov/pa/underwater-grass-comeback-helps-chesapeake-bay.

Vick, T.J., Dodworth, J.A., Costa, K.C., Shock, E.L., Hedlund, B.P. 2009. Microbiology and geochemistry of Little Hot Creek, a hot spring environment in the Long Valley Caldera. *Geobiology, 8(2),* 140-154. http://doi.org/10.1111/j.1472-4669.2009.00228.

Vijayavel, K., Michael J. Sadowsky, John A. Ferguson, and Donna R. Kashian. 2013. The Establishment of the Nuisance Cyanobacteria *Lyngbya wollei* in Lake St. Clair and Its Potential to Harbor Fecal Indicator Bacteria. *Journal of Great Lakes Research, 39(4)*, 560–68. https://doi.org/10.1016/j.jglr.2013.09.018.

Vitousek, P., Howarth, R. 1991. Nitrogen limitation on land and in the sea: how can it occur? *Biogeochemistry, 13*, 87-115. https://doi.org/10.1007/BF00002772.

Ward, L.G. 1985. The influence of wind waves and tidal currents on sediment resuspension in middle Chesapeake Bay. *Geo-Marine Letters, 5*, 71–75.

Watkinson, A.J., O'Neil, J.M., Dennison, W.C. 2005. Ecophysiology of the marine cyanobacterium, *Lyngbya majuscula* (Oscillatoriaceae) in Moreton Bay, Australia. *Harmful Algae 4(4),* 697-715. https://doi.org/10.1016/j.hal.2004.09.001.

Wehr, J.D., Sheath, R.G., Kociolek, J.P. 2015. Freshwater algae of North America, 2nd edn. *Academic Press*.

Woebken, D., Burow, L. C., Prufert-Bebout, L., Bebout, B. M., Hoehler, T. M., Pett-Ridge, J., Spormann, A. M., Weber, P. K., & Singer, S. W. 2012. Identification of a novel Cyanobacterial group as active diazotrophs in a coastal microbial mat using NanoSIMS analysis. *The ISME journal, 6(7),* 1427–1439. https://doi.org/10.1038/ismej.2011.200.

Woese, C. R. 1987. Bacterial evolution. *Clinical Microbiology Reviews*, *51,* 221–271.

Woese, C. R., Stackebrandt, E., Macke, T. J., Fox, G. E. 1985. A phylogenetic definition of the major eubacterial taxa. *Syst. Appl. Microbiol., 6(2),* 143–151. https://doi.org/10.1016/S0723-2020(85)80047-3.

Woese, C.R., Fox, G.E. 1977. Phylogenetic structure of the prokaryotic domain: the primary kingdoms. *Proc Natl Acad Sci USA, 74*, 5088–5090.

Woese, C.R., Stackebrandt, E, Macke, T.J., Fox, G.E. 1985. A phylogenetic definition of the major eubacterial taxa. *Syst Appl Microbiol, 6*, 143–151.

Wolle, F. 1887. Freshwater Algae of the United States. The Comenius Press, Bethlehem, Pennsylvania, pp. 364.

Wood, S.A., Selwood, A.I., Rueckert, A., Holland, P.T., Milne, J.R., Smith, K.F., Smits, B., Watts, L.F., Cary, C.S. 2007. First report of homoanatoxin-a and associated dog neurotoxicosis in New Zealand. *Toxicon, 50(2)*, 292–301.

Yamaguchi, H., Suzuki, S., Kawachi, M. 2019. *Microseira wollei* NIES-4236. *NCBI* direct submission. Unpublished.

Yin, Q., Carmichael, W., Evans, W. 1997. Factors influencing growth and toxin production by cultures of the freshwater cyanobacterium *Lyngbya wollei* Farlow ex Gomont. *Journal of Applied Phycology, 9*, 55-63.

Zehr, J.P. 1992. Molecular Biology of Nitrogen Fixation in Natural Populations of Marine Cyanobacteria. *Springer Netherlands,* 249-264. https://doi.org/10.1007/978-94-015-7977-3_16.

Zehr, J.P., McReynolds, L.A. 1989. Use of degenerate oligonucleotides for amplification of the *nifH* gene from the marine cyanobacterium *Trichodesmium thiebautii*. *Appl Environ Microbiol., 55(10)*, 2522-2526. https://doi.org/10.1128/aem.55.10.2522-2526.1989.

Zhang, J., Yang, Y., Zhao, L., Li, Y., Xie, S., & Liu, Y. 2015. Distribution of sediment bacterial and archaeal communities in plateau freshwater lakes. *Applied Microbiology and Biotechnology, 99*, 3291-3302.

Zhe, L., Hongfeng, L., Yingyu, H. 2023. Gut bacterial profiles in Parkinson's disease: A systematic review. *CNS Neuroscience & Therapeutics, 29(1),* 140–157. https://doi.org/10.1111/cns.13990.